The Effect of Weldable Primer Paint Thickness on Weld Quality and Geometry

by Russell A. Phipps

University of Strathclyde

Department of Mechanical and Aerospace Engineering

Master of Philosophy

2020

Contents

List of Acronyms

ANN – Artificial Neural Networking

CE – Carbon Equivalent

CMTR – Certified Material Test Report

CTWD – Contact Tip to Work Distance

CV – Constant Voltage

DCEN – Direct Current Electrode Negative

DCEP – Direct Current Electrode Positive

DFT – Dry Film Thickness

ERW – Electric Resistance Welding

ESW – Electro Slag Welding

FCAW – Flux Cored Arc Welding

GCHAZ – Grain Coarsened Heat Affected Zone

GRHAZ – Grain Refined Heat Affected Zone

HAZ – Heat Affected Zone

HICC – Hydrogen Induced Cold Cracking

HV – Hardness Vickers

LOF – Lack of Fusion

MIG/MAG – Metal Inert Gas/Metal Active Gas

MMA – Manual Metal Arc

MPI – Magnetic Particle Inspection

NDT – Non-Destructive Testing

QC – Quality Control

RT – Radiographic Testing

SAW – Submerged Arc Welding

STT – Surface Tension Transfer

TIG – Tungsten Inert Gas

WPQR – Welding Procedure Qualification Record

WPS – Welding Procedure Specification

UT – Ultrasonic Testing

Acknowledgements

Abstract

The purpose of this project was to provide data that could be used to support work by Cairns *et al.* [1] that aimed to optimise robotic fillet welding by identifying key contributing factors. The focus of this thesis was the effect of weld-through primers on the geometry and quality of a fillet weld.

Steel samples were sent to a paint company, where the primer was applied to predetermined thickness ranges. The DFT of the sample plate and a randomly selected panel was then measured and systematically recorded for analysis. Test joints at three DFT ranges, were welded using five filler types and a mechanised welding rig at the University of Strathclyde. Varying test methods were used to identify any trends, that would suggest the coating was impacting the weld quality and/or geometry.

Findings from the measurement of DFT casts doubt on data supplied by paint companies. This is a result of the effects of overspray, creating areas with a considerably higher DFT. Weld-through primer and HAZ area, showed a possible relationship. The samples where the paint was mechanically removed seemed in some cases to produce larger HAZ areas. It was concluded that the primer may limit the spread of heat, resulting in a smaller HAZ. The analysis of weld penetration data showed a possible relationship between weld-through primer and weld penetration. The sample joints, where the paint was mechanically removed, have produced welds with less penetration than those coated with primer. Discussion suggests, this could be a result of a surface tension effect from the coating and/or gases from welding, contaminating the gas shield and increasing the arc temperature. This work has also highlighted the potential for a model that would provide manufacturers using weld-through shop primers with a method of estimating internal weld metal porosity by measurement of DFT.

The Effect of Weldable Primer Paint Thickness on Weld Quality and Geometry

1.0 Introduction

In order to fully optimise a process, all notable variables must be considered. In the fabrication industry, the inspection of fillet welds is seen as a relatively simplistic task. Specially designed gauges allow the welder to self-verify and quality engineers to inspect the weld by measuring the horizontal and vertical leg length. This ensures it is within the acceptance range stated in the project specification. To inspect the penetration of a fillet weld, destructive testing is required. According to BS EN ISO 15614-1 [2], the qualification of a welding procedure for a fillet weld, involves two macro sections being cut from a 300mm long sample. Next, they are etched to provide a visual image of the penetration achieved at those points in the welded joint. This procedure test is then seen as justification, that if the production welders operate within the parameter range specified in the WPS, they will produce a fillet weld with sufficient penetration. As field fillet welds cannot be destructively tested during project fabrication, there is no way to accurately measure penetration and internal geometry of a fillet weld. Cairns *et al.* [3] developed a technique using ANN, to identify the key parameters affecting fillet weld penetration and geometry. Cairns *et al.* [1] used current, voltage, travel speed, gun angle and travel angle as input parameters to provide model outputs of penetration, horizontal and vertical leg length.

Weld through shop primers have been available for several decades, to prevent corrosion occurring pre-fabrication and during the fabrication process. They also remove the need for grinding or cleaning of the weld area before welding. To benefit from the use of weld through primers, certain controls must be put in place. These controls will ensure that welds produced meet the quality requirements and are free

of defects. Boekholt questioned whether such stringent controls would be practical for large volume production [4].

Primer film thickness, welding parameters and the welding consumable used are the main influencing factors. Paint manufacturers generally supply guidelines within the product information document. The recommended film thickness is often 15μm; anything below this may not offer sufficient corrosion protection, and anything above this may have an adverse effect on weld quality. This could result in causing internal or surface breaking porosity. The guidelines will also often state, that film thicknesses above 25μm, should be avoided (see Appendix 10). Boekholt concluded that mechanised welding increases the risk of porosity due to high welding speeds and rapid freezing of the weld pool [4]. This risk on weld quality is further increased with the introduction of primer paint. The use of seamless flux-cored and metal cored wires is thought to reduce the adverse effect of the shop primers. This is due to their low hydrogen content (typically <3ml/ 100g of weld metal).

The purpose of this thesis was to generate further data that could be used to provide an ANN model for the optimisation of a fillet weld. A series of experimental procedures assessed the effect of primer paint on fillet weld geometry and quality. This work focused on primer paint. Steel test pieces with varying film thicknesses were welded and tested to provide evidence of the effect of paint thicknesses on weld quality.

2.0   Literature Review

2.1 Geometry and terminology of a fillet weld

It is commonly known that fillet welds generally make up around 80% of the welding of a fabricated structure. This makes it highly important that the welds are of acceptable quality [5]. For a fillet weld to be successful, there must be ample root penetration to break the axis of the joint. The weld must also be within the size tolerance provided in the project specification.

The Mitre fillet weld symbol (see Figure 2.1) is used when calculating the fillet weld size requirement. It is also displayed in a technical drawing, when working to BS EN ISO 2553 [6]. A Mitre fillet weld symbol will also often provide the weld size required for the joint as a throat thickness (a), or as a leg length (z) (see Figures 2.1 & 2.2). The throat thickness of a fillet weld is a more accurate interpretation of the section of weld metal providing strength to the joint. When calculated, this is known as the design throat. In a practical sense, it would be impossible to achieve a fillet weld exactly the same size and geometry as the Mitre fillet. For this reason, the throat thickness produced after welding, is known as the actual throat. The actual throat thickness includes any excess weld metal from the weld profile. The leg length of a fillet weld is a term used for the distance from the axis of the joint to the toe of the weld. This terminology can be broken down again into the horizontal and the vertical leg length.
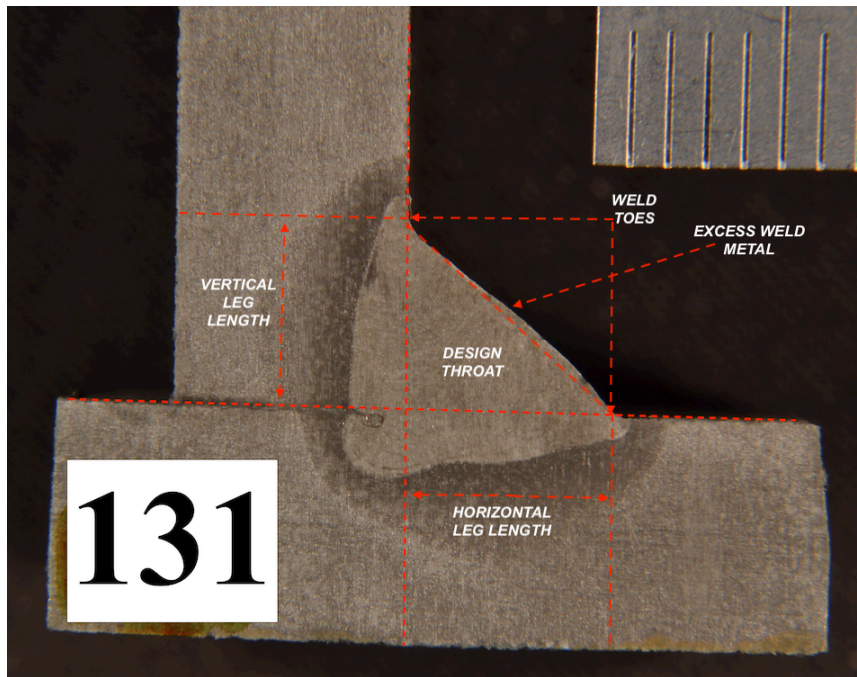
Figure 2.1 – Fillet Weld - Throat thickness (a) and Leg Length (z) – Design Throat (Mitre Fillet). This macro etched fillet weld was one of the sample joints welded and tested during the experimental schedule as part of this work.
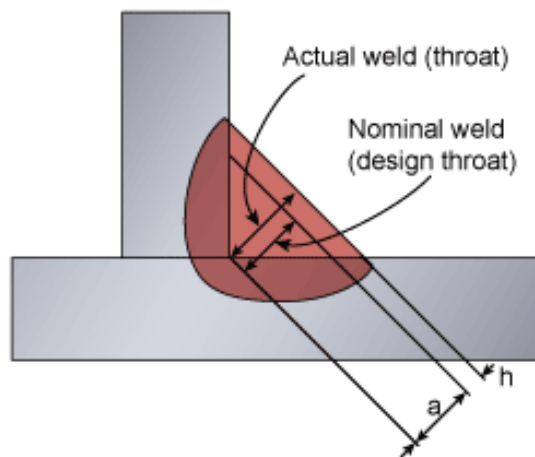
Figure 2.2 – Design throat and actual throat thickness. Adapted from The Welding Institute [7].

2.1.1 Over-welding

A problem regularly encountered within the fabrication industry is over-welding. This is generally a problem associated with fillet welding, although wide root gaps in butt joints are also a common problem. If the specification requires a 5mm leg length fillet weld, and welders lay down a 7mm leg length weld, the weld volume is increased by 93%. This almost doubles the required heat input and consumable cost, while increasing distortion and structural weight (see Figure 2.3). For these reasons, it is important that welders and welding operators use the correct welding parameters and they self-verify fillet weld leg length and throat thickness.
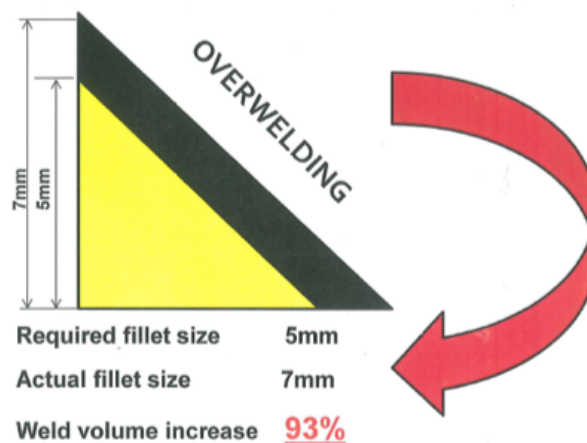
Figure 2.3 – This diagram was used as part of a shop floor toolbox talk, to educate production welders on the importance of maintaining the correct fillet size and the effect over-welding can have on weld volume. Reproduced with permission from BAE Systems Maritime, Glasgow.

2.2 Heat input and the Heat Affected Zone

Along with the practical and engineering aspects of welding, welding engineers have to have an understanding of the metallurgy associated with the processes. Having that knowledge, will lead to a greater overall control of the process. So, an understanding of microstructural development, is essential in the case of the weld metal and HAZ. Normally, this would be related to the heat input and as a consequence to cooling rate too. For the weld metal, the effect of the filler wire and dilution have to be assessed.

Heat Input

2.2.1 The Effect of Heat During Welding

During welding, the weld metal is in the molten state, and this is a solidification issue that has to be dealt with. The heat input governs the amount of heat in the process. High heat input leads to higher temperatures and as a consequence, slower cooling rates and a coarsened microstructure. The converse is true for low heat inputs, where a faster cooling rate occurs, which in turn generates a finer microstructure. There is an additional factor in cooling rates, and that is plate thickness. A thick plate combination creates an effective heat sink and slows cooling rate. The opposite is the case for the thin plate combinations, with heat spreading out over a wider area and contributing to issues such as distortion.

As cooling progresses, nucleation occurs within the weld, normally in a dendritic form. A high cooling rate results in a large number of fine dendrites, with very small inter-dendritic spaces and low levels of segregation. Slow cooling leads to large dendrite growth, with larger inter-dendritic spacing and potentially more inter-dendritic segregation. The combination of heat input and cooling rate are key components of microstructural control in the weld metal. There are other secondary factors, such as oxides acting as nucleation sites, or the use of heat sinks. These can be added in, but merely serve to illustrate the complex nature of the process. This is

relatively easy to describe for a single pass weld. However, multiple pass welds add a significant level of complexity to the microstructural analysis.

The HAZ is quite simply the area of the overall weld, which was not molten but that has been affected metallurgically by the heat imparted into the weld. It has been stated, that the unaffected base material for a carbon manganese steel, is around 400°C [8]. The HAZ also has a number of sub zones, all with their own microstructures. The nearer to the weld boundary, the coarser the grain structure. This is due to the slower cooling rate. Moving away from the weld metal, the microstructure becomes more refined and as a result, there can be a range of mechanical properties across the HAZ (see Figures 2.7 and 2.8). Normally, toughness is the property which attracts the most attention. The HAZ area nearest the weld region is the most susceptible to a reduction in toughness.

Beyond this, there are situations where the grain growth in the HAZ can be restricted by the presence of microalloying elements. These are normally, niobium, vanadium and titanium. So, steels such as Lloyds Naval grade DH36, have a good range of strength and toughness when compared to lower grade steels, e.g. A grade. In addition, there are significant benefits in weld region properties, with the presence of micro alloys minimising grain growth.

2.2.2 High Heat Input Welds

Processes such as SAW and ESW, produce large weld beads and high levels of dilution with the parent metal. These processes are associated with high heat inputs and slow cooling rates that allow sufficient time for austenitic grain growth. If a cross sectional macro is taken of such a weld, there will be a visibly coarsened grain structure with large columnar grains (see Figure 2.4). This kind of microstructure will, in most cases result in low toughness properties in the weld metal and the GCHAZ.
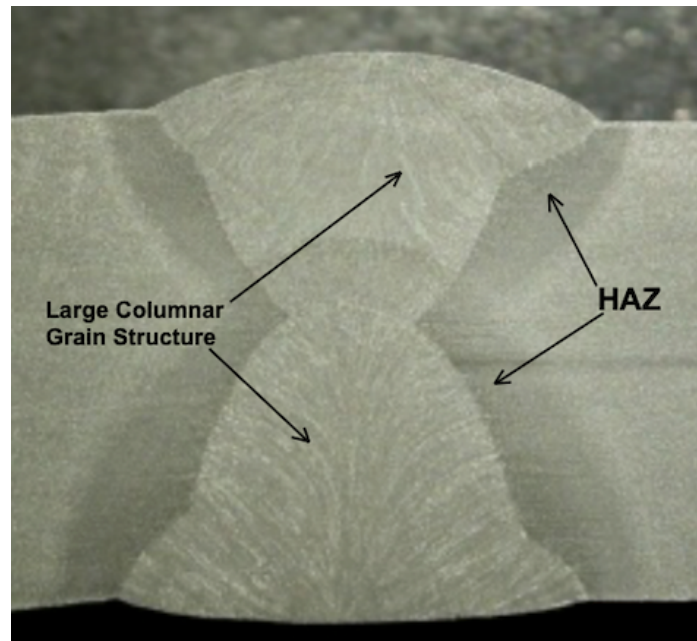
Figure 2.4 – High heat input double sided submerged arc weld. Noticeably large HAZ and columnar grain structure. This macro section was created during double sided SAW trial work at BAE Systems, Glasgow. Reproduced with permission from BAE Systems Maritime, Glasgow.

2.2.3 Low Heat Input Welds

When smaller weld beads are required, higher travel speeds are used, resulting in less heat input and faster cooling rates (see Figure 2.5). These faster cooling rates can produce a hard, brittle microstructure in the HAZ, due to the formation of martensite. This brittle structure will increase the risk of HICC occurring in a low temperature service environment. The risk of creating an area of high hardness in the GCHAZ can be reduced by the introduction of a minimum preheat. The minimum preheat temperature is calculated using the base material CE, heat input and combined material thickness. The use of an annealing pass during the welding of a butt joint, will also reduce the risk of high hardness in the GCHAZ due to the tempering effect. An annealing pass involves placing the final capping pass within the weld metal area.
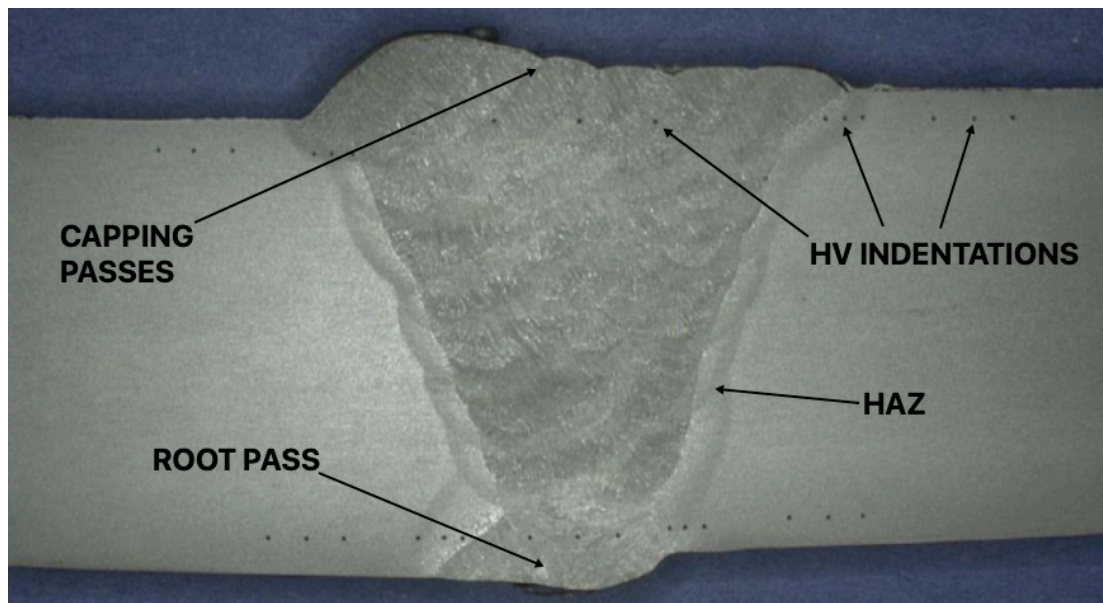
Figure 2.5 – Flux-cored C-Mn butt weld, welded in the horizontal (PC/2G) position. Visible indentations from Vickers Hardness test as part of WPQR qualification carried out by Cammell Laird shipyard. Reproduced with permission from Cammell Laird ship building and repair yard.

2.2.4 Calculating Heat Input

Alongside calculating heat input during welding, the heat input formula is used to establish a parameter range for the WPS. This document can then be issued to the shop floor as part of the welding procedure qualification process. Failure to operate within the heat input range in the WPS, can result in reduced toughness or high hardness zones. When qualifying a WPQR in plate material to BS EN ISO 15614-1 [2] a butt joint must be welded in the highest heat input position (Vertical up) and the lowest heat input position (Horizontal). This provides the qualification range required for all positional welding.

Heat input is calculated using current, arc voltage, travel speed and arc efficiency, which is dependent on the welding process and shielding gas used. The arc efficiency can be determined using a method dictated in work by Grong [9]. This method allows the engineer to calculate the arc efficiency for a shielding gas mixture. For this work, using MIG/MAG and an 80%Ar/20%CO_2 shielding gas, the calculated arc efficiency is 0.73. This figure was used to calculate heat input during the experimental stage of this work.

$$Heat\ Input\ \left(\frac{kJ}{mm}\right) = \frac{Volts\ (V)\ x\ Amps\ (A)x\ 60\ x\ \eta_{THERMAL}}{Travel\ Speed\ \left(\frac{mm}{\min}\right)}$$

Figure 2.6 – Formula for calculating heat input, as provided in
BS EN ISO 18491:2015 Welding and allied processes. Guidelines
for measurement of welding energies [10].

2.2.5 Areas of a Welded Joint

In any joint fusion welded using a filler metal consumable, there are three main areas of the welded joint. As described by Higgins [11] these are the weld metal, the heat affected zone and the unaffected parent metal (see Figure 2.7 & 2.8). The weld metal is primarily made up of the filler metal deposited from the welding consumable, with some dilution from the parent metal. The heat affected zone is mostly the parent material, with some dilution with the filler metal as a result of fusion welding. The unaffected parent metal is the base material out with the area affected by heat from the fusion process.
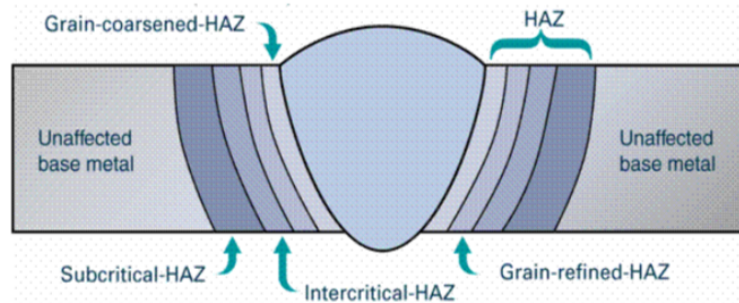
Figure 2.7 – Areas of a welded joint from the fusion line. Adapted from The Welding Institute [12].
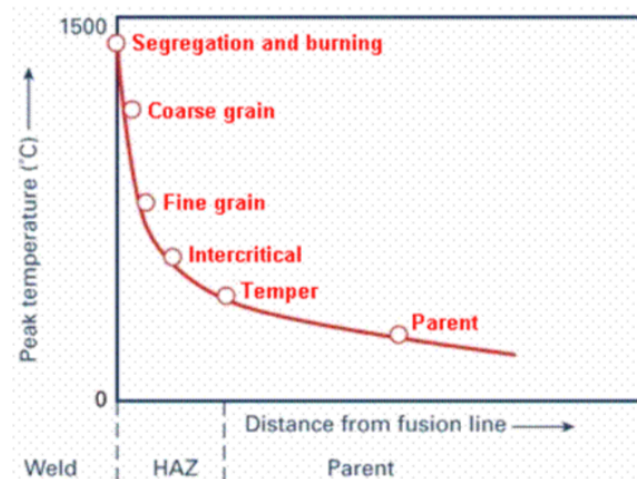
Figure 2.8 – Areas of a welded joint from the fusion line. Adapted from The Welding Institute [12].

Areas of the Heat Affected Zone

2.2.6 Grained Coarsened Heat Affected Zone

The GCHAZ is the area of the HAZ located closest to the fusion line of the weld. During welding, the temperature of the molten metal weld pool is in the region of 2500-3000°C, well above the melting point of iron (~1510°C) [13]. Temperatures within the GCHAZ will be around 1100°C, providing sufficient time for grain growth and full austenitisation to occur. Fast cooling rates will produce a GCHAZ with high hardness and reduced ductility, due to the formation of a martensitic microstructure (see Figure 2.9). This area is associated with low toughness in single pass welds, this is down to slower cooling rates producing a ferrite and carbide microstructure (see Figures 2.10 & 2.11).
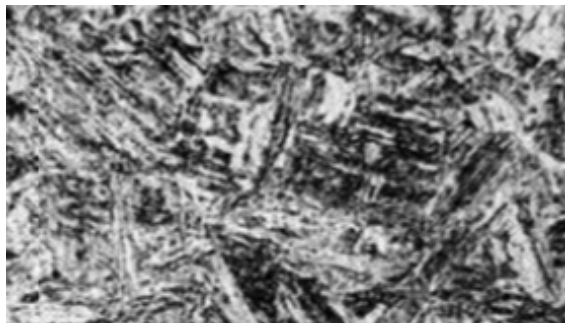
Figure 2.9 – GCHAZ microstructure of a C-Mn steel weld. The formation of a Martensitic microstructure generally produces high hardness (>350HV) and low toughness. Adapted from The Welding Institute [12]
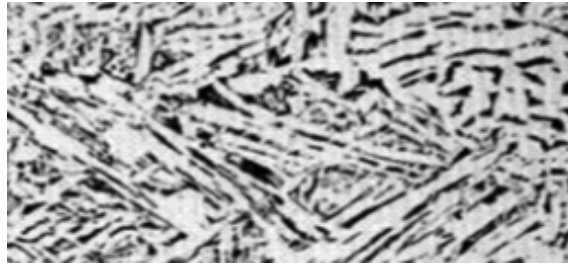
Figure 2.10 – Micrograph of a GCHAZ – Ferrite with aligned second phase which has poor toughness. Visible Columnar grained microstructure. Adapted from The Welding Institute [12].
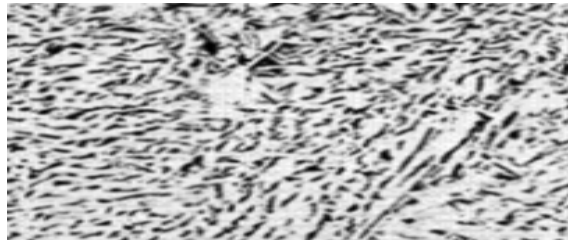
Figure 2.11 – Micrograph of a GCHAZ – Ferrite with non-aligned second phase. This section has better toughness. Adapted from The Welding Institute [12].

2.2.7 Grain Refined Heat Affected Zone

The next defined section in the HAZ is the GRHAZ. This area is far enough away from the fusion line that it reaches temperatures just above A_3 on the iron - carbon phase diagram (see Appendix 1). This means that cooling rates are faster and there is not enough time for grain growth. This section will have higher toughness and lower hardness than the GCHAZ, due to the finer grain structure (see Figure 2.12).
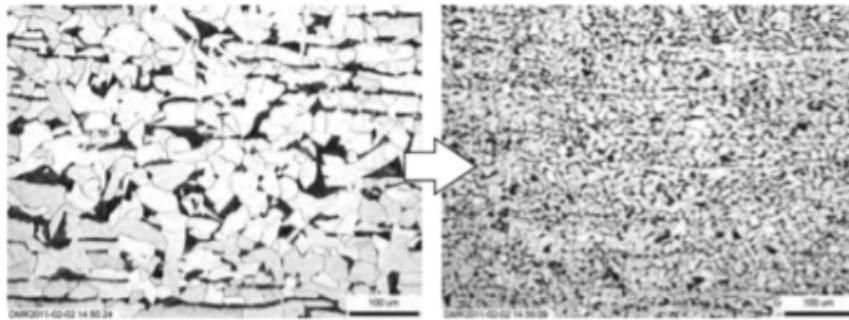
Figure 2.12 – Microstructure of the GRHAZ of a high heat input weld on C-Mn steel (right). Parent material microstructure (left). The Welding Institute [12].

2.2.8 Inter-critical Heat Affected Zone

The next area along from the GRHAZ is the inter-critical HAZ (see Figure 2.13). This area reaches temperatures between A1 and A3 on the iron – carbon phase diagram (~710-910°C – see Appendix 1&2). Partial austenitisation will occur in this area. Fast cooling rates in welds can lead to low toughness in this area, due to the formation of martensite in the austenite regions newly formed as a result of welding.
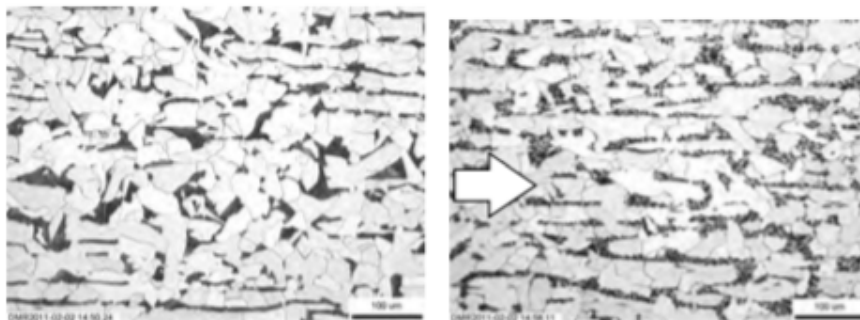
Figure 2.13 – Microstructure of the Inter-critical HAZ of a high heat input weld on C-Mn steel (right). Parent material microstructure (left). Adapted from The Welding Institute [12].

2.2.9 Sub-critical Heat Affected Zone

Reaching approximate peak temperatures of 580-720°C, there is no real notable change in the microstructure in the sub-critical HAZ when welding C-Mn steels. There is some slight spheroidization noticeable (see Figure 2.14). Temperatures remain below A_1 (see Appendix 1) which means there is no phase transformation. So, much like a tempering heat treatment, this area is often relieved of internal residual stresses due to slight softening occurring. If temperatures do not reach above ~580°C, then there is no effect on the parent plate in this area.
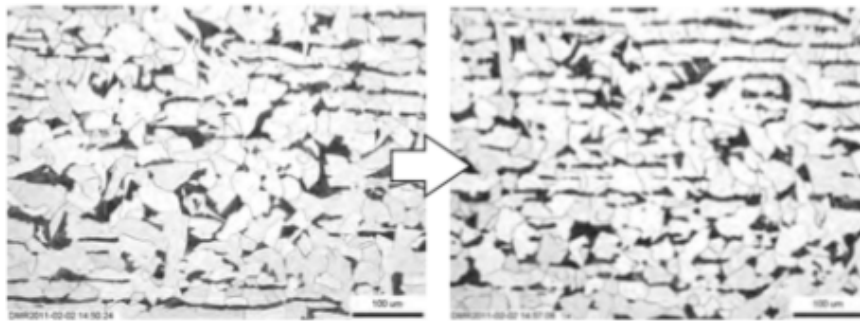
Figure 2.14 – Microstructure of the sub-critical HAZ of a high heat input weld on C-Mn steel (right). Parent material microstructure (left). The Welding Institute [12].

2.3 Metal Inert/Active Gas Welding Process

As discussed by Davies, the MIG/MAG welding process is now internationally recognised as the most cost-effective welding process for heavy engineering projects, where SAW is not feasible [14]. This is due to its adaptability to joint designs and welding position.

To create a fusion weld, an arc is struck between a wire electrode and a workpiece, with both melting to form a weld pool. The arc acts as the heat source, while the wire electrode is fed from a feeding unit through a welding torch and copper contact tip. As the wire passes through the contact tip, it picks up the present current, creating and maintaining an arc. This arc will continue until the torch trigger is pressed, stopping the flow of current (see Figures 2.15 & 2.16).
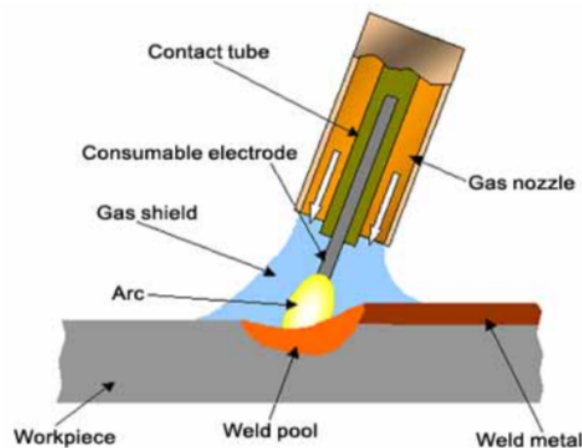
Figure 2.15 – Schematic showing the setup around a MIG/MAG welding arc. Adapted from The Welding Institute [15].
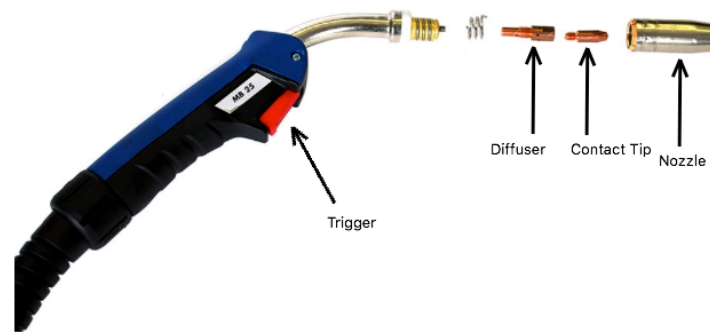
Figure 2.16 – Schematic showing MIG/MAG welding torch setup. Binzel-Abicor UK [16].

As the weld pool is molten, it must be protected from the atmosphere. For this, a gas shield is used (see Figure 2.15). The most common shielding gases used are Argon and CO_2, with a mixture of both being the most commonly used gas in Europe (Ar-80%/CO_2-20%).

MIG/MAG is suitable for welding most metallic materials, from heavy steel at 150mm and thicker, to 1mm thick sheet metal. The ability to select the mode of metal transfer, allows this wide range of material thicknesses to be welded. Adjusting the welding parameters to the low end of the range, will mean that the system uses the short circuit transfer mode. Here, the wire makes contact with the weld pool and transfers a droplet of filler metal. This method of metal transfer provides the control required from thin base materials and the root pass, when open gap welding is required. When welding thicker base materials, the equipment can be taken to the high end of the parameter range, creating a metal transfer mode known as spray transfer. This mode fires small droplets of metal from the wire electrode to the weld pool, depositing more filler and providing greater penetration.

As MIG/MAG is a semi-automatic process, where welder controls the travel speed and the wire electrode positioning. The current and voltage, although pre-set by the welder, are controlled by the power source. Arc length is also fully

controlled by the power source. If the welder's CTWD changes during welding, the power source adjusts the amperage, in order to maintain a constant voltage and arc length.

DCEP is the most commonly used polarity for the MIG/MAG welding process. The positively charged heat flow in the electrode improves wire burn-off and helps to maintain stability in the arc. Some basic flux-cored wires are more suited to DCEN, but these are less common, restricted to non-positional welding and generally for specialised applications. If a rutile flux-cored wire is incorrectly setup to run on DCEN, it can cause defective welds. A standard MIG/MAG welding set operating on DCEN, will produce weld beads with less penetration than that of a set operating on DCEP (see Figure 2.17). Not taking due care to ensure the correct polarity can lead to LOF defects.
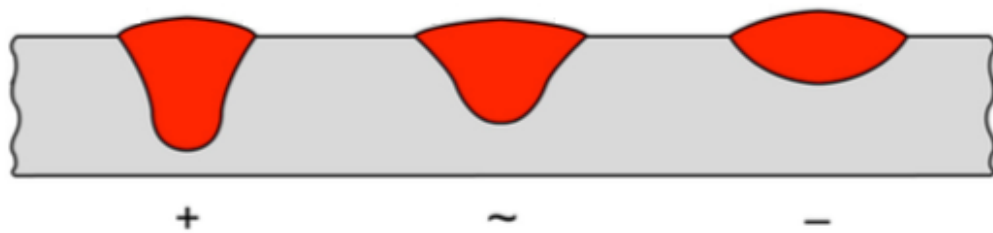
Figure 2.17 – The effect of polarity on welding penetration. The Welding Institute [17].

2.3.1 Arc Stability

Arc stability when using the MIG/MAG welding process, can be affected by a number of factors. The most liable include the welding equipment setup, welding polarity and welding consumable.

In recent years there have been many advancements in welding equipment, with synergic welding sets and controlled short circuit transfer systems such as Lincoln Electric's STT. This process provides good penetration while maintaining a low heat input, ideal for an open gap root pass or thin plate material. The standard welding plant for everyday use has also improved, with modern sets being more reliable with consistent wave forms and current flows. This move forward helps to create a stable welding arc.

Most solid and cored welding wires will operate on both DCEN and DCEP polarity, but due to the reduction in penetration (see Figure 2.17) DCEN is not often used. For this reason, welding consumable suppliers will commonly only approve wires to DCEP, unless the wire is specifically designed for DCEN (e.g. self-shielded). As suggested by Phillips, welding while operating on DCEN reduces the wire burn-off effect that is aided by a DCEP polarity; this cutback in filler wire burn-off has a negative effect on arc stability [18].

The welding consumable used will also have an effect on the stability of the welding arc. Seamless cored wires allow for copper coating, as there is no open seam. This coating provides good conductibility with the copper contact tip, and so has better arc stability than a non-copper coated folded type cored wire (see Appendix 21). A solid filler wire can be copper coated but does not have the advantage of the internal flux or metal powder used for cored wires. Such fluxes and powders can contain arc stabilising elements through the process of chemical refinement.

2.4 Automation/Mechanisation

To achieve as high a productivity as possible while producing good quality weld beads, mechanised welding systems are commonly used. Automation and mechanisation started to become a big part of heavy engineering when it started to evolve within the shipyards of Japan in 1975 [4]. The mechanised systems consist of a tractor unit and are often designed to run on a steel or aluminium track (see Figure 2.18). The track will usually be flexible, allowing the system to be run on curved structures such as ship hull sections and heavy bore pipes. These specially designed tracks allow excellent arc on times over long lengths. Millar suggested that shipyards using automation, greatly improves their competitive edge, producing welds faster than their competitors [19].

Although it may require two people to position and attached the track, the welder can solely operate the machine. After positioning the welding head and wire electrode in the desired area, the operator can set the travel speed on the control panel. The welding parameters are generally still controlled from the wire feeder unit. When the system is in operation, the welder may be required to adjust the travel speed on the control panel and the weld head positioning.

When using mechanised systems designed for fillet welding, it is essential that primer paint thicknesses are kept within the range recommended by the paint manufacturer. If paint thicknesses are too high, then travel speeds must be greatly reduced to prevent weld metal porosity. This in turn will not provide the same high levels of productivity that should be achieved from the use of automated systems.

Figure 2.18 – KAT300 Mechanised welding system. Adapted from the Gullco International product catalogue [20].

2.5 Different Types of Filler Materials

2.5.1 Solid Wire

When MIG/MAG welding was first developed, solid wire was the consumable of choice. When welding in the flat position (PA/PB), a higher parameter range can be used and so the mode of metal transfer is a spray condition. A solid wire will produce a large amount of spatter in spray transfer, but a continuous feed of filler wire means productivity levels can be much higher than that of MMA. However, when welding out of the flat position, short circuit transfer must be used, this can lead to LOF defects in heavier sections.

Solid wires are still widely used in the structural steel industry, this is due to their low cost and fitness for purpose. However, they do have their disadvantages, such as spatter, LOF risk and a welding arc that has a tendency to be unstable.

Solid wire is manufactured by drawing round sections of steel down to the desired diameter, annealing the wire if needed, and spooling on to either plastic or steel reels.

2.5.2 Flux Cored Wire

In the mid-1980s, flux-cored welding filler wire was developed, and this was a huge steppingstone in the use of MIG/MAG in the heavy fabrication industry. The introduction of cored wires allowed a wider range of materials to be welded, due to the metallurgical benefits of the flux addition. In comparison to a solid wire, cored wires will achieve greater burn-off and deposition. This is down to the reduction in cross sectional area, and in turn increase in current density through the wire sheath around the core.

Flux-cored wires will almost always be used in spray transfer, and so the likelihood of LOF defects is dramatically reduced. As the weld metal solidifies, there is a slag formation on the surface of the weld, which helps to support the molten metal. This slag allows for fully positional welding, unless specifically designed otherwise.

2.5.3 Folded Type vs. Seamless Flux Cored Wires

There are currently two main types of flux-cored wires being used in industry; folded type and seamless. The main difference in the wires is the manufacturing process [21]. A folded wire begins as a steel strip which is formed into a U-shape. Flux is laid into the formed steel, before the steel is then rolled with both edges brought together and folded, creating a tubular section. The welding wire can then be drawn down to the desired diameter, typically 1.0-1.6mm (see Figure 2.19).

As explained by Millar, seamless flux-cored wires provide all the benefits of a flux-cored wire, but with the additional reassurance that the wire will not pick up any moisture [19]. Typically, H_2 levels will remain under 5ml/per 100g of weld metal, which is a commonly used maximum tolerance for H_2 levels of a welding consumable. The open seam of a folded type wire means the H_2 content will begin to increase when the wire reel is removed from its sealed packaging and open to the environment. The low hydrogen assurance of a seamless cored wire makes them

increasingly more popular with the heavy fabrication industry; this is down to the minimisation of the risk of HICC.

In most instances, seamless wires are manufactured by forming a steel strip into a hollow tube. The seam is welded using ERW or a laser welding technique and the flux is poured in to fill the tube. As the flux is poured, the now seamless tube is vibrated to pack the flux tightly and help in the avoidance of flux voids. The wire is then drawn down for the first time before dehydrogenation and annealing takes place. Hydrogen levels are typically reduced to below 3ml/per 100g of weld metal, with some manufacturers reaching below 1ml per/100g of weld metal (see Figure 2.22). The product can then be copper coated to prevent surface rust formation, before the wire is drawn down to the desired diameter and spooled (see Figure 2.20).

Another method of manufacturing seamless cored wire involves laying the flux while the steel strip is in the U-shape, similar to the process for manufacturing a folded type wire. After the flux is uniformly laid, the strip is fully formed with the flux inside. The seam is then welded before annealing, dehydrogenation, drawing down to diameter and spooling (see Figure 2.21). This technique removes any chance of flux voids, which can be an issue with the vibration fill technique. If there is a small void in the flux fill, it will be stretched to become a far larger void during the drawing process.
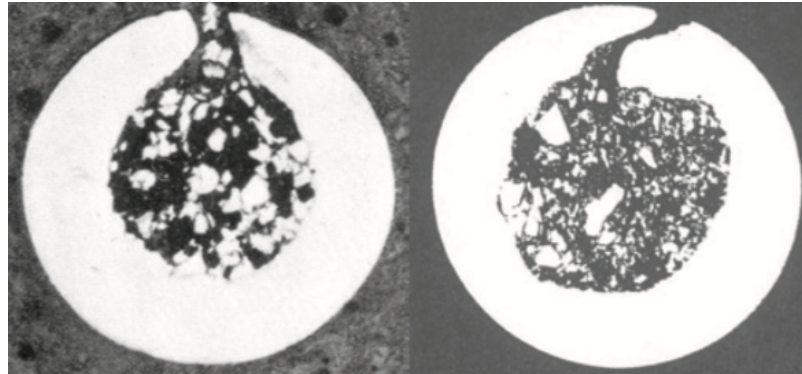
Figure 2.19 – A cross-section of two variations of folded type 1.2mm diameter flux-cored wires. These images were used in a technical promotional brochure by Nittetsu [22].
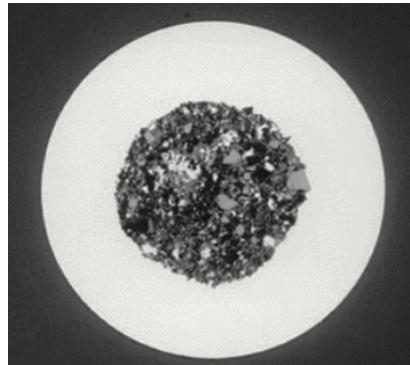
Figure 2.20 – A cross-section of a 1.2mm diameter seamless flux-cored wire from NSSW in Japan. This image was also used in a technical promotional brochure by Nittetsu [22].
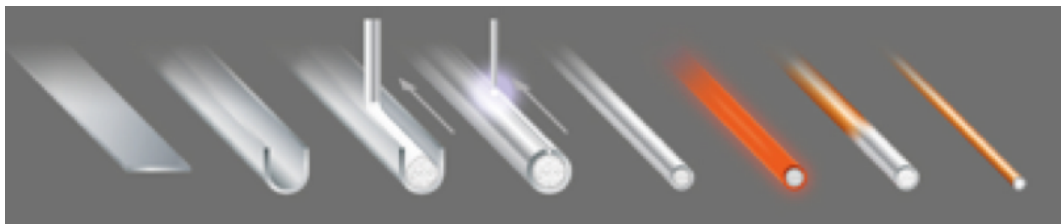
Figure 2.21 – A schematic showing each stage of the manufacturing process for a seamless flux-cored wire. Note with this method, the flux is laid in before welding to ensure continuous flux fill with no risk of voids. Image used with permission from NST Welding (UK) Ltd [23].

4. Hydrogen Content of Deposited Metal (Acc. to ISO 3690)		
HDM (ml/100g)	Ave.	Spec.
0.4, 0.5, 0.4	0.4	5 Max.

Figure 2.22 – Hydrogen levels of a seamless flux-cored wire from NSSW in Japan. This data was included in the CMTR received on purchase of the wires from NSSW (see Appendix 5).

2.5.4 Metal Cored Wire

Metal-cored wires are manufactured using the same techniques as are used for flux-cored wires; the difference being that inside the steel outer sheath is a granulated metal powder. As with the flux-cored wires the reduction in cross-sectional area provides more current density, so greater burn-off and deposition. Myers [24] suggests that the addition of the metal powder will further increase the achievable deposition rates. While operating in spray transfer mode, metal-cored wires are limited to welding in the flat position. However, they are also widely used in short circuit transfer mode for positional welding on thin base materials (~<7mm) and open gap rooting.

2.6 BS EN ISO 15614-1

British standard 15614-1 – Specification and qualification of welding procedures for metallic materials – Welding procedure test – Part 1: Arc and gas welding of steels and arc welding of nickel and nickel alloys [2] is a European harmonised standard regularly referred to by welding engineers. The contents provide information on terminology, procedure test piece dimensions/shape, details of testing requirements, range of qualification and a basic WPQR template. Along with other quality standards, this provides manufacturers with guidance and a set of rules, which if adhered to will aid in minimising defects and failures.

A WPQR is designed to provide the client with evidence that the manufacturer can produce repeatable sound welds, that meet metallurgical requirements. When

qualifying a T-joint, a test piece is setup (see Figure 2.23). Next, the joint is welded with a chosen filler metal, using predetermined welding parameters. A surface defect detection method (magnetic particle or dye penetrant inspection) is used to ensure there are no surface cracks or surface breaking porosity. If the joint is free of surface defects, both the end and start of the test piece are cut and discarded. A total of 2 macro sections are then cut from the sample (see Figure 2.24). This provides the inspector with a visual sample of the penetration achieved at the root of the weld. In order to qualify a fillet weld to BS EN ISO 15614-1, a hardness test must be performed. If all requirements are met, the WPQR is signed off by the welding engineering manager and the third-party insurer. The welding procedure pack can then be submitted to the client for review. If the WPQR is approved by the client, a WPS is created and welding activities can commence on the project.

Key
1   Joint preparation and fit-up as detailed in the preliminary Welding Procedure Specification (pWPS)
a   Minimum value 150 mm
b   Minimum value 350 mm
t   Material thickness
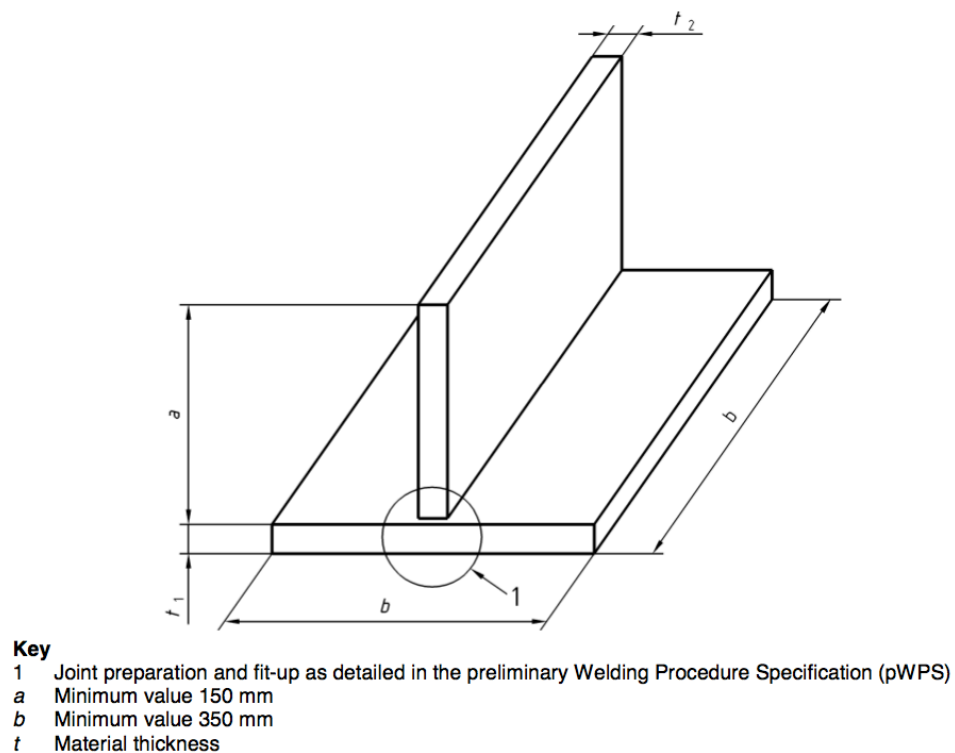
Figure 2.23 – Setup of T-Joint test piece
- as per BS EN ISO – 15614-1 [2].
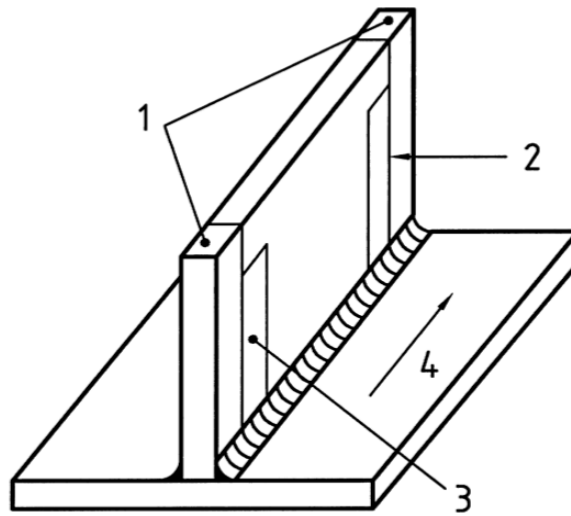
Key

1   Discard 25 mm

2   Macro test specimen

3   Macro and hardness test specimen

4   Welding direction

Figure 2.24 – Location of test specimens in a
T-joint - as per BS EN ISO – 15614-1 [2].

2.7 <u>Weld Metal Porosity</u>

2.7.1 <u>Causes of Weld Metal Porosity</u>

All welding processes use some form of shield to atmospheric gases, such as oxygen, nitrogen and hydrogen. Such gases can be detrimental to the soundness of a weld. A common weld defect or imperfection, known as weld metal porosity, occurs with the presence of nitrogen and oxygen. These are drawn into the weld metal due to deficient shielding.

The entrapment of as little as 1% air, can cause small pockets of porosity. Entrapment of 1.5% air can result in the formation of large areas of surface breaking pores. According to Widgery, H_2 gas is the most common cause of porosity in steel weld metal and so detrimental to the welding process [21]. It can be picked up from a number of sources, moisture from welding consumables such as fluxes and weld area surfaces not correctly dried or prepared. Contaminants such as oil, grease and paint are also common causes.

Welding over surface finishes, such as primer paints or zinc coatings will create a great deal of fume. These fumes/gases can become trapped during the process of welding, occurring more easily with T-joints than with butt joints. The likelihood of porosity occurrence increases again when welding a T-joint from both sides. This is a result of there being no outlet for the gas to escape. In heavy fabrication, specifically shipbuilding, weldable primers are widely used to prevent rust formation on pre and post fabricated steel. Weldable primer paints are low in zinc and specifically designed to allow welding, with no detrimental effect to the soundness of the weld. To achieve the desired results, primer paint thicknesses must be carefully monitored, ensuring they are within the range predefined in the manufacturers recommendations (see Appendix 10). The recommended range is typically 13-20μm.

2.7.2 <u>Prevention of Weld Metal Porosity</u>

As explained by Kobelco, most methods for preventing porosity during welding are simple [25]. The first preventative measure should be, to protect the weld pool from the gases in the atmosphere by providing it with a sufficient gas shield. When using TIG or MIG/MAG welding, the gas pressure should be set at the manifold and then tested at the nozzle/shroud. When using TIG, the flow at the torch should be approximately 14L/min and with MIG/MAG should be 15-20L/min. However, it may be possible to reduce the gas flow rate with the right conditions. It is important that gas hoses are checked for leaks regularly and repaired if required. Work areas open to drafts, such as ship construction linkups or fabrication sheds with large open doors, can be detrimental to gas shielded welding processes. Doors must be kept shut during operations, and field welding should be tented in, using scaffolding and shrink-wrap where necessary. Some welding consumables offer a higher resistance to reduced gas shielding, this is due to higher levels of deoxidants.

The control of hydrogen levels will not only reduce the risk of HICC defects but will also reduce the risk of weld metal porosity. The correct storage of MMA electrodes and folded type flux-core wires will greatly reduce hydrogen introduced into the weld from the consumables. An increasingly more common method is the use of vacuum-packed electrodes and seamless cored wires.

The weld area should be cleaned and degreased, if it has been in contact with substances that would act as hydrogen additions (oil, water ingress, paint). Surface coatings must be controlled to minimise the risk of porosity. Weld areas should be dressed to remove the coating, or if weldable primers are used, the thickness must be within the range recommended by the manufacturer. Paint thickness checks can be carried out during QC checks, using an Elcometer.

2.7.3 <u>Different Appearances of Porosity</u>

Weld metal porosity can be present in many different forms, a form known as worming, produces long elongated surface breaking porosity. On a radiograph, worming can resemble the bone structure of a herring, so is often referred to as herring bone porosity (see Figure 2.25). This form of porosity is associated with gases from contaminants becoming trapped in the weld area. Due to the geometry of the joint design, a T-joint is the most susceptible to this form of porosity. During application of weldable primers, paint can collect at the edges of stiffening bars and so should be ground off in a production environment. Weldable primer paints can be left on other sections of the panel and stiffening bar within the weld area, if thickness levels are maintained within the manufacturer's recommendations. Worming porosity can be prevented by ensuring the weld area is clean of contaminants and weldable primers are kept within a suitable thickness range. Techniques such as stitch welding, can be adopted where possible to prevent gases becoming trapped.
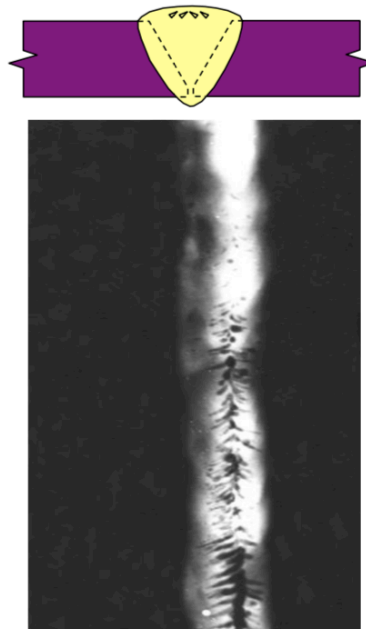
Figure 2.25 – Herring bone porosity as shown on a radiograph. Adapted from The Welding Institute [26].

Cluster porosity is the formation of many small gas pockets in an area of the weld (see Figure 2.26). This is most often due to loss of shielding gas, as a result of incorrect torch angle, or a drop-in shielding gas pressure. Poor access to the joint, can prevent the welder from maintaining the correct CTWD.
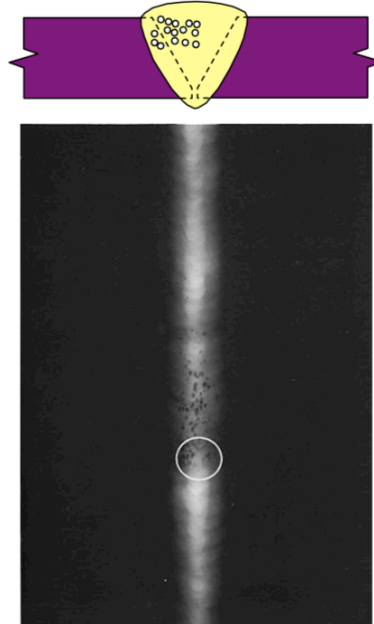
Figure 2.26 – Cluster porosity as shown on a radiograph.
Adapted from The Welding Institute [26].

Another form of porosity is a stop/start crater pore. A crater pore is not caused by trapped gases or loss of shielding, but by rapid weld metal shrinkage during solidification of the weld pool. Due to varying modes of metal transfer used for different welding processes, the risk of crater pores occurring is very dependent on the process. With the MMA process, the risk is very low and with the slope-down functions available on modern TIG welding sets, prevention is easy. When using MIG/MAG welding, the chance of a crater pore occurring is much greater. Most modern MIG/MAG sets will include a crater-fill function, preventing the formation of a pore by providing a pulse of current and filler as the welder stops. However, this function will not prevent the formation of a crater pore during the root pass when using ceramic backing tiles for single sided welding. Due to rapid cooling, a large

crater pore will always form when the welder stops during the root pass on to a ceramic backing (see Figure 2.27). Small cracks can propagate from these pores and they cannot be filled with any confidence, so must be removed by grinding, before welding recommences. If the joint allows, run-off tabs can also be used to leave the crater pore outside of the welded joint.
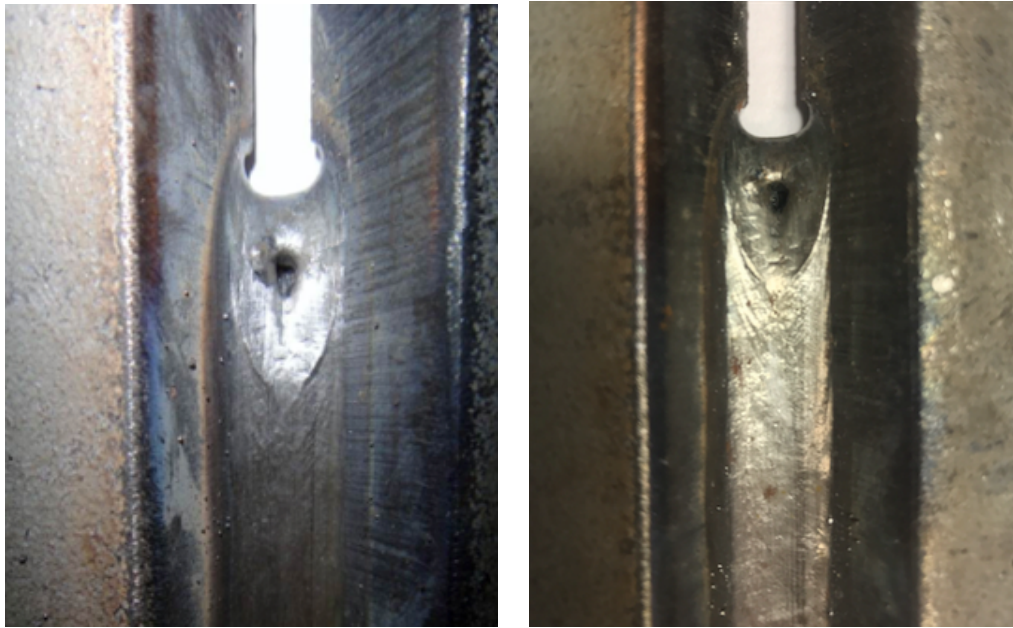
Figure 2.27 – Two examples of a stop/start crater pore in the root pass of a joint welded using FCAW and a ceramic backing tile. Both root passes were welded in the PA/1G position. These samples were used by NST Welding (UK) Limited as a training tool during a course on single sided welding using ceramic backings. Reproduced with permission from NST Welding (UK).

2.7.4 <u>Detection and Remedial Action</u>

During inspection of welded joints, weld metal porosity can be detected by a visual inspection, dye penetrant or MPI, if the porosity is surface breaking. When examining for internal porosity, UT or RT must be used. RT is the most effective for detecting porosity, but it can be difficult to detect small pores in thick sections.

If porosity is detected and recognised to be out with the acceptance criteria defined in the fabrication standard, then it must be removed. Small areas of porosity can be removed using grinding or gouging, but if the porosity is throughout the weld, then the weld must be removed. In these cases, porosity is often also present in the parent metal, due to penetration and dilution when welding. This must also be removed before re-welding.

2.8 Non-Destructive Testing of Fillet Welds

2.8.1 Visual Inspection

Moore and Booth argue that visual inspection is the first stage of NDT [27]. It is also, potentially the most important inspection method. This is due to its simplicity, low cost and the fact it is the first line of defect detection. If there are visible flaws that are out with the specification, these should be repaired before any further inspection methods are used. After a welder has produced a weld bead, the welder should then visually self-verify the weld, ensuring there are no visible defects. Notably, undercut or surface breaking porosity. The welder can then use a specifically designed weld gauge, ensuring the weld bead has the desired leg length and throat thickness to meet the specification. When welding operations are complete, a qualified QC inspector will also check for any visible defects and ensure fillet sizes are within the allowable tolerance. A high percentage of fillet welds on fabricated structures will be visually inspected only.

2.8.2 Magnetic Particle Inspection

Magnetic Particle Inspection is described by The James F. Lincoln Arc Welding Foundation, as a method of locating and defining discontinuities in magnetic materials [28]. It is an inexpensive, simple NDT method of testing for surface and slightly sub-surface defects in welds. The process involves the magnetisation of the area around the weld, and for this reason the material must be ferro-magnetic. The magnetic field is introduced using an electrically powered yoke or prods and cables (see Figure 2.28). The operator applies a white contrast paint and then magnetises the area around the weld. A ferro-magnetic ink is then sprayed over the test area. If there is a defect in the base material or the weld, such as a crack, a leakage field is created, attracting the particles from the ink. The defect can then be easily identified as a dark indication against the contrast of the white paint. Florescent particle sprays are also

available, these use ultraviolet light to display the collection of particles around the defect, removing the requirement for contrast paint. This method of NDT is popular with manufacturers, due to its low cost and ability to provide instant results.

2.8.3 Radiographic Testing

The first X-Rays were discovered in 1895 by WC Roentgen, while he was passing an electric current across a tube containing an anode and a cathode. The current caused an emission of radiation in the tube and created an image on a photographic plate nearby. It was the 1920's before further experiments on different materials and material thicknesses led X-Rays to become a tool for NDT. The large-scale navy shipbuilding program, during the second world war saw a huge increase in the use of X-Rays for NDT. RT is still widely used in the heavy engineering industry to this day.

The principles of RT have not changed much over the years. Varying degrees of radiation can be transmitted through the test object, the variation dependent on the density of the material (see Figure 2.29). Halmshaw describes how thinner areas of the material and areas of less density are visibly darker, this usually indicates a cavity or defect in a welded joint [29]. If there is internal porosity in the weld, this will show on the radiograph as darker spots. Visibly lighter areas are thicker areas with greater density (see Figure 2.30).

The James F. Lincoln Arc Welding Foundation argues that radiographic inspection is one of the most widely used NDT techniques [28]. Providing manufacturers with a trusted method of locating the presence and nature of macroscopic defects and other discontinuities in the interior of a weld. Radiographic testing holds many advantages over NDT methods such as UT and MPI. A permanent record is created with project and location identification, this can then be reviewed at any time, if the radiograph is stored correctly. There is also very little surface preparation and operator skill involved. RT provides a test method for aluminium, exotic metals, composites and can be used on thin material. Radiographic

testing is an NDT method used by specialised NDT companies or a specialist team within large engineering firms. This is due to equipment costs and the many precautions that must be taken, to ensure safe practices when working with harmful radiation. There are other disadvantages to this process, in that results are not instantaneous, and the engineer must have access to both sides of the weld. Interpretation of planar defects (LOF & cracks) are not always easy to identify and the defect depth can be difficult to determine.
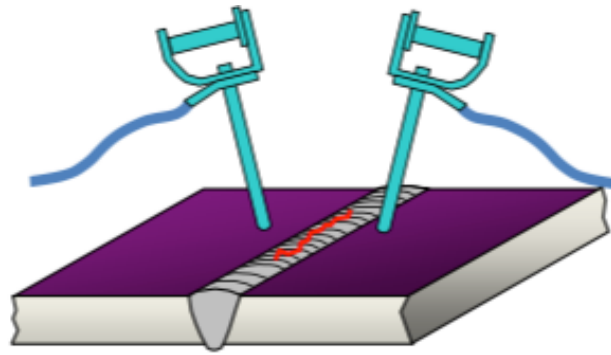
Figure 2.28 – Electro-magnet (DC or AC). Also known as a Yoke. Adapted from The Welding Institute Ltd [26].
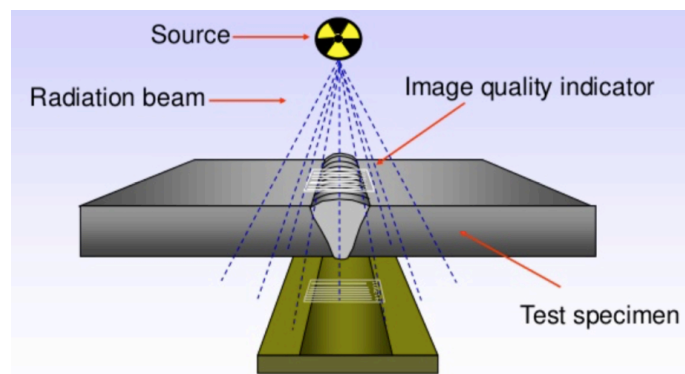
Figure 2.29 – Typical setup of the X-ray process for a butt weld on plate. Adapted from The Welding Institute Ltd [26].
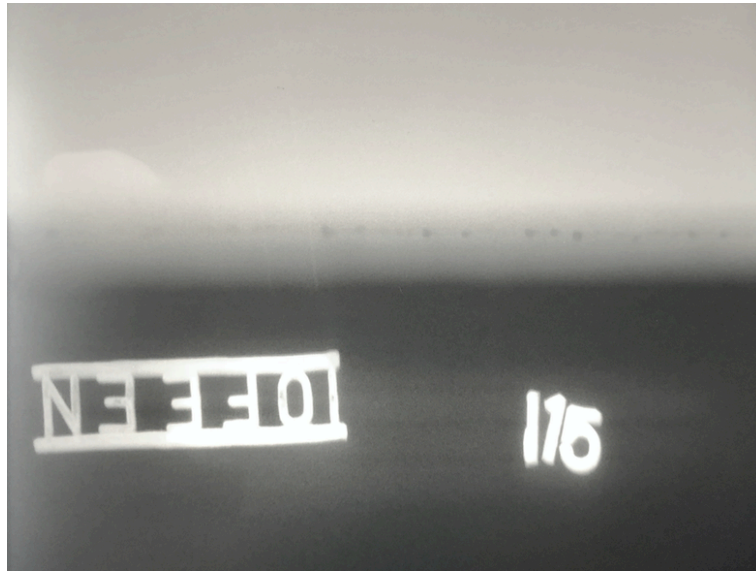
Figure 2.30 – Radiograph of a T-joint welded during the experimental schedule of this work. There are clear indications of internal porosity at the root of the weld. The radiograph was produced by a trained QC inspector at BAE Systems, Glasgow in support of this work.

2.9 Destructive Testing of Fillet Welds

2.9.1 Macro Etching

A macro examination, as described by the British Standards Institution, is used as a method of checking the quality of a welded joint [30]. This method allows a certified person to analyse the weldment, from an angle that is not possible in a production environment. The weld is checked for porosity, lack of fusion, lack of penetration and poor weld profile. If the weld contains imperfections out with tolerances defined in the specification, then it is deemed a defective weld and a failure (see Figure 2.31). If the welded joint meets the requirements, then it is deemed as acceptable (see Figure 2.32). This test is commonly a requirement when qualifying a WPQR, as assurance that the consumable, the technique and the method used produce a sound weld.

Macro samples are prepared and examined at a registered test house by qualified technicians. Firstly, the welded joints are collected and sent to the test house where they are cut down to size and ground flat. The test surface is then polished using various grains of abrasive disc. When the surface is polished sufficiently, acid is used (typically 10-20% nitric acid), to highlight the weld metal, its grain structure, the HAZ and the parent material. This allows the technician to check the sample meets the acceptance criteria.

2.9.2 Vickers Hardness Test

The hardness of a material is determined by its resistance to an indenter. According to the American Society for Metals, the Vickers hardness test was introduced in England in 1925 by R. Smith and G. Sandland [31]. The indenter must be made of a material that is much harder than what is being tested. In the case of the Vickers Hardness test, a pyramid shaped diamond indenter is used. A pre-determined weight of 5 or 10kgs, is applied at right angles to the sample for a

given period of time before releasing the pressure. This process leaves an indentation. The hardness is then calculated by measuring the depth or cross-sectional area of the impression using a function in the eyepiece. If hardness testing is being carried out as part of the qualification of a WPQR, then the relevant standard must be referred to. The hardness values are then checked, ensuring they are below the maximum allowance. The allowance is commonly dependant on material and client specification (e.g. 350HV).

Specimen 2
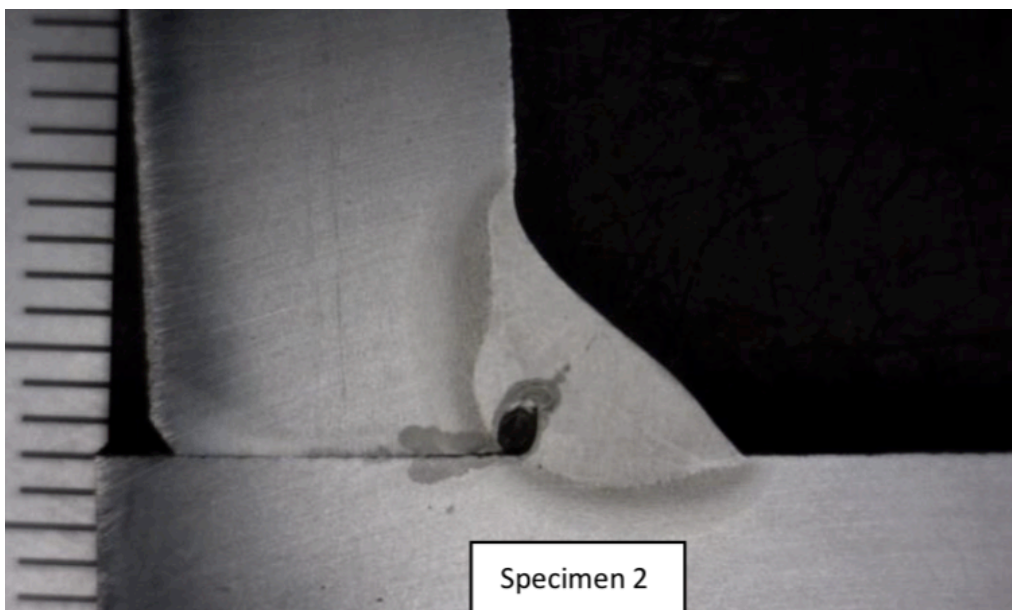
Figure 2.31 – Example of a macro section of a rejected single pass fillet weld in the flat (PB/2F) position. This fillet weld was part of WPQT to qualify a flux cored wire. The reason for the failure was thought to be the thickness of the primer paint as a result of incorrect application method. Reproduced with permission from Seaspan ULC.
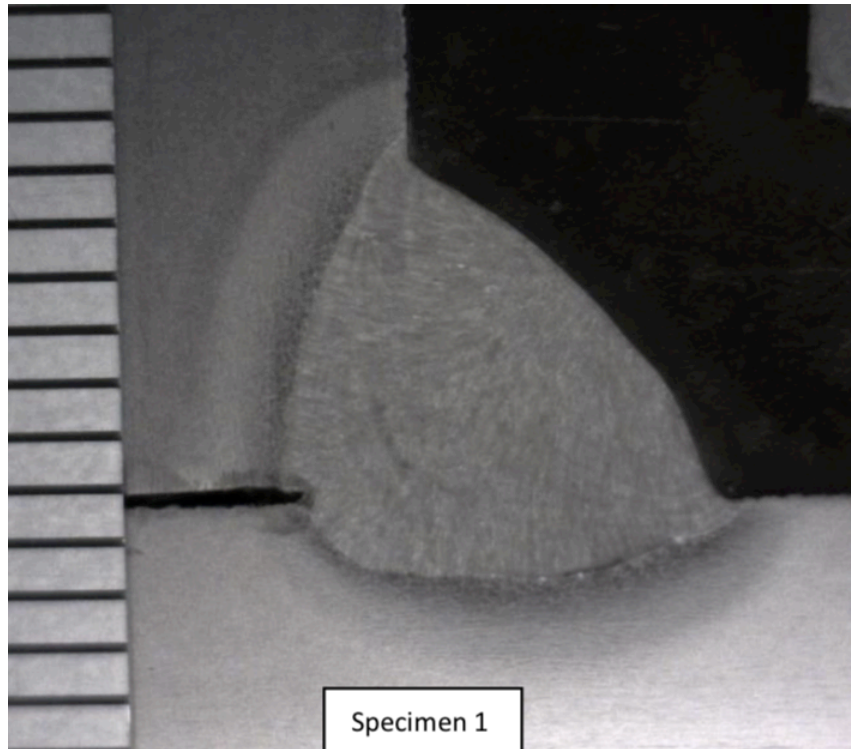
Figure 2.32 – An example of a macro section of an acceptable single pass fillet weld in the vertical (PF/3F) position. As with Figure 2.31, this weld was also part of a WPQT to qualify a flux cored wire. Although the primer paint was of the same thickness as the failed flat fillet weld, the heat input was greater, and the travel speed was slower. This meant the paint did not cause porosity in the weld. It is also likely the small gap in fit-up provided space for gases to escape. Reproduced with permission from Seaspan ULC.

2.10 <u>Shop Primer</u>

Shop primers, also known as weldable primers, were patented by Feldt, Montle and Skiles [32] and are commonly used in the steel fabrication industry [33]. They create a corrosion-resistant barrier while the material is in transport and during the fabrication process. The paint coating offers protection to a limit of three or six months, depending on the choice of primer. The application of shop primers must be controlled, monitored and measured to ensure the correct DFT is achieved. Methods described by Khanna and Kumar [34] help to achieve thicknesses within the narrow window, providing sufficient corrosion protection without having an adverse effect on weld quality. A DFT out with this window, will result in reduced barrier properties, as explained by Mallik [35]. If the DFT is too thick, weld metal porosity will likely occur. A questionnaire (see Appendix 22), carried out during research by Boekholt, shows that almost all of the shipyards visited had experienced issues with weld metal porosity [4]. A common factor of the weld porosity problems being, the combination of weldable shop primers and automated welding systems.

Porosity occurs during welding, when organic materials are broken down, forming hydrogen and carbon dioxide, which become trapped in gas pockets within the weld metal. As the weld metal solidifies, these pockets remain. Despite risk of weld porosity, if the appropriate controls are not in place, shop primers are widely used, due to the potential cost savings they can provide.

Common Types of Primers Used in Steel Construction

2.10.1 Etch Primers

Etch primers are single packed metal primers which contain low levels of phosphoric acid which etches the surface of the metal, providing improved adhesion. The coating also contains zinc phosphate and low volumes of solids which allows film thicknesses to be kept low (10-20μm). Etch primers are suitable for ferrous metals and non-ferrous metals such as aluminium. They can also be used on zinc coated surfaces. In most cases, it is not possible to weld through etch primers. However, there are etch primers available which provide a weld-through function.

2.10.2 Zinc Epoxy Primers

As explained by Kanitkar, zinc epoxy primer paints are designed to be part of an anti-corrosive paint system for use in maintenance, marine applications and automotive coatings [36]. They are also commonly used as shop primers for structural steel, before fabrication. These zinc rich primers produce a coating containing a solids volume ranging from approximately 50% to 85%. The minimum DFT for this kind of pre-fabrication primer is generally around 50μm, which makes it unsuitable for welding directly over.

2.10.3 <u>Zinc Silicate Primers</u>

Zinc silicate primer consists of zinc dust, an organic/inorganic vehicle and selected additives as required [37]. They are most commonly used as construction primers, this is due to the manufacturer having the option to create an organic or inorganic low zinc primer. This function improves weldability and minimises weld metal porosity. The lifespan and durability of the protection is affected by the advantage of not having to pre clean the weld area before welding. If using as a weld-through primer, the DFT must be maintained within a range of 10-18μm. This DFT range is provided in the paint data sheet (see Appendix 10).

2.11 BS-EN-ISO 17652-2

Workmanship standards are developed and adhered to, to provide customers with assurance that a degree of quality and safety standards are met. ISO 17652-2 is no different [38]. This standard provides details of two methods of testing the performance of weldable shop primers. This work focused on the weldability test method.

The weldability test creates a method for evaluating the performance of shop primers of a certain thickness and various welding processes. A T-joint, setup with a tight fit-up, is used to create conditions most susceptible to porosity. The fillet weld is then welded from both sides in the flat position (PB/2F). Welding is not simultaneous, but within 30 minutes of each other, producing a typical leg length of 6mm. Welding parameters (current, voltage and travel speed) are also provided in the standard. Next, the joint is broken open to allow evaluation of the weld root.

The sample material for this test is advised as 500mm x 80mm x 10mm and in good condition with ragged edges removed. The surface finish should be SA 2 ½ (as per ISO 8501-1), which defines a surface which has had very thorough blast cleaning [39]. The primer paint should be applied as per manufacturer's instructions and to the data sheet specified DFT. The test requires application to the horizontal plate and the vertical plate, but not the edge of the vertical plate (see Figure 2.33). Any paint on the edge of the vertical plate should be removed before the test, as paint can collect around this area during application. Small tack welds at the end of the plates are used to restrain the vertical plate in position, ensuring no fit-up gaps, with the standard requiring <0.05mm.

The weld evaluation is a visual examination of the inside of both welds against an acceptance criterion. Any visible pores that are 0.5mm or larger are measured and recorded. The number of pores, or the total pore area can be used to indicate the weldability of the consumable/welding process against the primer paint type and DFT.
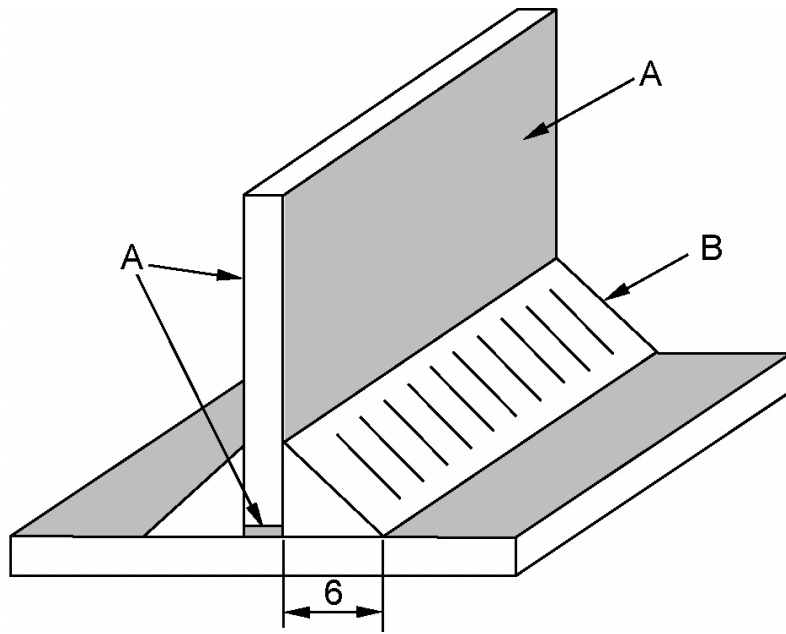
Figure 2.33 – Joint setup for weldability test as per ISO 17652-2 [38]

A – primed steel, B – Weld, leg length 6mm.

2.12 Optimisation of Robotic Fillet Welds

Work by Cairns *et al.* looked at optimisation of fillet welding by performing extensive experimental work, to better understand the impact of welding torch parameters [1]. Parameters such as torch angle, travel angle and shielding gas flow rate were analysed, to assess their effect on the geometry of the fillet weld. The experimental work, also involved assessment of how the significant parameters impact thermal load of a T-joint, resulting in distortion. With a significant amount of past work looking at obvious parameters (current, arc voltage and travel speed), Cairns *et al.* focused on less obvious parameters [3]. The interactions between all input parameters were analysed, looking at the impact on the geometry, metallurgy and thermal loading of the fillet welds. The data was developed and analysed using an ANN model.

This research was important for several reasons, with fillet welds representing a large percentage of the construction of a naval ship. Optimising fillet welding provides an opportunity to reduce build cost and keep weight to a minimum, improving in-service performance and running costs. At BAE Systems Naval Ships, fillet welding is primarily a manual/semi-automatic process. A short study found there to be significant variation in torch angle among welders. It also found that information from welding consumable suppliers can be contradictory and mostly generic for fillet and butt welds.

With the continued drive to reduce weight, there is increased use of thin plate material (<6mm). Working with such thicknesses, requires much care and attention, to keep distortion at a minimal. Improved control over fillet welding will help minimise over-welding, heat input and so reduce distortion. Quality assurance/control departments rely on adherence to the WPQR, visual inspection and welder training to provide an optimal fillet weld. This leaves the process open to variation.

3.0 <u>Experimental Technique</u>

3.1 <u>Base Material</u>

The base material that was selected for this research is a commonly used, shipbuilding, Lloyds Register approved low carbon steel known as DH36. The 'DH' of the designation, relating to the delivery condition of the steel and the temperature at which the impact testing is conducted (-20°C). The '36' relates to the minimum yield strength, which in this case was 355MPa (see Appendix 3).

This steel grade has been used for many years in the shipbuilding industry. DH36 was the primary steel used on recent well-known projects, such as the HMS Daring class destroyers and the Queen Elizabeth Carriers. These ships were constructed by BAE Systems and Babcock Marine in the United Kingdom. In support of this research, BAE Systems supplied 200 sample plates 200mm x 100mm x 6mm of DH-36 (see Appendix 4), to allow for experimental work. As is common production practice for BAE Systems, the plate samples were thermal cut to size from a single sheet of steel using an underwater plasma cutting technique. This method produces a clean, smooth cut with a narrow HAZ and little to no distortion.

3.2 <u>Welding Consumables</u>

The welding consumables for this project, were selected as Lloyds approved filler wires commonly used in the shipbuilding and heavy fabrication industries. The four filler wires selected were; NSSW SF-1A (a rutile seamless flux-cored wire), NSSW SM-3A (a seamless metal-cored wire), Lincoln SupraMIG (a solid wire) and Lincoln Outershield 71E-H (a rutile folded type flux-cored wire). All consumables are 1.2mm in diameter. See Appendix 5, 6, 7 and 8 for consumable information.

When a fabrication company is selecting a welding consumable for a project, they must first qualify a WPQR with an appropriate filler, suited to the base materials involved. Next, they must order the desired filler wire from the wire manufacturer or

a distributor with access to the product. On receiving delivery of the welding wire, they will also receive a BS EN 10204, Type 3.1 CMTR, or a batch test certificate as it is otherwise known. The CMTR provides the fabricator with a record of the wire manufacture date, the batch number and the welding parameters used for the all-weld-metal batch test. It also details test results (tensile and impact tests), the chemical composition and the hydrogen content of the deposited weld metal. The hydrogen test is only a requirement for cored wires, due to the hygroscopic properties of the flux/metal powdered core. The hydrogen test provides a value at the point of manufacture. This means that the H_2 content of a folded type flux-cored/metal-cored may increase when removed from its sealed packaging. The wire then must be stored correctly to avoid H_2 levels increasing to such that the H_2 content is out with the specification.

Storage of seamless wires is less stringent, as there is no risk of moisture pick up when the packaging is removed. Storage and handling documents are commonly available from the wire manufacturer on request (see Appendix 9).

3.3 Application of Primer Paint

To ensure the application of the primer paint was done correctly, resulting in a consistent and accurate film thickness, the expertise of International Paint (AkzoNobel Group) was used. Initially four film thickness ranges were requested, 0-10μm, 10-20μm, 20-30μm and 30-40μm. On request for these thickness ranges, a lab technician advised against the range of 30-40μm, as there was potential for the paint to crack due to poor drying. As a result of this advice, it was decided that the film thickness ranges would be, 0-10μm, 10-20μm and 20-30μm. The steel was securely packed and sent to AkzoNobel in Gateshead, Tyne and Wear. After only two weeks the plate samples were returned with the primer paint applied (see Appendix 11).

International Paint, a subsidiary of AkzoNobel, is a multinational company which creates paints and coatings. They supply them to the manufacturing industry and consumers worldwide. International Paint specialises in the marine industry,

providing paint and coatings to protect ships and yachts from the corrosive effect of sea water. Their products also aid ship builders in creating aesthetically pleasing, finished products. As the world leader in their field, they were selected to apply the paint for this project.

The primer paint selected for this work was Interplate 855, from International Paint (see Appendix 10). This weldable shop primer is widely used in the marine construction industry, protecting steel pre and during the fabrication process. International Paint describe this product as having good heat resistance and suitable when using welding processes with high travel speeds.

As it was not possible to have the paint applied to an exact micron, ranges of paint thickness were selected for this work. A range of measurements was supplied by International Paint on delivery of the coated steel samples. However, it was decided, that it would also be beneficial to gather thickness data for each sample joint. After some research, an Elcometer 415 Model T was chosen as the film thickness measuring device. This gauge has an accuracy of ±2.5μm.

When testing the coated sample plates, it became clear that the thickness ranges were out with the grouped ranges first noted for the experimental work. With this finding, the paint thickness ranges were altered to reflect the paint thickness of the coated steel. The amended primer paint thickness ranges were 0-7μm, 7.1-20μm, 20.1-45μm. The thickness range of 0-7μm was achieved by removing the coated surface of the steel, using an angle grinder and a flapping disc (see Figure 3.1).

The samples were separated in to the 3 thickness ranges and each sample was marked using a paint pen and a template (see Figure 3.2). The horizontal plate and the vertical plate were marked for each sample joint (e.g. 10V & 10H). As each sample was 200mm in length, 14mm from each edge and 8 points between were marked, each with an equal distance of 19mm separating them. This would provide ten readings from each of the sample plates. This was devised as the best method for obtaining an average primer paint thickness for the vertical and horizontal plate of each sample T-joint. As advised in the instruction manual, the Elcometer was

calibrated using the smooth method. This required calibrating the gauge using a foil of known thickness, and an un-coated substrate. This process ensured the thickness gauge was operating at its most accurate. An in-date manufacturers calibration certificate was also provided on purchase of the device (see Appendix 12).

A total of 264 steel plates were measured and marked, allowing 132 sample T-joints to be assembled for welding. All measurements were recorded on an Excel spreadsheet, set up at the workstation (see Figure 3.3).
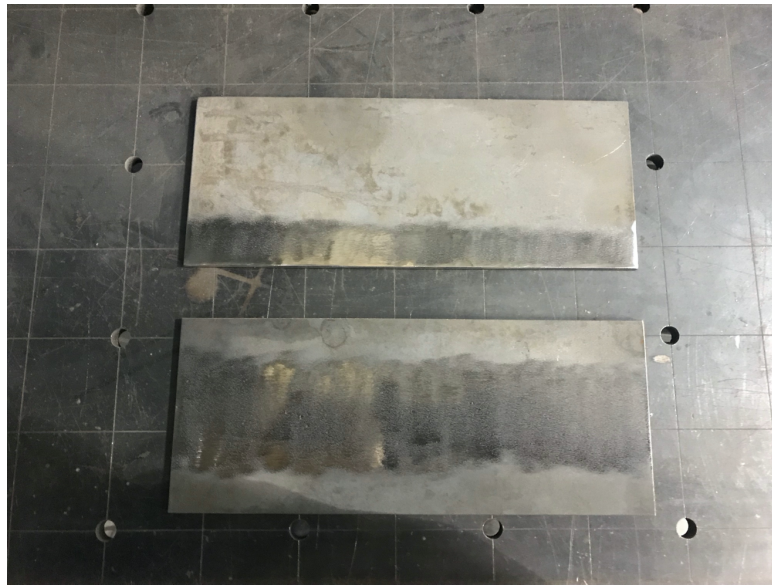
Figure 3.1 – Example of steel sample plate that has been dressed using a flapping disc to remove the surface coating. This process was used for paint thickness range of 0-7μm.
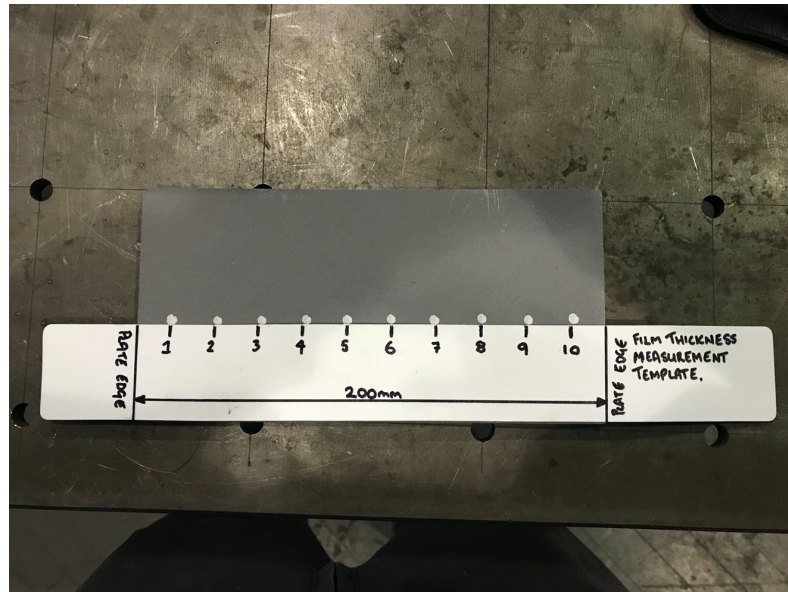
Figure 3.2 – Template used to mark a rough area for measurement of paint thickness on each horizontal and vertical plate of T-joint samples.

Figure 3.3 – Workstation for the measuring of primer paint thickness using Elcometer 415 Model T gauge.

3.4 <u>Welding of T-joint Samples</u>

To ensure each joint was setup correctly and as accurate as possible, magnets were used to temporarily hold the vertical plate in position. Next, tack welds were suitably placed (see Figure 3.4). A Miller Integra 151S welding set and a 0.8mm solid MIG wire, were used to apply small tacks at both edges, on the back side of each T-joint. These tacks were suitably positioned and kept small in size so not to have any effect on the side of the joint that was to be fully welded. All joints were checked using an engineer's square, to provide assurance that the fit-up was correct (see Figure 3.5).

Built by the University of Strathclyde, the welding rig used for this project, provided a suitable method of mechanised welding (see Figure 3.6). The rig was used alongside LabVIEW software. To measure welding parameters, such as amperage, voltage and travel speed, a TVC PAM's unit was used. The system was programmed to record once each second. For welding, a Miller XMT 304 Series and a Miller wire feeder unit were used (see Figure 3.7). Before commencing welding, the welding set was checked to confirm it had an in-date and valid calibration certificate (see Appendix 13). A shielding gas from BOC, with the trade name, Specshield, classified under ISO 14175 as M21 (80%Ar/20%CO_2) was used for all welding. The reason for selecting this gas, was that this was a commonly used shielding gas in the fabrication industry. It was also a suitable choice for each of the filler wires selected. A gas flow of 17 L/min was used, as advised by the consumable manufacturers. Gas flow rate was set at the manifold and tested at the torch nozzle, using a portable gas flow meter to ensure accuracy.

The selection of an appropriate arc voltage and amperage setting was not straight forward. Each consumable would have an optimum welding condition with different parameters. An amperage range of 220-250 amps across all consumables was used, with the aim of achieving an amperage setting of 235 amps. The arc voltage was then set around this, to such that a smooth stable arc with minimal spatter was obtained.

During welding, penetration is controlled by the amperage, which the welder can manually adjust with the wire feed speed on the feeder unit. MIG/MAG welding commonly uses a CV power source. This characteristic helps to maintain a stable arc, ensuring that there is no fluctuation in the arc voltage. Amperage is automatically adjusted if there is movement in the electric stick-out used by the welder. A reduction in electric stick-out when welding increases the amperage and so, in theory produces a weld with greater penetration. If the electric stick-out length is increased, amperage will be reduced and so less penetration will be achieved. For this reason, it was important that the electric stick-out was maintained at the same length for all welded samples, this was set at 20mm.

A total of 132 samples were welded, 4 samples were not suitable for testing, due to poor weld quality, caused by technical issues with the welding rig. Each sample was left as welded, with no dressing or removal of spatter.

During the experimental work, several of the joints were welded on DCEN polarity. This occurred as a result of other students using the rig, and the correct checks not being carried out, between days of welding trials. Welding on DCEN, was not originally in the scope of work for this project, as the welding consumables used are all designed to operate on DCEP. When DCEN is used, it produces a welding arc that is unstable, creating a large volume of spatter. Welding on DCEN also produces less penetration (see Figure 2.17). This was taken into account when measuring penetration and establishing a comparison between welding consumables.
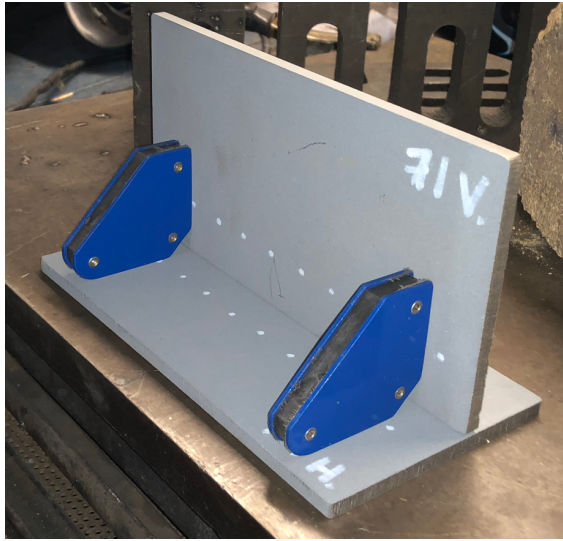
Figure 3.4 – Magnets used to aid in alignment of joint before tack welding.

Figure 3.5 – Engineers square used to check squareness after tack welding.
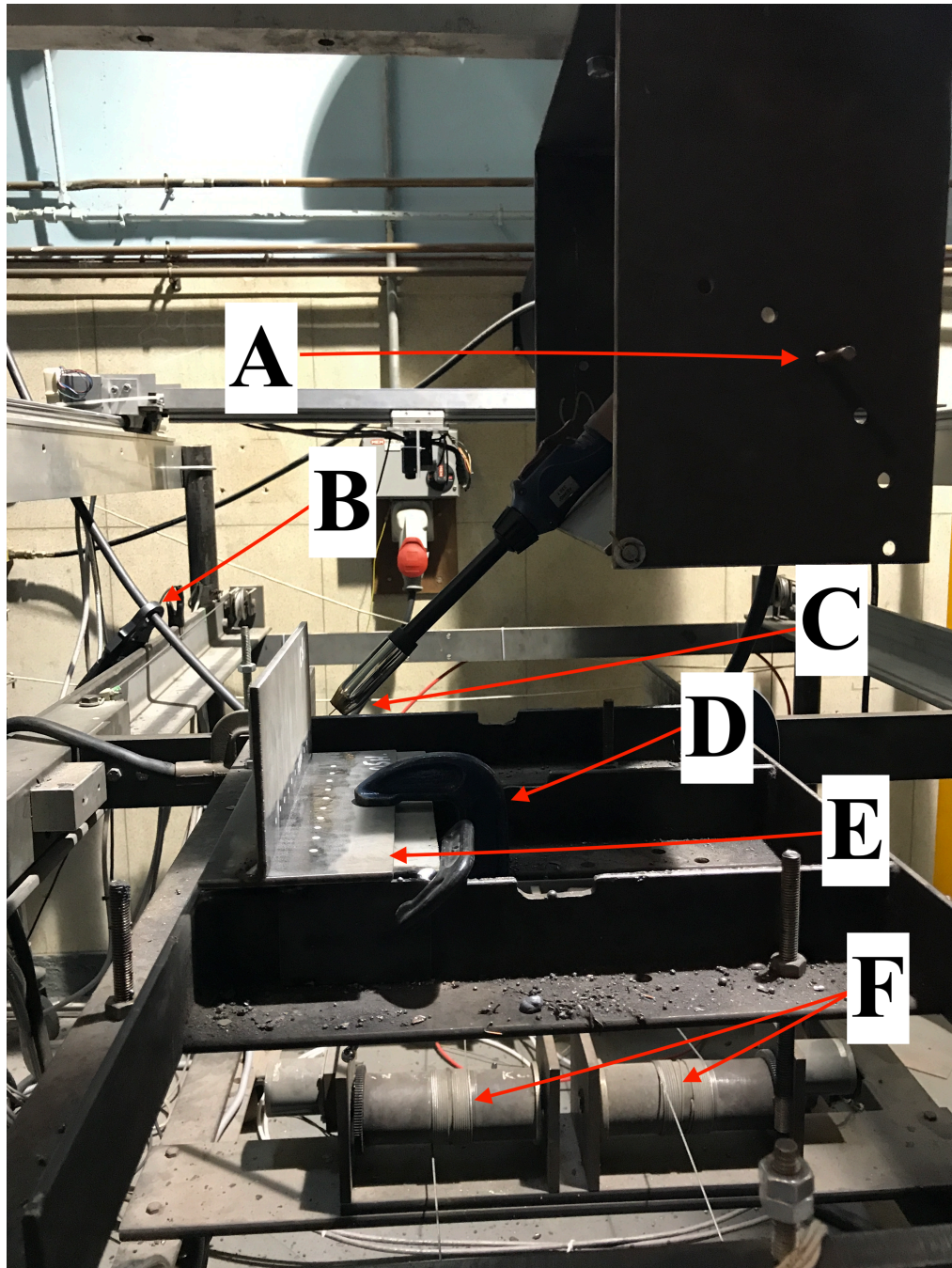
*Figure 3.6 – Welding rig setup, with sample secured in place prior to welding. **A** - Welding torch secured and positioned at 45 degrees using jig. **B** - Clamp used to measure welding current. **C** - MIG/MAG welding head. **D** – G-Clamp used to maintain position of sample joint. **E** – Sample T-joint. **F** – Motor system powered by steel cables and an electric motor.*

Figure 3.7 – Miller XMT 304 Series constant voltage welding power source.

3.5 Testing of Welded Samples

When all welded samples were complete, various testing methods were identified as ways of producing data that could be collated and used to highlight trends. RT was selected as the best method of detecting internal porosity. HV testing, was selected to provide data on a metallurgical level, and etched macro sections allowed analysis of the internal geometry of each welded sample.

3.5.1 Macro Sections

Etched macro sections were taken from 80 welded samples, allowing analysis of the weld geometry, weld area, penetration and the HAZ. The 80 samples, consisted of 5 macros from each setup (paint thickness and filler type).

Each sample was prepared using the same method, with the tools available at the University of Strathclyde. The welded joints were cut in the center using a band saw. Next, a Struers Discotom was used to cut each sample down to a manageable size. A bridge port mill was then used to mill the face of the samples flat, before creating a smooth surface finish with a surface grinder. The face surface finish of each sample was then suitable for etching.

As advised by the university metallography technician, an acid based solution was created to etch the sample surface. The solution was made up of 100ml of 20% Nitric Acid and 500ml of ionised water. Each sample was placed in the solution for approximately 10 seconds, before being removed, rinsed under a running tap and dried. A single sample for each setup (a total of 15 samples), was molded in a resin, to prevent discolouration and rusting (see Figure 3.8).

A high resolution Nikon DX AF-S NIKKOR camera and camera stand was used to provide photographs of each macro section. The photographs were then analysed using Image J software. The camera stand consisted of a fixed camera head, a spotlight, an adjustable platform and a steel rule, used to create a reference of scale. Each sample was identifiable through a number visible within the image. All photos

were saved to an SD card, before being transfered to an external hard drive for storage. Each file was named to provide traceability.

3.5.2 Radiographic Testing

Samples approximately 100 millimeters in length, were cut from 15 welded joints, 1 from each paint thickness range, for all 5 of the filler wire/polarity setups. RT was then performed on the 15 samples, each labelled allowing traceability. This testing allowed the 15 samples to be checked for internal porosity, caused by trapped gases during the welding process.

The RT was carried out on request, by a trained welding inspector at BAE Systems Glasgow, as support to this project. Photographs were taken of each radiograph, using a backlight and a high resolution Nikon DX AF-S NIKKOR camera. This allowed for easy interpretation of the radiographs, highlighting any pores (see Figure 2.29 & 3.9).

3.5.3 Vickers Hardness Testing

For hardness testing, 15 joints were chosen from the welded samples, one from each paint thickness range for all 5 of the filler wire/polarity setups. This provided data that could be used to identify any notable changes in hardness levels, when welding over different thicknesses of shop primer. This data was then used to conclude if certain DFT ranges, would or would not affect the metallurgical performance of the steel and weld metal after welding.

The samples selected for HV testing, were the samples etched and molded in Bakelite, a thermosetting phenolic conductive resin. This was due to the good surface finish, improving the likelihood of locating the desired areas of the welded joints.

The HV testing equipment in the Advanced Materials Research Laboratory at the University of Strathclyde, is calibrated annually and regularly used for commerical and student projects. Training and guidance was provided by metallography technician, James Kelly. This support has provided many students with an understanding of the correct method, ensuring accurate data was obtained. As is typical for the HV test method, a diamond shaped indenter was used, with a 5kg weight. The smaller impression, provided for better accuracy when measuring hardness within the HAZ of a weldment.

A total of 3 indentations, were taken in 5 different locations of each welded sample. As shown in Lloyds Naval Rules, for a single pass fillet weld (see Figure 3.10). There were 6 readings taken from the parent material, 3 from the weld metal and 6 from the HAZ. Next, 2 measurements were taken from each indentation using the eye piece. These measurements were then converted, to a single hardness value using Part 1 of British Standard 427 Method for Vickers hardness testing (see Appendix 14). Each hardness value, was recorded on a template (see Appendix 15). All values were then transfered to a spreadsheet for review and comparison.

3.5.4 Image J Analysis – Macro Sections and Radiographs

Image J, is a software widely used for microscopy image analysis. This made it a suitable choice for collecting data from the high resolution images of the macro sections and radiographs.

Firstly, the scale was set using the steel rule, which was included in the image. This process was carried out on each image, before recording any measurements. A total of 7 measurements were taken from each macro. This included, horizontal leg length, vertical leg length, throat thickness, weld area, HAZ area, penetration area and joint angle (see Figure 3.11). The measurements taken allowed for analysis of all aspects of weld geometry (see Figure 2.1 & 2.2). They also provided data, that would give an indication as to whether an increase in primer paint thickness affected weld

penetration and the HAZ. Joint angle was recorded, but in order to focus on the areas most likely to be affected by primer paint, at this point it was not used in the thesis.

The radiograph images taken with the high resolution camera, were also analysed using the Image J software. This provided data that could be evidential in recognising a possible trend, between volume of weld metal porosity and primer paint thickness. The scale was set on each image using the steel rule included in the photos, before collecting any data. As the samples were of varying lengths, only the initial 70mm was checked. Porosity was calculated as a total area, with the area of each pore being measured and then totalled.

All of the data collected using Image J software, was input in to a Microsoft Excel document for further analysis.

Figure 3.8 – Sample etched and hot moulded in Bakelite to prevent discolouration, rusting and to allow final surface preparation for imaging quality and hardness testing.

Figure 3.9 – Image of clear radiograph showing no visible signs of porosity. This radiograph was produced by a trained NDT engineer at BAE Systems, Glasgow in support of this work.
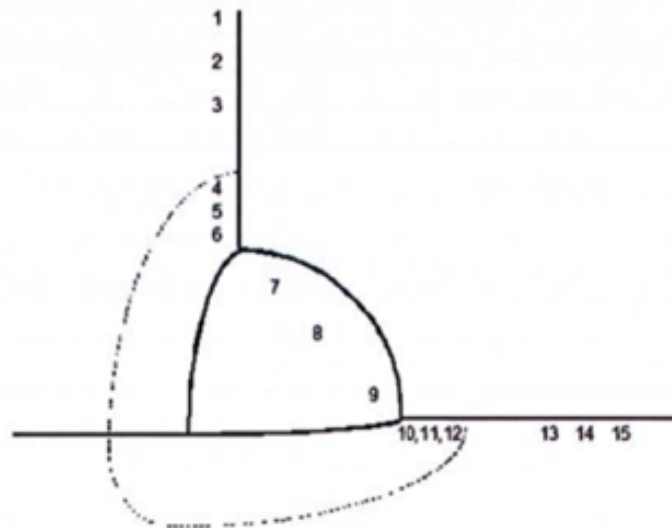
Figure 3.10 – Schematic providing instruction on locations of Vickers Hardness indentations for a single pass fillet weld. Adapted from Lloyds Naval Rules – Manufacture Testing and Certification of Materials 2016.
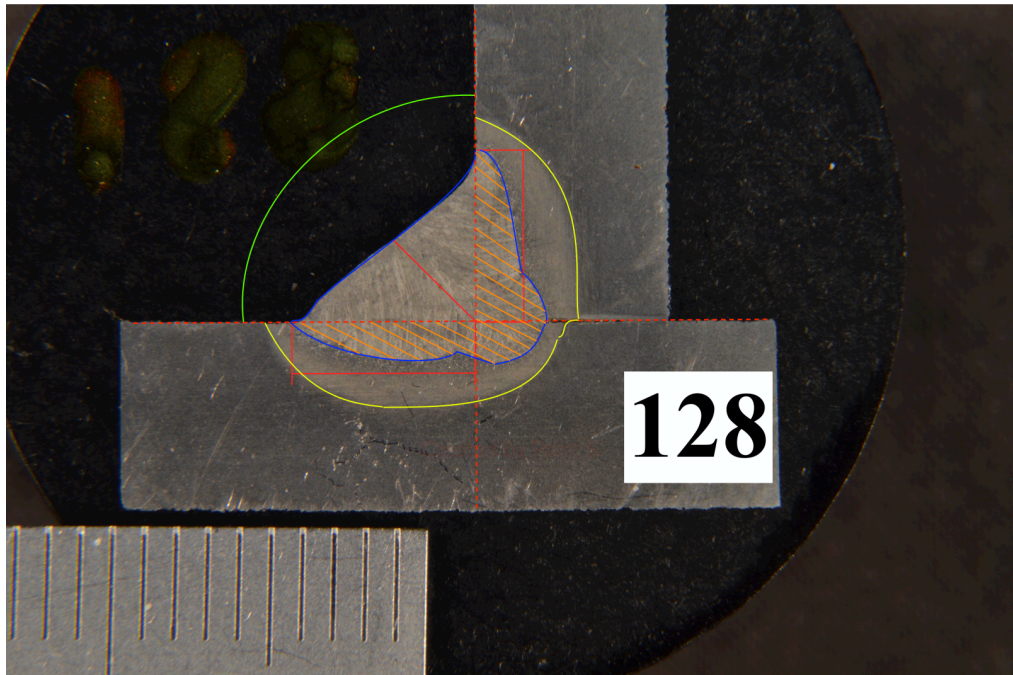
Figure 3.11 – Schematic providing seven measurements taken from images of macro sections. Red arrows – horizontal/vertical leg lengths and throat thickness. Blue outline – weld area. Yellow outline – HAZ area. Orange hatched markings – penetration area. Green radius – joint angle.

4.0 <u>Results</u>

4.1 <u>Measuring Dry Film Thickness</u>
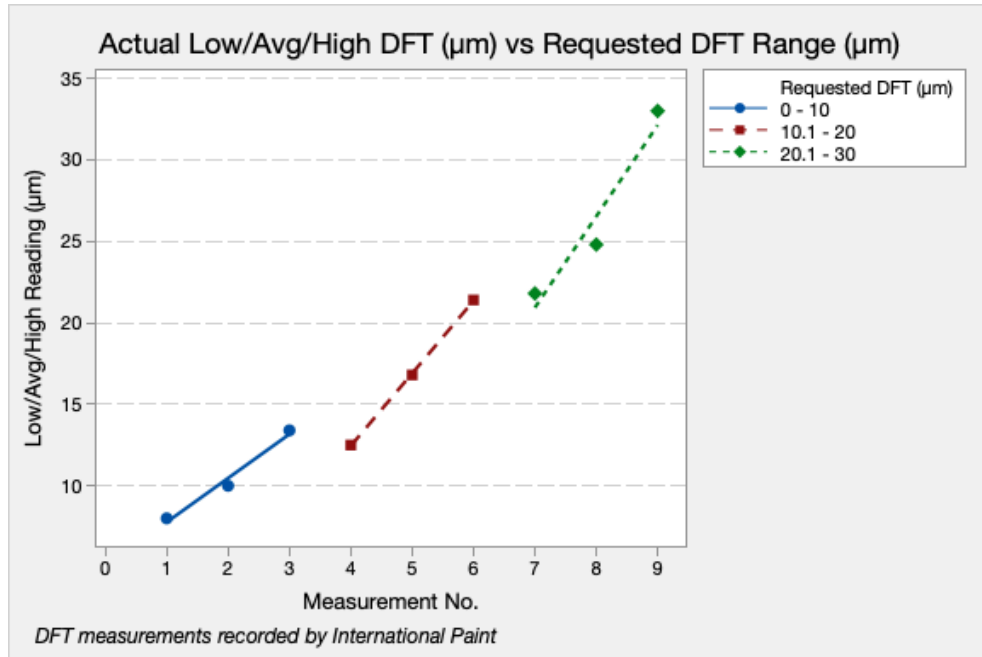
*Figure 4.1 – Actual DFT values (as measured by
International Paint) vs. requested DFT ranges.*

Figure 4.1 displays data supplied by International Paint. The data shows a comparison between the DFT ranges requested for this work, and the actual DFT readings measured by International Paint prior to delivery of the samples. The lowest reading, the highest reading and the average of all measurements taken, was provided.

Working from the average DFT, the samples supplied by International Paint were within the DFT ranges that were requested. However, some of their readings would have been out with the requested ranges.
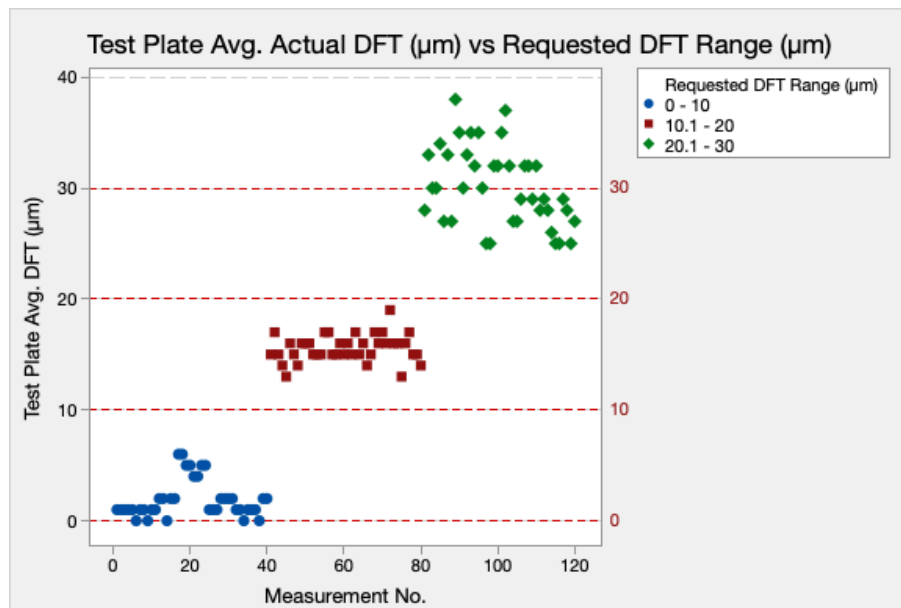
Figure 4.2 – Actual DFT values (as measured during experimental work) vs. requested DFT ranges.

As explained in section 3, paint thickness readings were taken from each individual sample plate. This testing was carried out in the University of Strathclyde workshop, using an Elcometer 415 Model T (see Figure 3.3). A total of 10 readings were taken from each of the 264 plates. Measurements were taken from the centre of the horizontal plate and the edge of the vertical plate. Next, 8 sample plates were randomly selected (4 vertical and 4 horizontal) and an average was taken from the 10 readings on each sample plate. This data was then used to create Figure 4.2. This figure displays the requested DFT ranges and the scatter of the average recorded measurement from each plate and thickness range.

It is visible from Figure 4.2, that the averages taken from DFT ranges 0-10µm and 10-20µm were achieved. This is clear, with the figure showing 80 of 80 readings within the requested DFT range. However, only 23 of the 40 readings from the DFT range 20-30µm were within the requested tolerance.

- DFT Range 0-10µm – 40/40 – 100% accuracy according to available data.
- DFT Range 10-20µm – 40/40 – 100% accuracy according to available data.
- DFT Range 20-30µm – 23/40 – 58% accuracy according to available data.
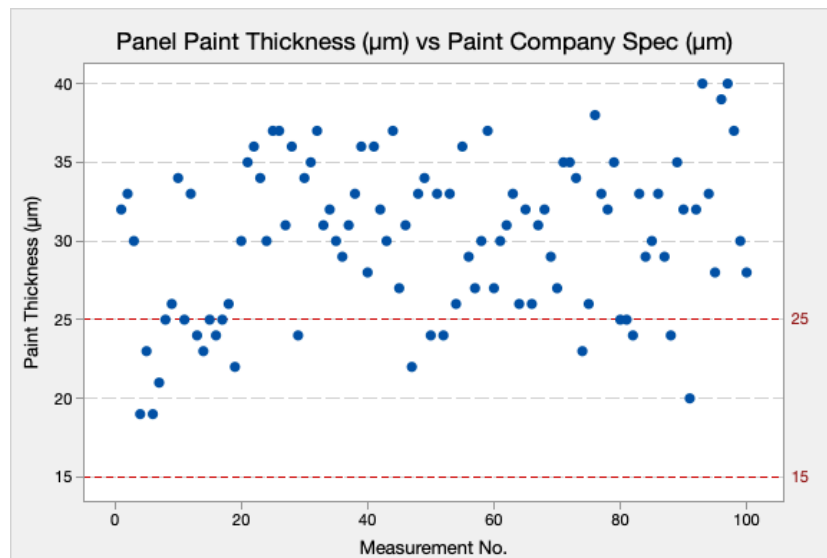
Figure 4.3 – Production panel DFT thickness vs paint company specification.

Figure 4.3 displays data collected from a single steel panel, from the production line of a large steel fabricator. A total of 100 readings were taken and compared, against the DFT range specified in the data sheet for the shop primer used (see Appendix 10). The minimum value for primer DFT was taken from the limitations section of the data sheet. There it states, "Film thickness below the specified 15 microns may result in breakdown of the shop primer and substrate corrosion…".

The limitations section of the data sheet also provides information on the maximum value of primer DFT (see Appendix 10). It reads, "Film thickness above the specified 15 microns may adversely affect welding and cutting properties and may affect the performance of subsequently applied coating systems. Thicknesses above 25 microns should be avoided".

Working with the minimum and maximum values specified in the data sheet, the panel readings were input to a scatter diagram. This diagram provided a figure of accuracy of the paint application to the desired thickness. Only 22 of the 100 readings were within the range advised in the data sheet, with the average reading being 30 microns.

- DFT Range 15-25µm – 22/100 – 22% accuracy within specification.
- Average DFT across 100 readings - 30µm.

4.2 <u>Hardness Testing – Heat Affected Zone</u>

As explained in Section 3.5, 15 samples were tested, each with 15 indentations made in the locations specified in Lloyds Naval Rules (see Figure 3.10). The same locations are used during the qualification process of a single pass fillet weld. In order to best highlight any notable changes in the material hardness at different DFT ranges, only 4 measurements from each DFT range were taken. All measurements were taken from the HAZ, which is commonly the area of the parent plate most affected by the welding process.

Figures 4.4 to 4.8, display the hardness data for each welding filler type at the selected 3 DFT ranges.
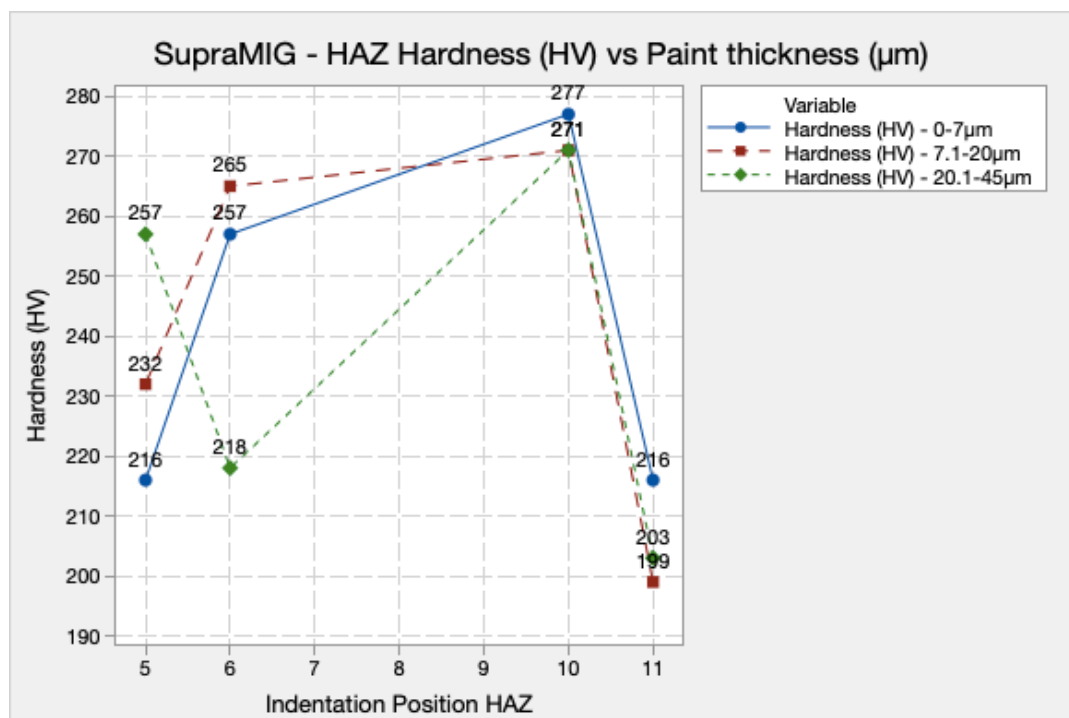
Figure 4.4 – HAZ hardness at varying DFT ranges using SupraMIG solid wire.

Figure 4.4 shows a tight scatter of hardness values at indentation position 5, with a small drop in HV value for DFT 20.1-45µm. HV values for all 3 DFT ranges, were consistent at indentation positions 10 and 11.
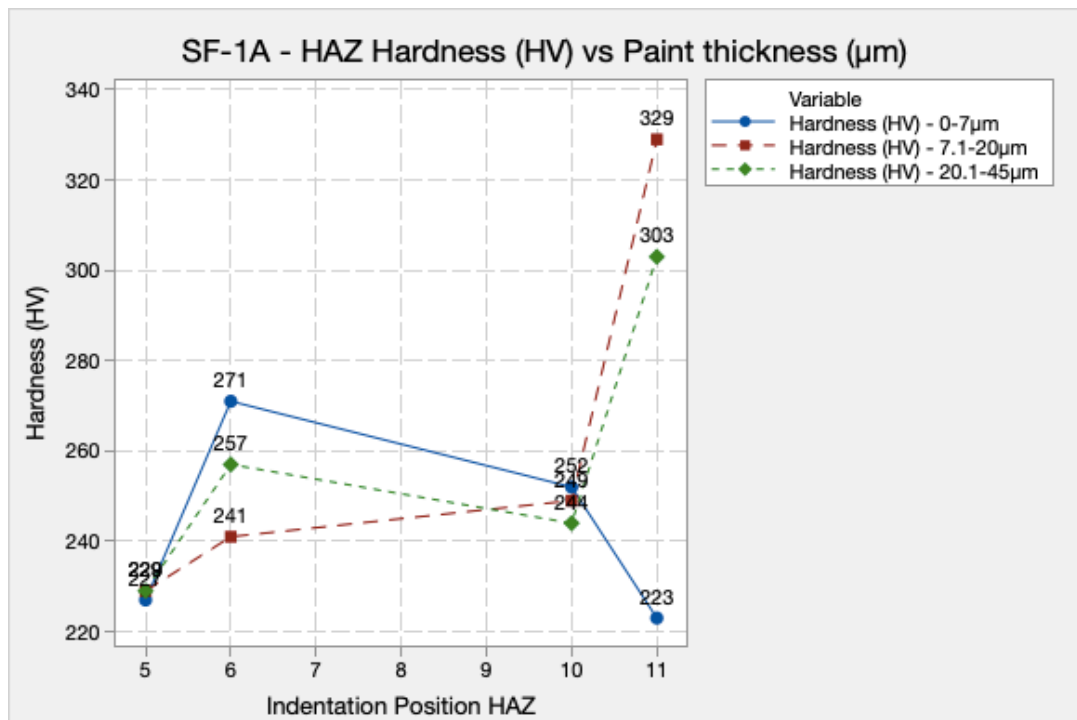
Figure 4.5 – HAZ hardness at varying DFT ranges using
SF-1A seamless flux cored wire.

The scatter diagram in Figure 4.5, shows very similar HV values at indentation positions 5 and 10, for all 3 DFT ranges. There was tight scatter in the DFT ranges at indentation 6. DFT range 0-7μm shows a notably lower HV value at indentation 11.
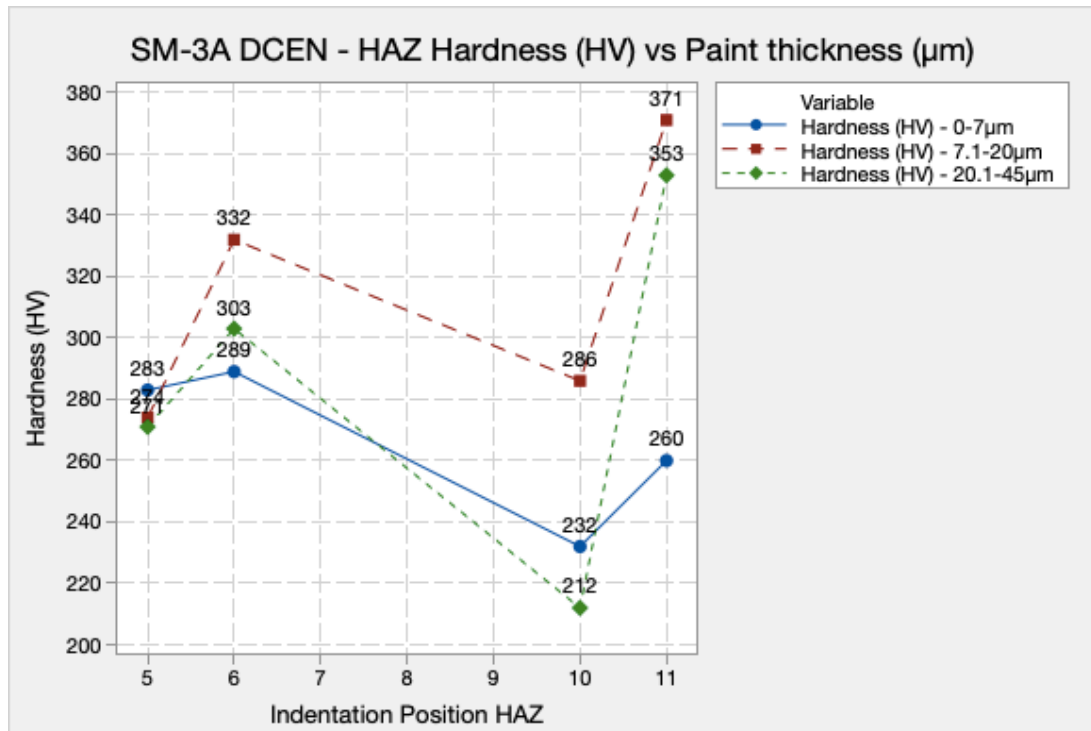
Figure 4.6 – HAZ hardness at varying DFT ranges using SM-3A seamless metal cored wire on DCEN.

Figure 4.6 shows HV similar values at indentation position 5, and a tight scatter across all 3 DFT ranges at indentation 6. There was a wider scatter at indentation 10. DFT range 7.1-20μm showed a higher HV value and DFT range 0-7μm shows a notably lower HV value at indentation 11.
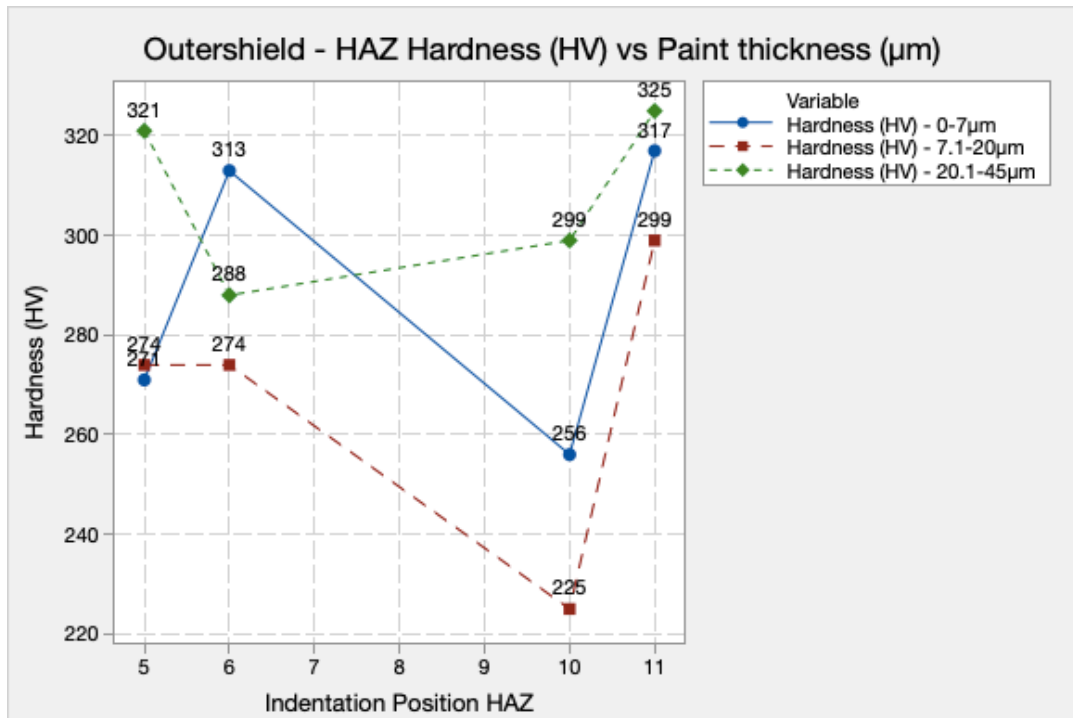
Figure 4.7 – HAZ hardness at varying DFT ranges using Outershield folded type flux cored wire.

Figure 4.7 shows varying degrees of scatter across all indentation positions and DFT ranges. The most noteable difference being at identation 10, with the lower HV value of DFT range 7.1-20μm and the higher DFT range 20.1-45μm.
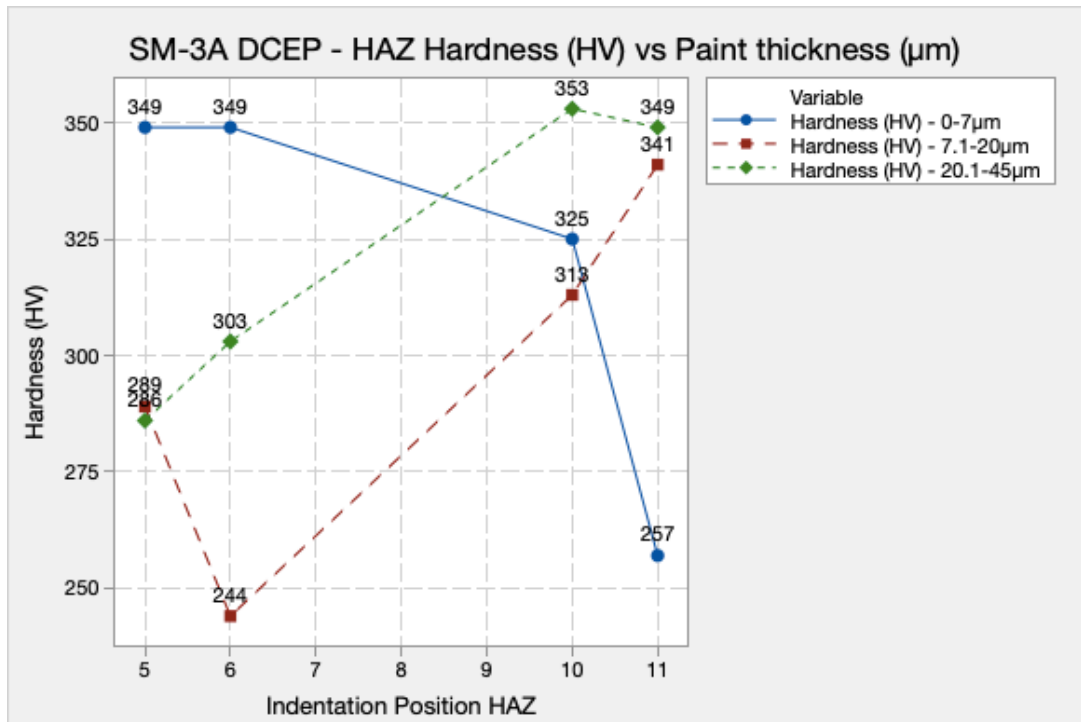
Figure 4.8 – HAZ hardness at varying DFT ranges using SM-3A seamless metal cored wire on DCEP.

Figure 4.8 shows high HV values for DFT range 0-7μm at indentation positions 5 and 6 when compared with the other DFT ranges. The most notable, being the high value for DFT range 0-7μm and the low value for DFT range 7.1-20μm at indentation 6. The HV values at indentation positions 10 and 11 are above 300HV, but still within BS EN ISO 15614-1 acceptance for a single pass fillet weld (380HV). DFT range 0-7μm is noticeably lower at 257HV.

4.3 <u>Etched Macro Sections</u>

4.3.1 <u>Heat Affected Zone Area</u>

The following 5 diagrams, show HAZ area results taken from 15 macro sections, with 5 at each DFT range. Each of the diagrams, provides data on the performance of different welding fillers, against a change in DFT within the ranges chosen for this work. Welding parameters and condition were maintained for each filler, with only DFT being adjusted. Results were displayed on a scatter diagram, where they were arranged in numerical order to aid analysis.
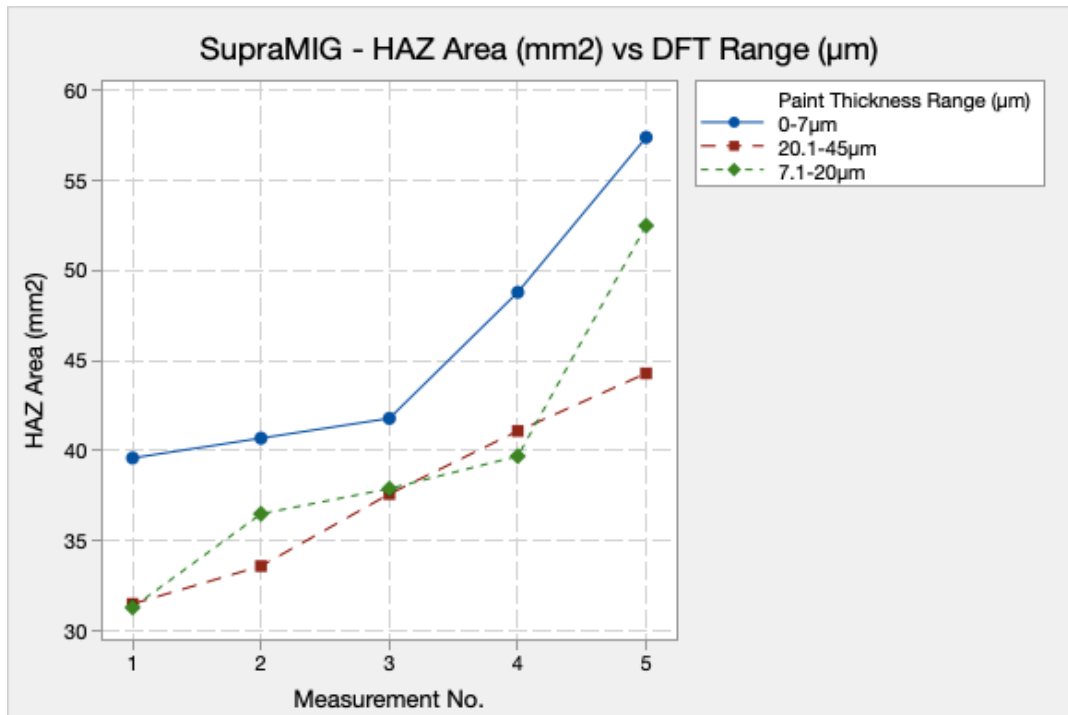
Figure 4.9 – HAZ area at varying DFT ranges using SupraMIG solid wire.

Figure 4.9 shows HAZ area, when SupraMIG solid wire was used. Samples at 3 varied DFT ranges were welded, using the same welding parameters and condition. Across 5 macro sections, the HAZ area was visibly larger for DFT 0-7µm. DFT ranges 7.1-20µm and 20.1-45µm follow a similar trend, although measurement 5 for DFT 7.1-20µm had the second largest HAZ area.

- DFT Range - 0-7µm - Total HAZ area across 5 macro sections – 228.3mm^2
- DFT Range - 7.1-20µm - Total HAZ area across 5 macro sections – 197.9mm^2
- DFT Range - 20.1-45µm - Total HAZ area across 5 macro sections – 188.1mm^2
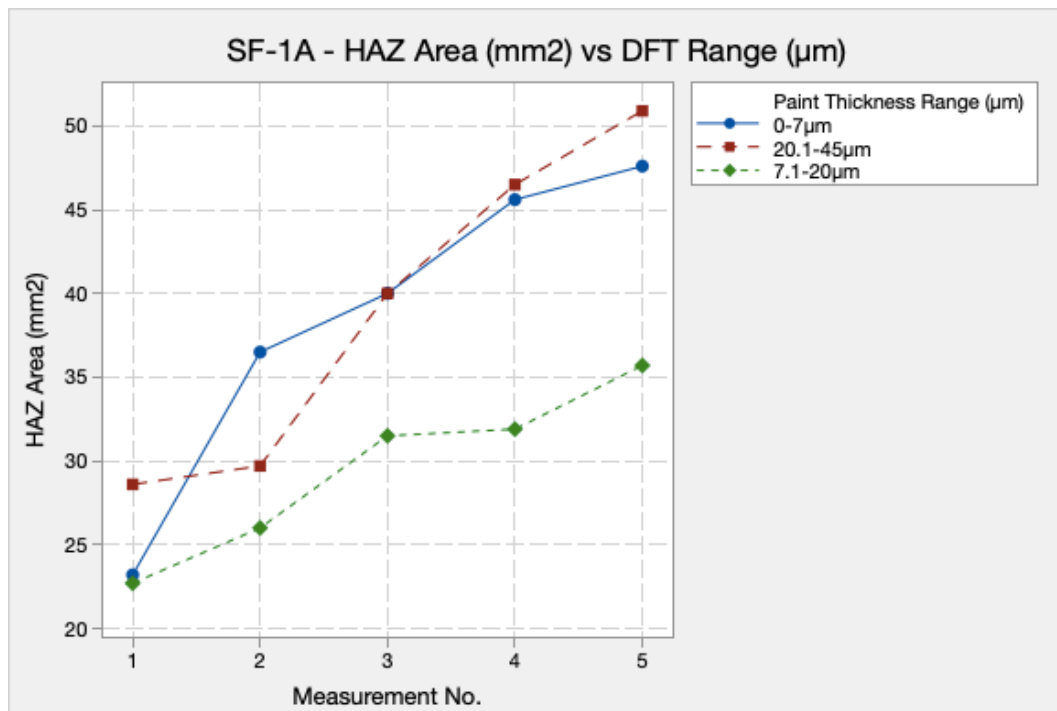
*Figure 4.10 – HAZ area at varying DFT ranges using SF-1A
seamless flux cored wire.*

Figure 4.10 provides HAZ area results when SF-1A flux-cored wire was used as
the filler. The same welding parameters and condition were maintained, with only
the DFT adjusted. DFT ranges 0-7µm and 20.1-45µm seemed to follow a similar
trend across measurements 3, 4 and 5. The HAZ Area at measurement 1 was almost
the same for DFT 0-7µm and DFT 7.1-20µm. The HAZ area was notably smaller
across measurements 2, 3, 4 and 5 for DFT 7.1-20µm.

- DFT Range - 0-7µm - Total HAZ area across 5 macro sections – 193.2mm^2
- DFT Range - 7.1-20µm - Total HAZ area across 5 macro sections – 147.8mm^2
- DFT Range - 20.1-45µm - Total HAZ area across 5 macro sections – 195.7mm^2
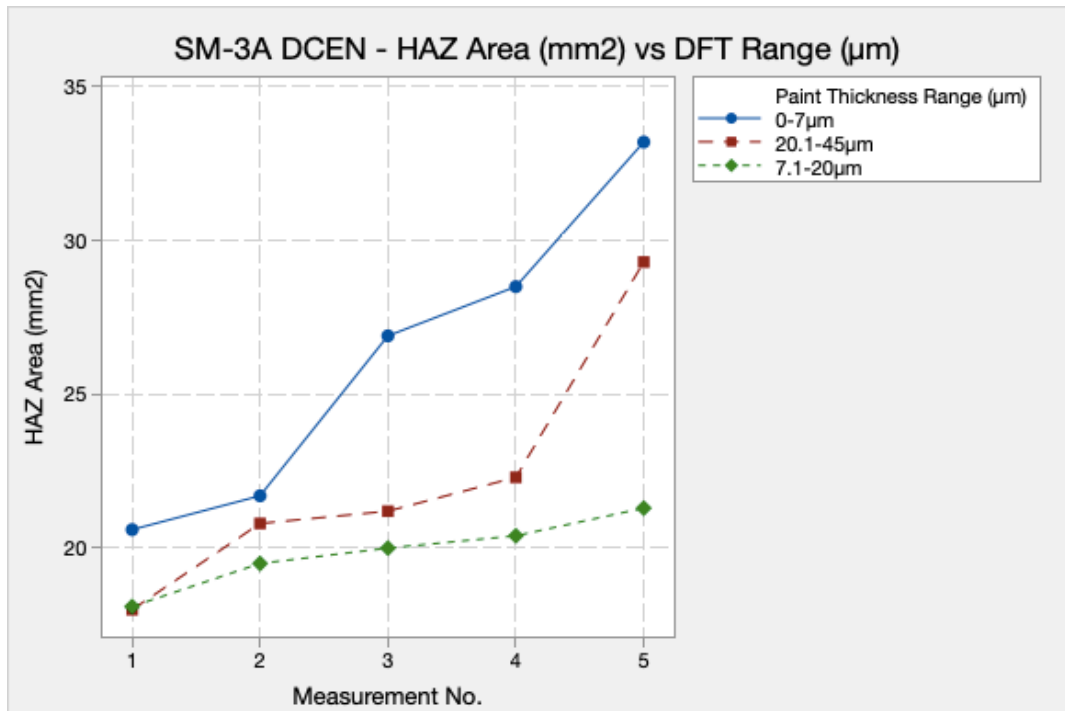
Figure 4.11 – HAZ area at varying DFT ranges using SM-3A seamless metal cored wire on DCEN.

Figure 4.11 shows HAZ area when welding was completed with SM-3A metal-cored wire. During testing, the wire was operating on DCEN, welding samples at 3 varied DFT ranges, using the same welding parameters and condition. DFT 0-7μm showed the largest HAZ area across all 5 measurements. DFT 7.1-20μm displayed a tight scatter of results. DFT 0-7μm showed a much wider scatter in results.

- DFT Range - 0-7μm - Total HAZ area across 5 macro sections – 130.9mm^2
- DFT Range - 7.1-20μm - Total HAZ area across 5 macro sections – 99.3mm^2
- DFT Range - 20.1-45μm - Total HAZ area across 5 macro sections – 112.2mm^2
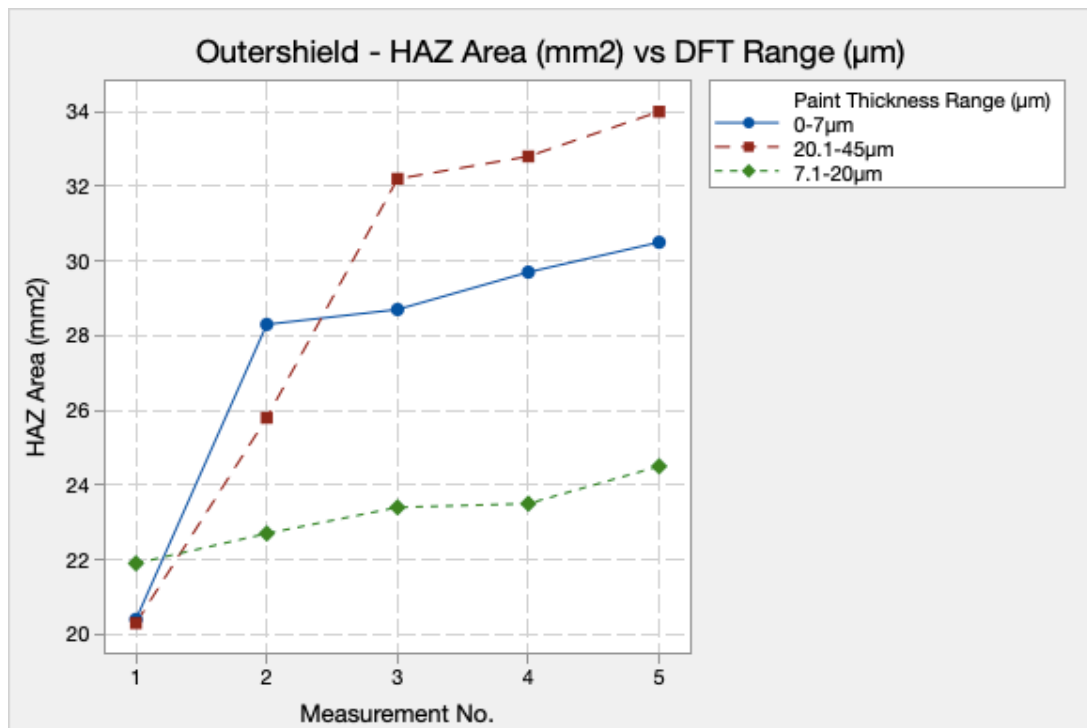
Figure 4.12 – HAZ area at varying DFT ranges using Outershield folded type flux cored wire.

Figure 4.12 displays HAZ area when Outershield flux-cored wire was used. Samples at 3 varied DFT ranges were welded using the same welding parameters and condition. The smallest HAZ area measurement, for each DFT range, was found to be almost the same. DFT range 20.1-45µm, showed the largest HAZ's in a tight scatter across measurements 3, 4 and 5. DFT 0-7µm also displayed a tight scatter across measurements 2, 3, 4 and 5.

- DFT Range - 0-7µm - Total HAZ area across 5 macro sections – 137.6mm^2
- DFT Range - 7.1-20µm - Total HAZ area across 5 macro sections – 116mm^2
- DFT Range - 20.1-45µm - Total HAZ area across 5 macro sections -148.1mm^2
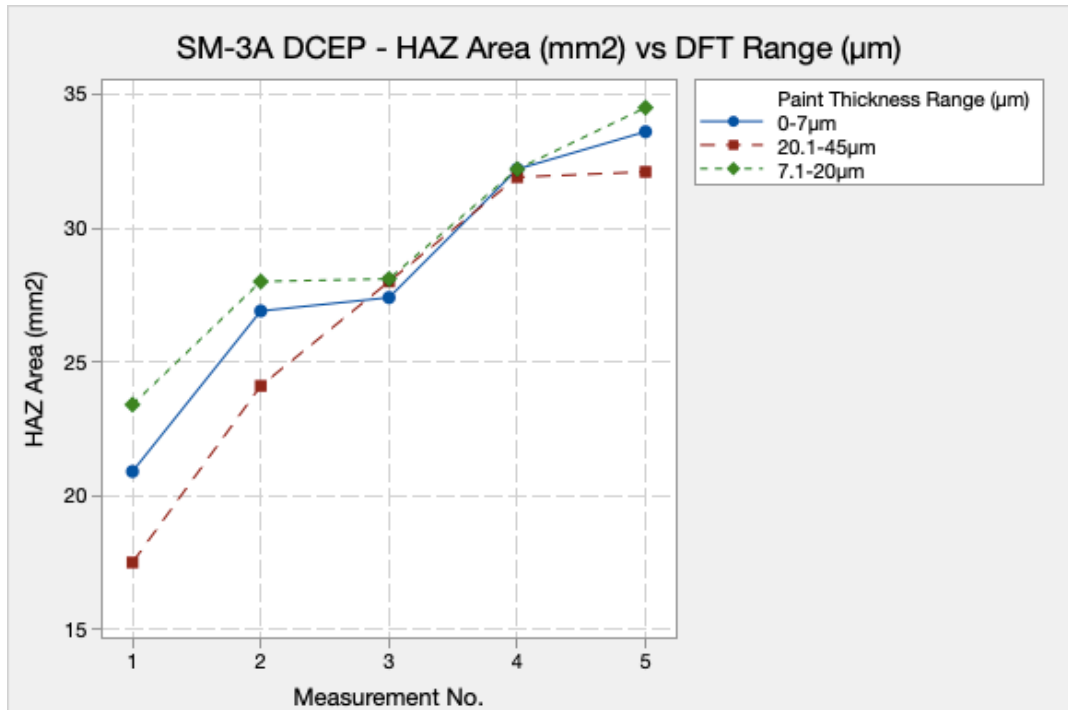
Figure 4.13 – HAZ area at varying DFT ranges using SM-3A seamless metal cored wire on DCEP.

Figure 4.13 displays HAZ area when welding was completed with SM-3A metal-cored wire on DCEP polarity. Again, the 3 varied DFT ranges were welded, while using the same welding parameters and condition. Measurements 1, 2 and 5 showed slight scatter, while there was almost no scatter visible at measurement 3 and 4.

- DFT Range - 0-7µm - Total HAZ area across 5 macro sections – 141mm^2
- DFT Range - 7.1-20µm - Total HAZ area across 5 macro sections – 146.2mm^2
- DFT Range - 20.1-45µm - Total HAZ area across 5 macro sections – 149.3mm^2

4.3.2 Penetration Area

The following 5 diagrams show penetration area results. As with section 4.3.1, the findings were taken from 15 macro sections, with 5 at each DFT range. Each of the diagrams, provides data on the performance of different welding fillers, against a change in selected DFT range (See Section 3.3). The welding parameters and condition was maintained for each filler, with only DFT being adjusted. Results were displayed on a scatter diagram, where they were arranged in numerical order to aid analysis.
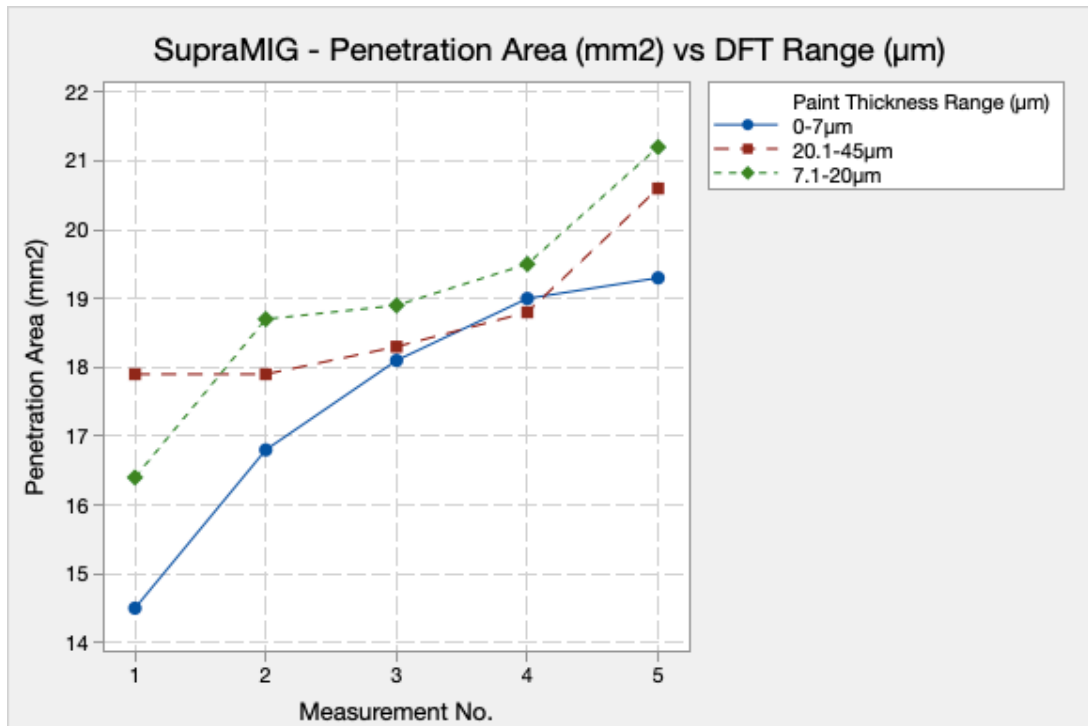
Figure 4.14 – Penetration area at varying DFT ranges using SupraMIG solid wire.

Figure 4.14 displays penetration area results when welding was completed with SupraMIG solid wire at 3 varied DFT ranges using the same welding parameters and condition. DFT 0-7µm showed the smallest penetration area across measurements 1, 2, 3 and 5. There is a notable trend for DFT ranges 7.1-20µm and 20.1-45µm across measurements 2, 3, 4 and 5.

- DFT Range - 0-7µm - Total penetration area across 5 macro sections – 87.7mm^2
- DFT Range - 7.1-20µm - Total penetration area across 5 macro sections – 94.7mm^2
- DFT Range - 20.1-45µm - Total penetration area across 5 macro sections – 93.5mm^2
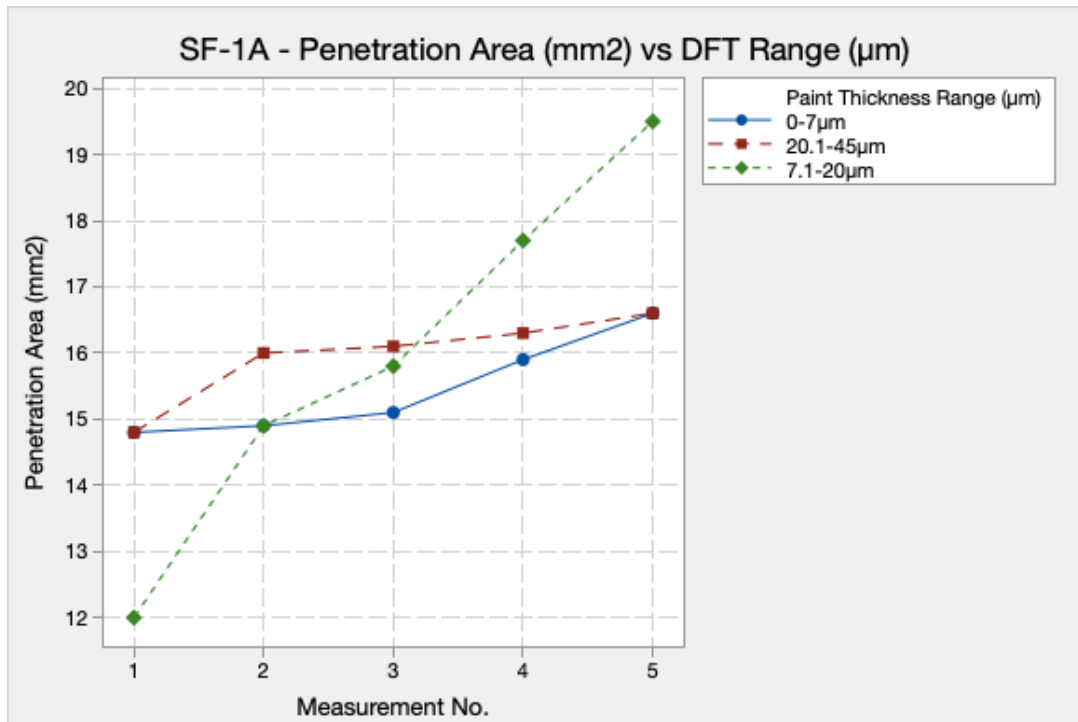
Figure 4.15 – Penetration area at varying DFT ranges using SF-1A seamless flux cored wire.

Figure 4.15 displays penetration area when SF-1A flux-cored wire was used as the filler. Samples with 3 varied DFT ranges were welded using the same parameters and condition. DFT ranges 0-7μm and 20.1-45μm followed a similar trend with measurements 1, 4 and 5 showing very similar areas. DFT 7.1-20 displayed a much wider scatter of results, with a smaller area at measurement 1 and larger areas at measurements 4 and 5.

- DFT Range - 0-7μm - Total penetration area across 5 macro sections – 77.3mm^2
- DFT Range - 7.1-20μm - Total penetration area across 5 macro sections – 79.9mm^2
- DFT Range - 20.1-45μm - Total penetration area across 5 macro sections – 79.8mm^2
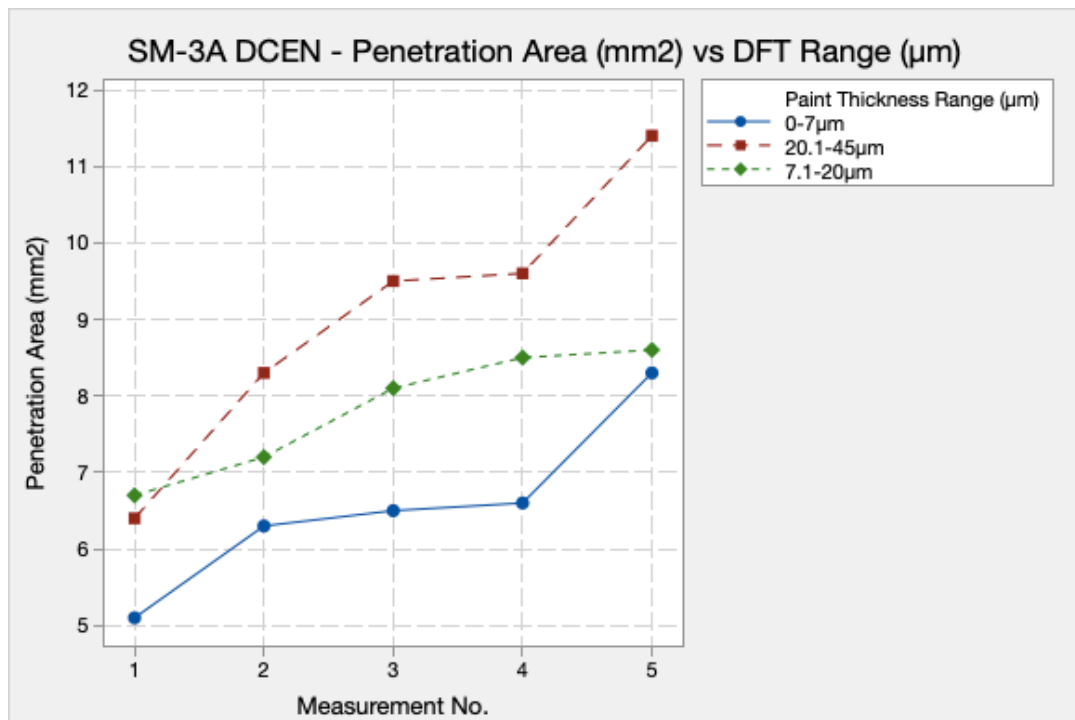
*Figure 4.16 – Penetration area at varying DFT ranges using
SM-3A seamless metal cored wire on DCEN.*

Figure 4.16 shows penetration area when welding was completed using SM-3A metal-cored wire operating on DCEN. Samples with 3 varied DFT ranges were welded using the same parameters and condition. DFT range 0-7µm showed notably smaller penetration areas across measurements 1, 2, 3 and 4. Results are similar for DFT ranges 0-7µm and 7.1-20µm at measurement 5. DFT range 20.1-45 showed considerably larger penetration area results at measurements 2, 3, 4 and 5.

- DFT Range - 0-7µm - Total penetration area across 5 macro sections – 32.8mm^2
- DFT Range - 7.1-20µm - Total penetration area across 5 macro sections – 39.1mm^2
- DFT Range - 20.1-45µm - Total penetration area across 5 macro sections – 45.2mm^2
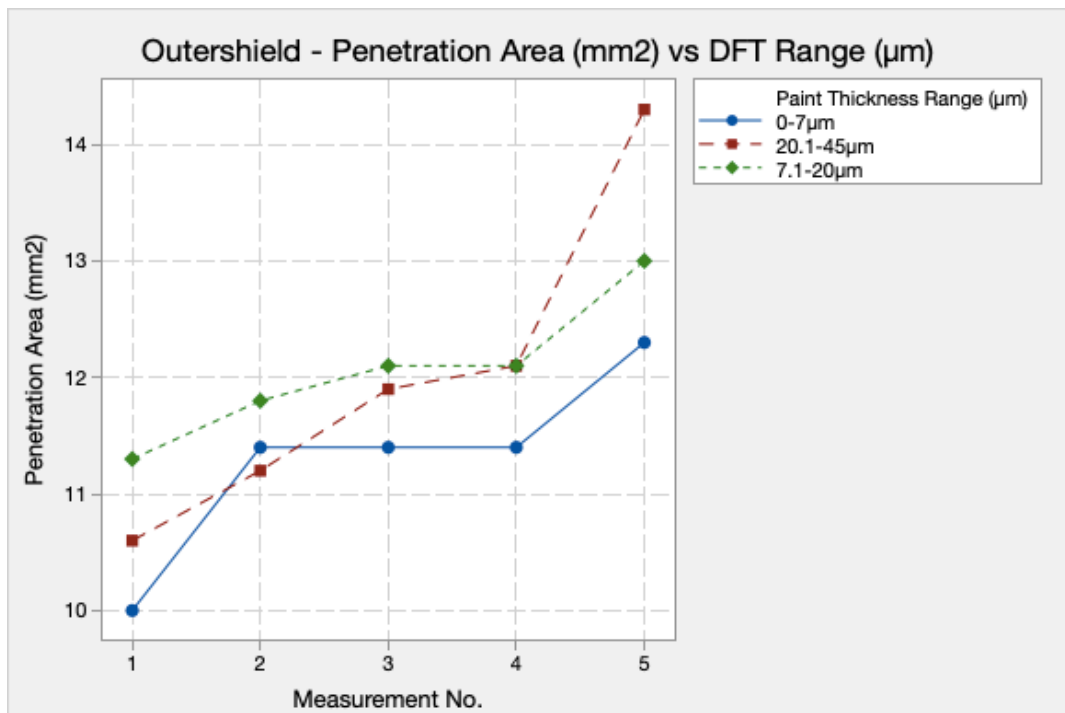
Figure 4.17 – Penetration area at varying DFT ranges using Outershield folded type flux cored wire.

Figure 4.17 shows penetration area results, from the Outershield flux-cored filler at 3 varied DFT ranges, using the same welding parameters and condition. DFT range 0-7µm showed smaller penetration areas across measurements 1, 3, 4 and 5. DFT ranges 7.1-20µm and 20.1-45µm showed a similar trend at measurements 1, 2, 3 and 4.

- DFT Range - 0-7µm - Total penetration area across 5 macro sections – 56.5mm^2
- DFT Range - 7.1-20µm - Total penetration area across 5 macro sections – 60.3mm^2
- DFT Range - 20.1-45µm - Total penetration area across 5 macro sections – 60.1mm^2
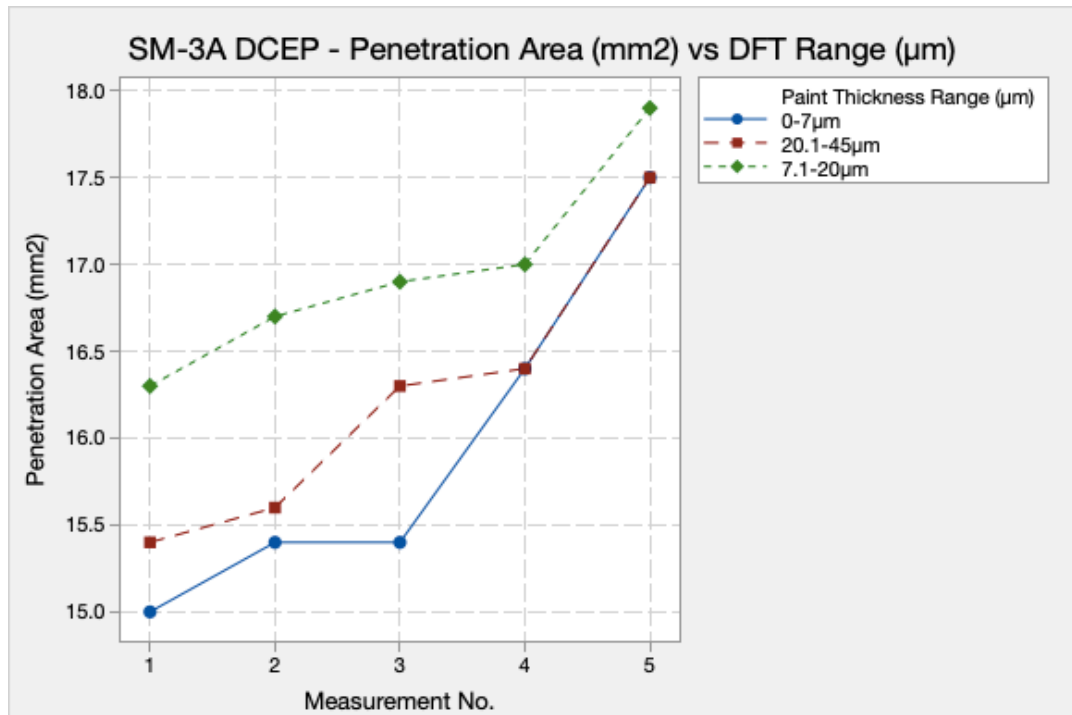
Figure 4.18 – Penetration area at varying DFT ranges using SM-3A seamless metal cored wire on DCEP.

Figure 4.18 displays penetration area, as a result of welding with SM-3A metal-cored wire at 3 varied DFT ranges using the same welding parameters and condition. Penetration area results for DFT ranges 0-7µm and 20.1-45µm followed a very similar trend across measurements 1, 2, 4 and 5. Results for DFT range 7.1-20µm showed visibly greater penetration areas across all measurements.

- DFT Range - 0-7µm - Total penetration area across 5 macro sections – 79.7mm^2
- DFT Range - 7.1-20µm - Total penetration area across 5 macro sections – 84.8mm^2
- DFT Range - 20.1-45µm - Total penetration area across 5 macro sections – 81.2mm^2

4.4 <u>Radiographic Testing</u>

4.4.1 <u>Volume of Porosity with Varying Dry Film Thickness</u>

Figures 4.19 to 4.23, present data taken from 15 welded joints. A total of 5 joints at each DFT range. The figures compare the performance of the named filler wire at each DFT range. Adopting the method described in section 3.5, radiographs were analysed using Image-J software, providing a total visible porosity area across the first 70mm of the welded samples.
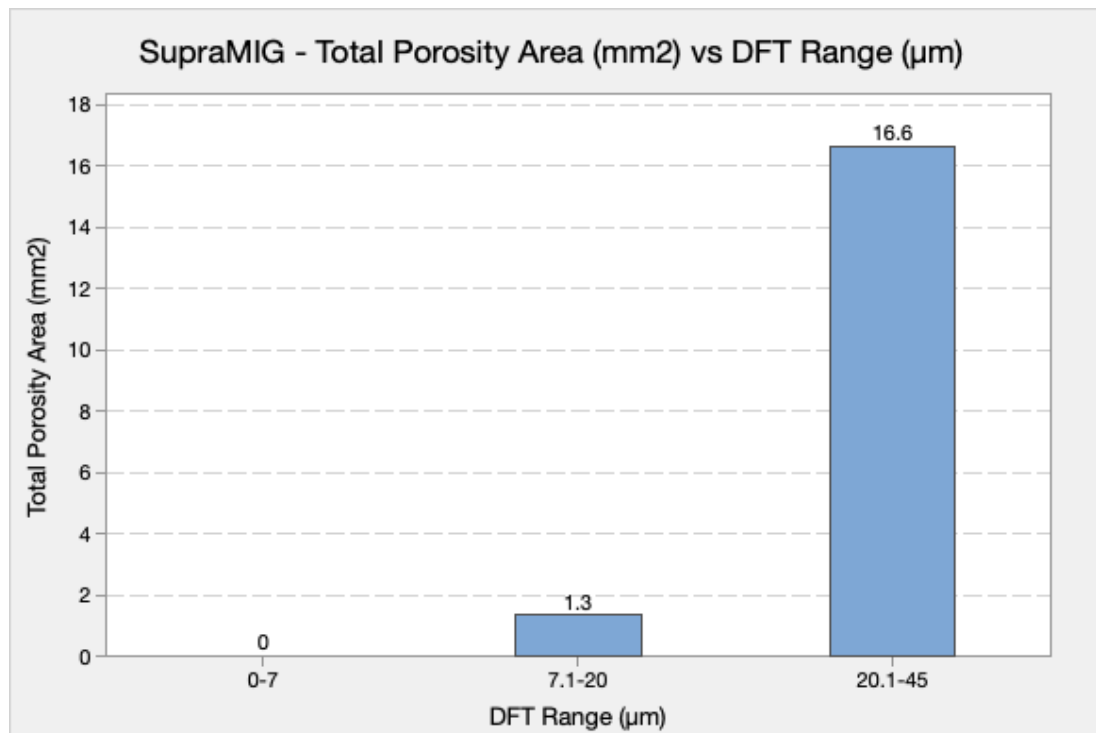
Figure 4.19 – Total porosity area at varying DFT ranges using SupraMIG solid wire.

- SupraMIG solid wire - DFT Range 0-7µm – No visible pores
- SupraMIG solid wire - DFT Range 7.1-20µm – Minimal porosity (1.3mm^2)
- SupraMIG solid wire - DFT Range 20.1-45µm – large volume of porosity (16.6mm^2)
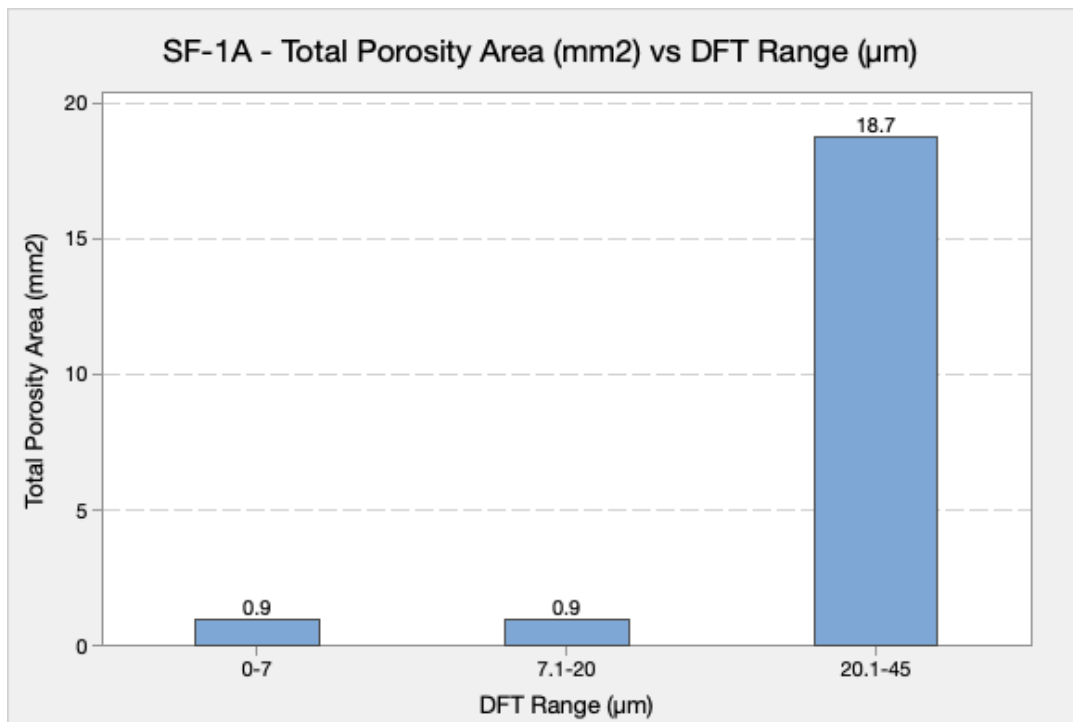
Figure 4.20 – Total porosity area at varying DFT ranges using SF-1A seamless flux cored wire.

- SF-1A FC wire - DFT Range 0-7µm – Minimal porosity (0.9mm^2)
- SF-1A FC wire - DFT Range 7.1-20µm – Minimal porosity (0.9mm^2)
- SF-1A FC wire - DFT Range 20.1-45µm – large volume of porosity (18.7mm^2)
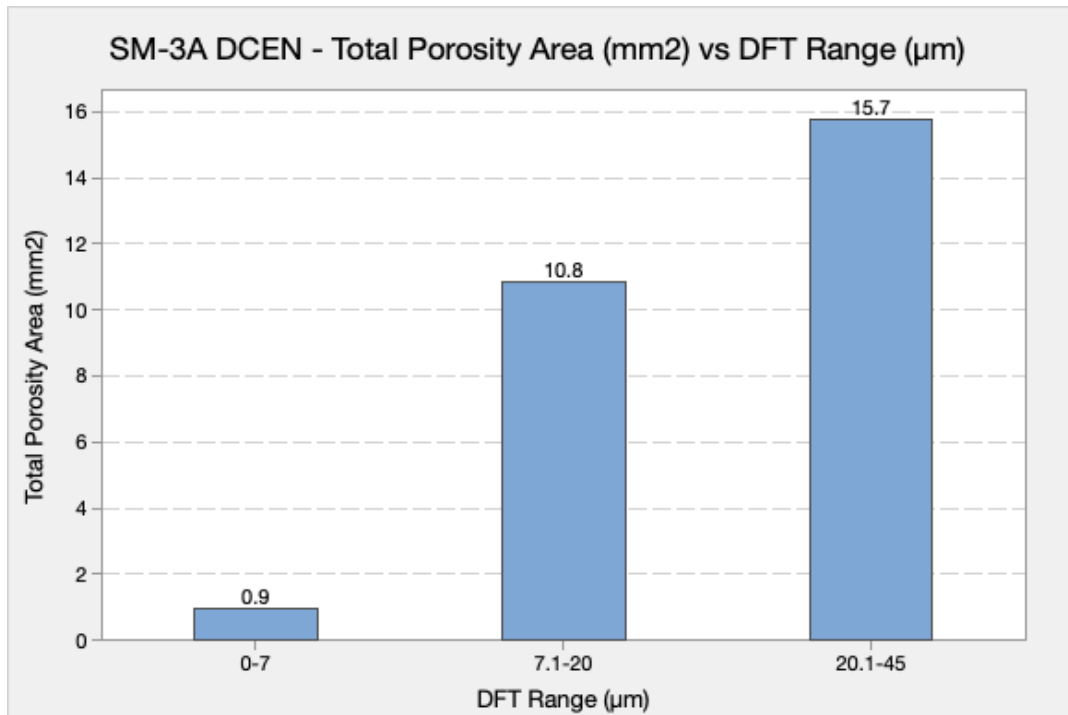
Figure 4.21 – Total porosity area at varying DFT ranges using SM-3A seamless metal cored wire on DCEN.

- SM-3A (DCEN) MC wire - DFT Range 0-7µm – Minimal porosity ($0.9mm^2$)
- SM-3A (DCEN) MC wire - DFT Range 7.1-20µm – Moderate/Large volume of porosity ($10.8mm^2$)
- SM-3A (DCEN) MC wire - DFT Range 20.1-45µm – large volume of porosity ($15.7mm^2$)
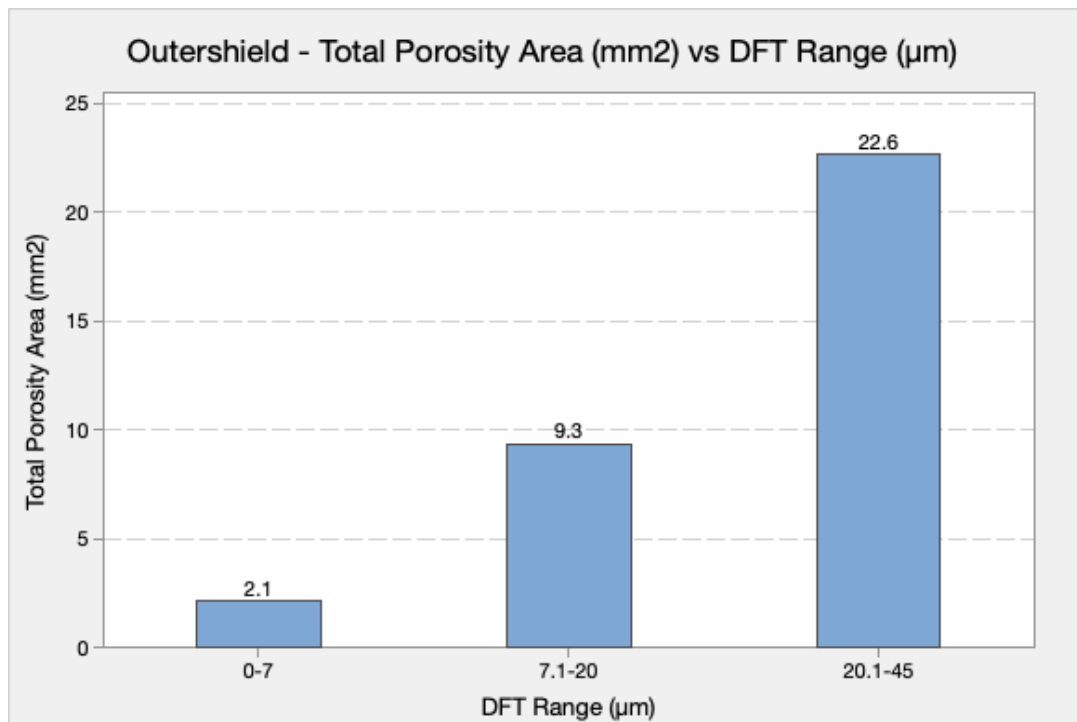
Figure 4.22 – Total porosity area at varying DFT ranges using Outershield folded type flux cored wire.

- Outershield FC wire - DFT Range 0-7µm – Minimal porosity (2.1mm^2)
- Outershield FC wire - DFT Range 7.1-20µm – Moderate volume of porosity (9.3mm^2)
- Outershield FC wire - DFT Range 20.1-45µm – large volume of porosity (22.6mm^2)
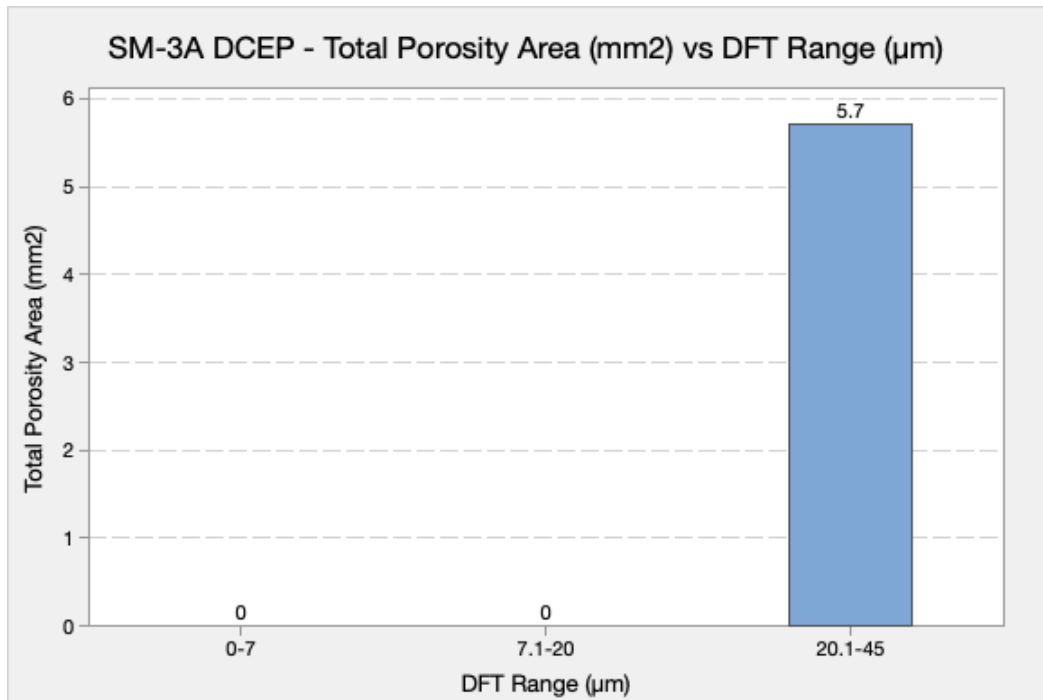
Figure 4.23 – Total porosity area at varying DFT ranges using SM-3A seamless metal cored wire on DCEP.

- SM-3A (DCEP) MC wire - DFT Range 0-7µm – No visible pores
- SM-3A (DCEP) MC wire - DFT Range 7.1-20µm – No visible pores
- SM-3A (DCEP) MC wire - DFT Range 20.1-45µm – low/moderate volume of porosity (5.7mm^2)

4.4.2 <u>Volume of Porosity with Varying Filler Type</u>

Figures 4.24 to 4.26, display data taken from 15 radiographs. The box plot diagrams, provide a comparison of the filler type performance at a set DFT range. This data was again gathered from results obtained using the method described in section 3.5.
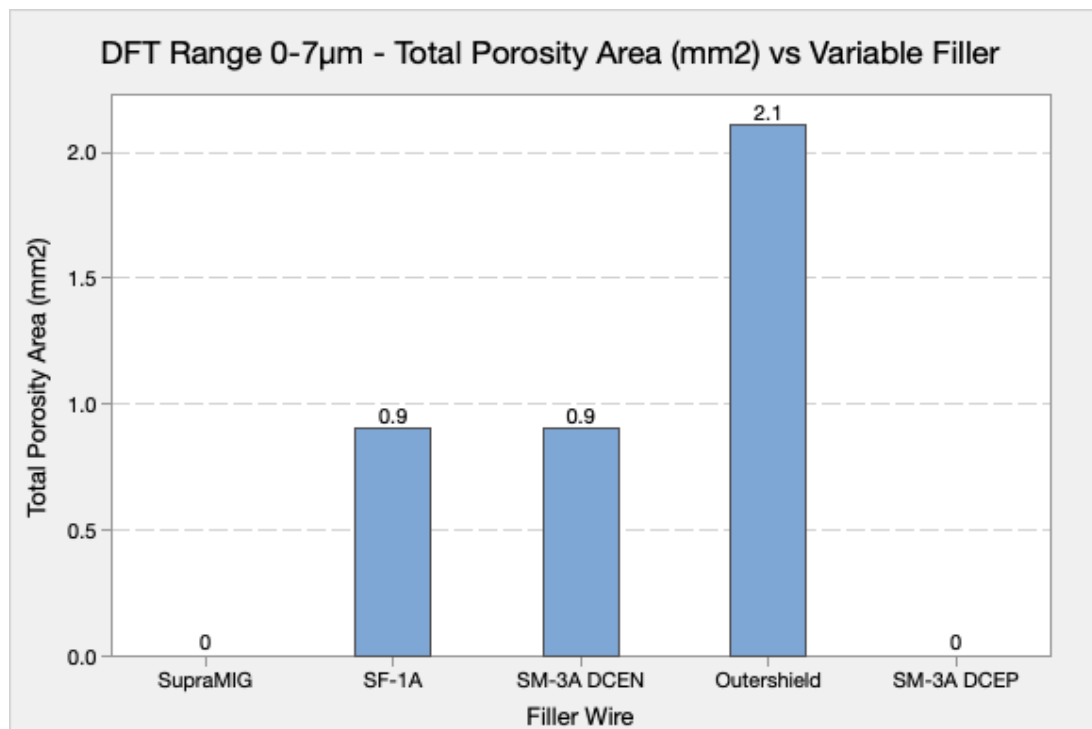
Figure 4.24 – Total porosity area at DFT range 0-7µm with varying filler type.

Figure 4.24 presents the results gathered for each filler type at the DFT range of 0-7µm. The SM-3A seamless metal-cored wire on DCEP polarity and the SupraMIG solid wire performed the best, with both producing welds with no visible porosity across the test area. Outershield folded type flux-cored wire, produced the most visible porosity, although it was of minimal volume.
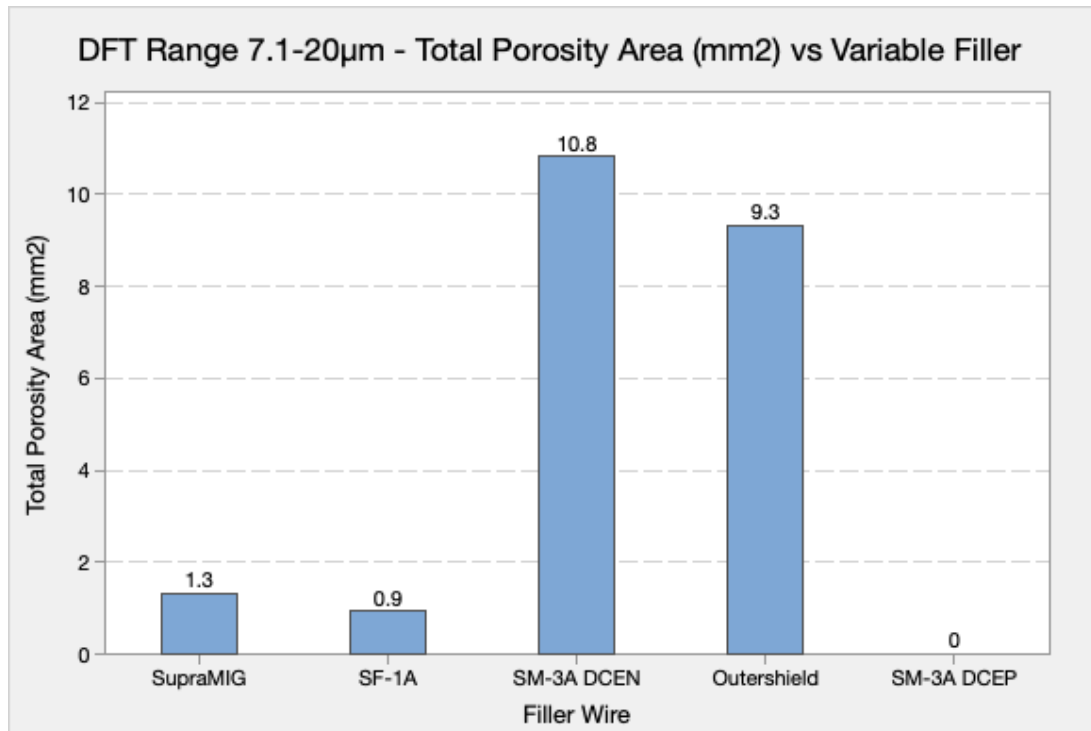
Figure 4.25 – Total porosity area at DFT range 7.1-20µm with varying filler type.

Figure 4.25 presents the results gathered for each filler type at the DFT range of 7.1-20µm. Again SM-3A metal-cored wire on DCEP polarity performed the best, producing a weld with no visible porosity across the test area. SupraMIG solid wire and SF-1A seamless flux-cored wire also performed well, producing welds with little porosity. The SM-3A metal-cored wire operating on DCEN polarity, created the most porosity, potentially due to the instability of the arc. Outershield folded type flux-cored wire produced similar results to the SM-3A DCEN.
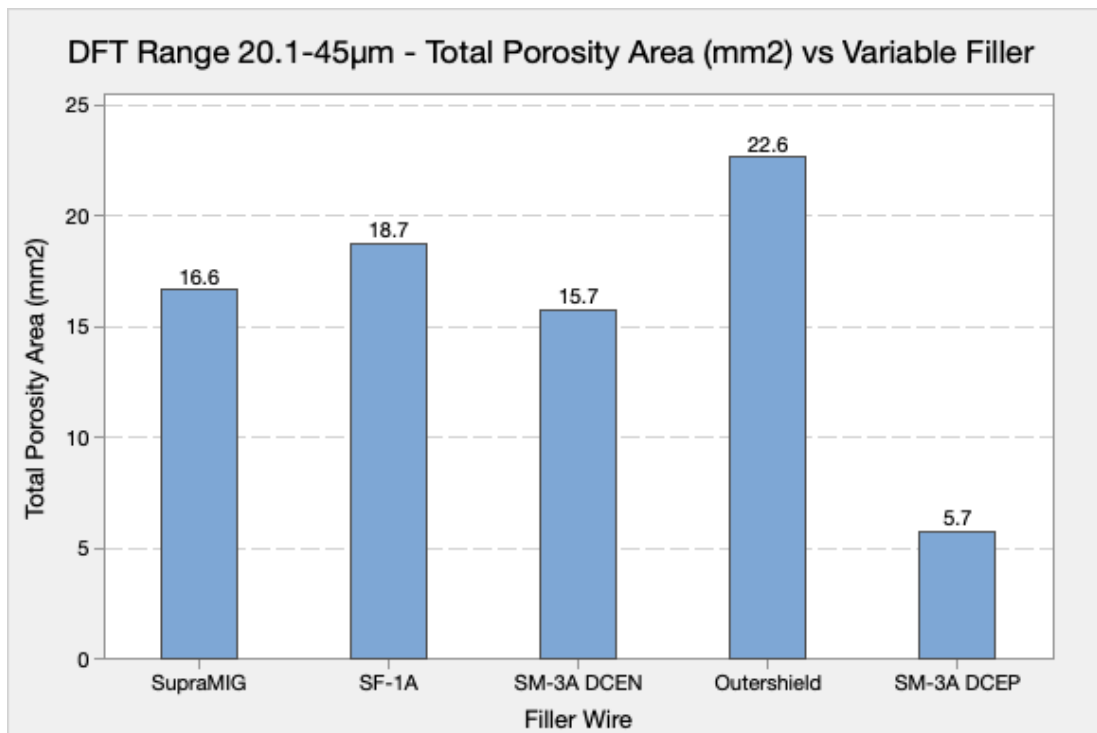
Figure 4.26 – Total porosity area at DFT range 20.1-45µm with varying filler type.

Figure 4.26 presents the results gathered for each filler type at the DFT range of 20.1-45µm. SM-3A seamless metal-cored wire on DCEP polarity performed the best, with the weld showing only a small volume of porosity across the test area. The flux-cored wires formed the most porosity, with the folded type Outershield wire producing slightly more than the seamless SF-1A. SupraMIG solid wire and SM-3A metal-cored wire operating on DCEN formed welds with similar volumes of porosity, again this could be a result of arc instability.

It should be noted, that SM-3A seamless metal-cored wire operating on DCEP showed to be the most tolerant to primer paint across all 3 DFT ranges.

5.0   Discussion and Analysis

5.1 Dry Film Thickness Measurements

The data provided in Figure 4.1, compares the DFT ranges that were requested of International Paint for this work and their actual DFT measurement results. The average reading at each DFT range, is within that requested. However, the lower range of 0-10μm had an average reading of 10μm. This indicates that a portion of the measurements taken by International Paint were above 10μm. Due to the nature of the spray application process, areas of overlapping are unavoidable, and so some high DFT readings are to be expected. Paint companies will take this into account and allow for some high DFT readings, if the average measurement is within the specification provided in the data sheet.

Using the University of Strathclyde workshop and an Elcometer 415 Model T, the DFT was measured on each sample piece. Following some initial measurements that were not recorded, it was obvious that there were a large number of sample plates out with the requested range. It was at this time that the DFT ranges were reviewed and altered from 0-10, 10.1-20 and 20.1-30μm to 0-7, 7.1-20 and 20.1-45μm. The lowest of the reviewed DFT ranges was achieved by using an angle grinder. The primer paint was removed from some of the plates that were not of a suitable DFT to use for testing. The ground plates could then be used for the T-joints in the 0-7μm DFT range. Even after using many of the plates that were reading above 30μm, there were still some that had to be used in the testing. For this reason, the high DFT range was revised to 20.1-45μm.

Figure 4.3 compared 100 DFT measurements taken from a panel on the production line of a large steel fabricator, to the primer data sheet tolerance (see Appendix 10). The DFT range selected as the tolerance, starts with the minimum of 15μm, this thickness ensuring the coating does not break down. The maximum of 25μm, is what the data sheet says should be avoided. However, the information states, that any DFT above 15μm may adversely affect welding and cutting

properties. This comment is likely a way for the paint manufacturer to cover instances of defective welds, where the DFT is under 25µm. It can be seen from figure 4.3, that out of 100 DFT measurements taken, only 22 readings were under the tolerance maximum of 25µm. This resulted in an accuracy of 22% and an average of 30µm for the randomly selected production panel. On close inspection, there were some visible surface breaking pores (see Appendix 16).

Inconsistences in the requested DFT ranges and a 22% accuracy to tolerance of a randomly selected panel, casts doubts on reported DFT. Such accuracy raises similar doubts on the achievability of the DFT tolerances provided in the data sheet by the paint manufacturer.

Based on findings from this work, there is reason to suggest that when using weld-through shop primers, the occurrence of internal porosity is highly likely. This theory is based on the assumption that some overspray will occur. In these areas the DFT will be considerably higher, even if the average reading meets the tolerance in the specification.

5.2 Heat Affected Zone Hardness

Figures 4.4 to 4.8 display data of Vickers Hardness test results taken from 15 welded samples, with 5 filler types across 3 variations of DFT. Hardness data was collected from the base material, HAZ and the weld metal. However, for the purpose of this work, only the HAZ measurements were used. This decision was due to the assumption that any notable changes in hardness, as a result of varying primer paint DFT would be most visible in the HAZ. In this area, the coating would fully vaporise. It is possible, that metallurgical changes to the weld metal may also have been present. However, repeatability of the hardness test location was thought to be less consistent, due to the possible occurrence of weld metal porosity.

Hardness results taken from Figures 4.4 to 4.8 were input into a table (see Appendix 17). The HAZ hardness readings were then totalled and an average was taken for each filler type and DFT range combination. The table provided a tool for

data analysis. This meant, any obvious metallurgical changes when maintaining the same parameters but adjusting the DFT of the shop primer, were easier to recognise.

When an average was taken for the results across 4 locations when using the SupraMIG solid wire filler, the results were almost identical at each DFT range. DFT ranges 0-7 and 7.1-20µm, both resulted in a hardness measurement of 242HV, with DFT range 20.1-45µm resulting in a hardness measurement of 237HV. These results were only marginally below both of the lower DFT ranges. Hardness results for the seamless flux-cored wire, SF-1A, are within a similar range to the SupraMIG solid wire. DFT ranges 7.1-20 and 20.1-45µm produced average measurements of 260HV and 258HV, slightly higher than the result of 243HV at DFT range 0-7µm. However, they were still within a relatively tight scatter of material hardness. Hardness measurements for seamless metal-cored wire SM-3A, operating on DCEN polarity, produced a larger spread of results. Hardness ranged from 266HV at 0-7µm to 316HV at 7.1-20µm. The DFT range 20.1-45µm showed an average value of 285HV. The Outershield folded type flux-cored wire, produced a similar spread of results to SM-3A on DCEN polarity. However, the DFT ranges were in a different order, according to material hardness. DFT range 20.1-45µm, produced the highest average hardness result at 308HV and 7.1-20µm produced the lowest average HAZ hardness at 268HV. The DFT range 0-7µm formed an average hardness value of 289HV. SM-3A seamless metal cored wire while operating on DCEP, showed a similar trend as the Outershield wire with DFT range 20.1-45µm. At this DFT range, the average material hardness was 323HV, followed by DFT range 0-7µm with a value of 320HV. DFT range 7.1-20µm produced the lowest average hardness value at 297HV.

Due to the variation in heat input of each filler type, it was difficult to compare and cross reference the results. For this reason, the focus of this discussion, compared results from each DFT range for each individual filler type. There were similar trends in the results from SF-1A and SM-3A on DCEN polarity. There were also similarities in results from Outershield and SM-3A operating on DCEP. However, a conclusion that a variation in DFT, has an effect on hardness in the HAZ of a weldment, is difficult to suggest or justify.

The temperature to which the weld pool and HAZ reaches, is largely a result of heat input, welding position and also shielding gas. Introducing some gases to a shielding gas mix, creates a hotter welding arc and so offers the benefit of improved penetration. An example of this, is the use of helium when welding aluminium to reduce the risk of LOF defects. Testing of hardness in the HAZ, was a method of identifying any transformation that may have been the result of changing temperature within the welding arc. A potential cause of this, could have been alterations in the gas shield composition, due to contamination from the vaporising primer paint.

The results from the hardness testing, showed no visible trend across all filler types. This suggests, that there was likely no significant change in the welding arc temperature, between primer paint DFT ranges.

5.3 Heat Affected Zone Area

Figures 4.9 to 4.13 are scatter diagrams that provide measurements of the HAZ areas of 5 samples at 3 varied DFT ranges. Using that data, the table in Appendix 18 provided the total HAZ area at each DFT range for each filler type. This information was then used to calculate, the average HAZ area across 5 samples.

When analysing the average HAZ areas for the SupraMIG solid wire, it is observable that DFT range 0-7μm produced the largest average HAZ area, at 45.7mm^2. DFT range 20.1-45μm produced the smallest at 37.6mm^2. The average HAZ area at DFT range 7.1-20μm, is placed between the others at 39.6mm^2. These results indicated a possible relationship between DFT of the primer paint and HAZ area. This relationship being, that DFT could potentially reduce the HAZ area of a welded joint. However, this trend did not carry over to the other filler types. SF-1A seamless flux-cored wire, created the largest average HAZ area at 20.1-45μm, with a measurement of 39.1mm^2. The smallest average HAZ area (29.6mm^2), occurred when the DFT range was 7.1-20μm. The average HAZ area of 38.6mm^2 at 0-7μm for SF-1A, also put any relationship between DFT and HAZ area in doubt. This doubt

arises from the minimal difference in the HAZ area, between the lowest and the highest DFT ranges.

The average HAZ area results recorded in Appendix 18, for SM-3A seamless metal-cored wire operating on DCEN, showed a different order again. For this combination, DFT range 0-7μm produced welds with the largest average HAZ area (26.3 mm^2), across all 5 welded samples. DFT range 20.1-45μm produced welds with the next largest HAZ area for SM-3A on DCEN polarity, with a result of 22.3mm^2. The smallest average HAZ area of 19.9mm^2, was produced where the DFT range was 7.1-20μm. These results are also the smallest HAZ areas, for all 15 combinations of filler type and DFT. The small HAZ areas from this combination, are most likely due to the DCEN polarity used to weld these samples.

When comparing Outershield folded type flux-cored wire and SF-1A seamless flux-cored wire, there was a similar trend in the order of HAZ area results (see Appendix 18). DFT range 20.1-45μm showed an average HAZ area of 29mm^2, the largest of the 3 DFT ranges. As with SF-1A, DFT range 7.1-20μm, produced welds with the smallest average HAZ area. However, the area was smaller than that produced by SF-1A, at 23.2mm^2. The DFT range 0-7μm showed an average HAZ area across 5 samples of 27.5mm^2, a result that sat between the other DFT ranges. Although the HAZ areas for the fillers are not directly comparable, the HAZ of both SF-1A and Outershield showed minimal variation at DFT ranges 0-7μm and 20.1-45μm. Both fillers also showed a drop off in average HAZ area for DFT range 7.1-20μm.

The average HAZ areas for SM-3A seamless metal-cored wire, showed little variation across all 3 DFT ranges. There was a difference of only 1.7mm^2, between the smallest average HAZ area (0-7μm – 28.2mm^2), and the largest average HAZ area (20.1-45μm – 29.9mm^2). DFT range 7.1-20μm, produced welds with an average HAZ area of 29.2mm^2. This tight group of results, visible in the scatter diagram in Figure 4.13, could have been a result of good arc stability. The stable arc, providing a continually consistent welding condition.

The most notable results from the HAZ area work, are those of flux-cored wires, SF-1A and Outershield. SF-1A seemed to produce a larger HAZ across all DFT

ranges. However, there was a trend, in that the area of the HAZ seemed to become smaller, when the DFT range was between 7.1-20µm. This was highlighted from the average HAZ area results, by the table in Appendix 18, Figure 4.10 and Figure 4.12. The results showed the majority of the HAZ areas for 7.1-20µm, dropped below those of DFT ranges 0-7µm and 20.1-45µm. However, a relationship between HAZ area and DFT within a range of 7.1-20µm seems unlikely and the results from Figures 4.10 and 4.13 were not definitive.

It was visible from the HAZ areas, that the SupraMIG solid wire created the hottest welding arc of all fillers used for this work (see Appendix 18). The results from testing with SupraMIG, showed some interesting findings at DFT range 0-7µm. This thickness range, where the primer was mechanically removed, produced welded samples with the smallest average penetration area (see Appendix 19). However, the same combination, produced the largest HAZ area (see Appendix 18). This outcome could have been a result, of a combination of the surface finish and the lack of surface coating. It could be suggested, that welding over the primer paint created a surface tension effect, that increased weld penetration. It could also be suggested, that the surface coating reduced the HAZ by slowing the spread of heat. This same trend was also visible with SM-3A while operating on DCEN polarity. However, this was not the case with SM-3A while operating on DCEP, which showed very little variation in HAZ area between all 3 DFT ranges.

When comparing SM-3A while operating on DCEN and on DCEP polarity, there was no unexpected results. All of the HAZ area and penetration area results showed lower values while the wire was operating on DCEN polarity. The area least affected by the change in polarity, was the HAZ area at DFT 0-7µm, which showed very little variation (see Appendix 18). However, there was a drop in HAZ area for DFT's 7.1-20 and 20.1-45µm. This could also suggest that the primer paint restricted the spread of heat. As previously mentioned in this section, there was little variation across all 3 DFT ranges for SM-3A on DCEP polarity. There was also no visible impact on the spread of heat, between any of the DFT ranges. This outcome could be relatable to the stable arc characteristics of the SM-3A DCEP wire. The stable arc could remove any prospect of the primer paint affecting the HAZ area. However, the absence of

any notable effect on the HAZ when welding with SM-3A on DCEN polarity and mixed results among the other filler types, casts doubt on any relationship. These factors make the theory, that the application of primer paint could reduce the size of the HAZ area of a welded joint, difficult to confirm.

5.4 Penetration Area

Figures 4.14 to 4.18 are scatter diagrams, that show the penetration area measurements taken from 5 welded samples for all 3 DFT ranges. There were 15 samples for each filler type and a total of 75. The table in Appendix 19 displays the totals and the averages for each filler type/DFT range combination. As with the previous sections, a table was used to highlight any notable trends in the relationship between DFT range and weld penetration.

SupraMIG solid wire produced an average penetration area at DFT range 7.1-20µm of 18.9mm^2 and 18.7mm^2 at DFT range 20.1-45µm. Both of these results showed little variation. However, the average penetration area for DFT range 0-7µm dropped down to a value of 17.5mm^2. This trend continued with SF-1A seamless flux-cored wire, where both DFT ranges 7.1-20µm and 20.1-45µm produced an average penetration area of 16mm^2 across the measured samples. DFT range 0-7µm created an average penetration area at the lesser value of 15.5mm^2. For Outershield folded type flux-cored wire, this trend was again visible. DFT range 0-7µm produced an average penetration area of 11.3mm^2, lower than that of DFT ranges 7.1-20µm and 20.1-45µm. Both higher DFT ranges, produced a greater penetration average of 12.1mm^2 and 12mm^2. As with SupraMIG and SF-1A, there was very little variation in average penetration between DFT ranges 7.1-20µm and 20.1-45µm.

SM-3A seamless metal-cored wire operating on DCEN polarity, showed a similar trend, in that DFT range 0-7µm produced the smallest average penetration area. However, unlike SupraMIG, SF-1A and Outershield, there is a larger variation in results between DFT ranges 7.1-20µm and 20.1-45µm. DFT range 7.1-20µm created an average penetration area of 7.8mm^2 and 20.1-45µm produced a larger average

penetration area at 9mm^2. Penetration values for SM-3A operating on DCEN, were the lowest recorded, this was likely due to the choice of polarity. When the polarity was switched to DCEP with SM-3A, it produced some of the largest penetration area measurements, similar to that of SupraMIG solid wire.

SM-3A seamless metal-cored wire operating on DCEP polarity, once again displayed a similar trend with DFT range 0-7μm. The combination produced the smallest average penetration area at 15.9mm^2. However, there was little variation between this and the result of 16.2mm^2 at DFT range 20.1-45μm. DFT range 7.1-20μm produced the largest average penetration area at 17mm^2.

Based on the experimental results, there is a notable relationship between weld penetration and primer paint DFT. The lowest DFT range of 0-7μm produced samples with the smallest average penetration area across 5 welded samples with all 5 filler types. As shown, the difference in penetration area at DFT range 0-7μm and the next largest, is of minimal value. SM-3A operating on DCEN polarity, shows a drop of 15% at DFT range 0-7μm, however this is likely affected by the DCEN polarity causing poor arc stability. The reduction in penetration among the commonly used filler types is only 2-6%.

- SupraMIG and DFT range 0-7μm – 6% less penetration
- SF-1A and DFT range 0-7μm – 3% less penetration
- SM-3A DCEN and DFT range 0-7μm – 15% less penetration
- Outershield and DFT range 0-7μm – 6% less penetration
- SM-3A DCEP and DFT range 0-7μm – 2% less penetration

It is difficult to understand, how a primer paint coating with a DFT of approximately 10-20μm, would increase the weld penetration of a near 3000°C welding arc. However, the testing carried out during this project, indicates that weld penetration may be marginally greater, when weld-through primers are used.

As mentioned in section 5.2, it is well known that adding some gases, such as helium, to an argon shielding gas mixture will create a hotter arc. This extra heat helps to increase weld penetration. It could be suggested, that zinc oxide and other gases from the primer compound or from thinners used during the application process, could have a similar affect. When these gases are released while welding over the primer paint, they may have an effect on the temperature of the welding arc. If an increase in welding arc temperature is present, there could be an increase in weld penetration.

As shown in Figure 3.1, the DFT range of 0-7μm was achieved by using a handheld grinder and a flapping disc. This produced a bright and mostly smooth surface finish. Another possible theory is that the introduction of the primer paint to the steel, created a surface tension effect that then increased weld penetration.

Further testing would be required, to allow analysis that would support or confirm, if primer paint has an effect on weld penetration.

5.5 Volume of Porosity with Varied Dry Film Thickness

Figures 4.19 to 4.26, display data taken from radiographic testing of 15 welded samples. A single sample was used for each combination of filler type and DFT range.

The results from the radiographic testing were displayed in the table in Appendix 20. For this section, SM-3A metal-cored wire operating on DCEN polarity was removed, to give the data more relevance to what would occur in a manufacturing environment. SM-3A is specifically designed for operation on DCEP polarity. So, it is likely that the high levels of porosity that are highlighted in Figure 4.21, were a result of the DCEN polarity.

Appendix 20 shows the results of the 4 filler types at the 3 DFT ranges, and the average porosity area across the 4 filler types at each DFT range. It may be possible, for similar data to be used as a rough guide for manufacturers who weld T-joint fillets on primed plate. This could allow them to forecast an approximation of

internal porosity over the weld length. With porosity being classed as a volumetric defect, should the manufacturer wish to use volume as the unit, it could be easily calculated using the known area. To create such a method, data would need to be collected from single sided and double-sided welding. The scope of experimental work for this thesis, included only single sided welding.

The following information, uses the data in Appendix 20 to display the relationship between the total area of internal porosity, over 70mm of weld and primer paint DFT. To simplify this data, an average of the DFT range was used for all 4 filler types. There is good cause to argue, that an increase in DFT will produce a greater volume of internal porosity. However, further trials with smaller DFT ranges and double-sided welding, would be required to fully establish and understand the relationship.

T-joint - Single sided fillet welding

Solid wire MAG using M21 shielding gas
- Avg. DFT 3.5μm produces ~ 0mm^2 per 70mm of weld length
- Avg. DFT 13.5μm produces ~ 1.3mm^2 per 70mm of weld length
- Avg. DFT 32.5μm produces ~ 16.6mm^2 per 70mm of weld length

Seamless FCAW using M21 shielding gas
- Avg. DFT 3.5μm produces ~ 0.9mm^2 per 70mm of weld length
- Avg. DFT 13.5μm produces ~ 0.9mm^2 per 70mm of weld length
- Avg. DFT 32.5μm produces ~ 18.7mm^2 per 70mm of weld length

Conventional folded type FCAW using M21 shielding gas
- Avg. DFT 3.5μm produces ~ 2.1mm^2 per 70mm of weld length
- Avg. DFT 13.5μm produces ~ 9.3mm^2 per 70mm of weld length
- Avg. DFT 32.5μm produces ~ 22.6mm^2 per 70mm of weld length

Seamless MCAW using M21 shielding gas
- Avg. DFT 3.5μm produces ~ 0mm^2 per 70mm of weld length
- Avg. DFT 13.5μm produces ~ 0mm^2 per 70mm of weld length
- Avg. DFT 32.5μm produces ~ 5.7mm^2 per 70mm of weld length

Although the principal purpose of this work, was to focus on each filler type and look at the changes occurring with varying DFT. It is also worth comparing the performance of the filler types at each DFT range. Figures 4.24 to 4.26 provide data that allowed for a performance analysis.

It is notable that the SF-1A seamless flux-cored wire performed better than the Outershield folded-type flux-cored wire across all 3 DFT ranges. It is likely that the reduced volume of internal porosity, was a result of the very low H$_2$ content of the

seamless wire. This reduction in H_2, means less residual gas formation during welding. These results coincide with research by Boekholt [4]. Non copper coated folded type cored wires are also commonly drawn down to the desired diameter with the aid of a soap substance. This substance can create more gas/fume that may also add to the volume of internal porosity.

SupraMIG solid wire performed better than both the seamless and folded type cored wires when the DFT range was 20.1-45µm. This could be due to the minimal H_2 content of the solid wire, having no hygroscopic core. This finding is contradictory to the research of Boekholt, which found solid MIG wire to be more susceptible to porosity, when welding over shop primers [4].

The filler type that showed the most resistance to porosity when welding over a primed surface, was the SM-3A seamless metal-cored wire operating on DCEP. This affirmed the same conclusion from research by Boekholt [4]. The research also showed seamless metal cored wire, to be the welding consumable least sensitive to porosity, as a result of weld-through shop primers. This wire showed porosity levels lower than all other filler types, across all DFT ranges, and only showed visible porosity when the DFT range was 20.1-45µm. At the highest DFT range of 20.1-45µm, the porosity area was $5.7mm^2$, over 70mm of weld. This was 66% less than the total porosity area of the next highest reading. The very low H_2 content of the seamless wire will have reduced the residual gas available to become trapped within the weld. However, there may also be the added advantage of good arc stability. This may have given, the metal-cored wire an advantage over the solid wire. It is also conceivable, that the deep, focused penetration achieved when using a metal-cored wire, helped to prevent residual gases becoming trapped, by forcing them out. Removal of these gases would reduce the chances of internal weld metal porosity forming during solidification.

6.0   Conclusions

6.1 Dry Film Thickness Accuracy

- This work casts doubt on the achievability of DFT ranges specified in manufacturer data sheets.
- This work has demonstrated that the measurement of DFT lacks a reasonable consistency and accuracy.
- Higher DFT levels are caused by overspray.
- The average DFT may be within specification but there is considerable variation around it.

6.2 Hardness

- Hardness has not been affected by variations in DFT.
- Hardness results suggest that there has been no significant change in arc temperature, as a result of gas shield contamination from the vaporising primer.

6.3 Heat Affected Zone Area

- There seems to be a relationship between DFT 7.1-20µm and HAZ area, i.e., smaller HAZ areas were found in the 7.1-20µm thickness range. Larger HAZ areas were found in the group < 7.1µm. This could indicate that the thicker average DFT was limiting the spread of heat, to some extent.

6.4 <u>Penetration Area</u>

- A tentative relationship existed between DFT and weld penetration, i.e., the thinner the DFT, then the smaller the penetration. This could be related to the surface tension effects created from the thicker primer. The preferential flow would be from the outside to the inside in the thicker DFT welds. That would agree, to some extent with the HAZ – DFT findings.
- SupraMIG solid wire produced the greatest penetration area.
- SM-3A metal-cored wire operating on DCEN, produced the least penetration area at all 3 DFT ranges, this reduction in penetration is a result of the DCEN polarity used.
- Outershield folded type flux-cored wire produced the smallest penetration area at all 3 DFT ranges, of the wires operating on DCEP polarity.

6.5 <u>Porosity - The Effect of Dry Film Thickness</u>

- The lowest DFT, had the lowest volume of porosity. This is explained by the lowest DFT having the lowest volatile levels which could lead to porosity.

6.6 <u>Porosity – Different Filler Types Reaction to Similar Dry Film Thickness</u>

- Different wires create different conditions for the generation of porosity with a weld.
- Seamless metal cored wire has the best overall performance when welding over primer.
- Solid wire performs best when compared to flux cored wires.
- Seamless flux cored wires perform better than conventional folded wires.

7.0   Recommendations for Future Work

7.1 The Effect of Surface Finish on Weld Penetration

- Quite clearly, the role of primers in the welding process is potentially very complex. This is due to the significant number of potential variables involved. Standards of surface preparation could be a factor and should be investigated against the main measurables, such as penetration and hardness.

7.2 Estimating Levels of Internal Porosity

- There may be a relationship between DFT and internal weld metal porosity. If tighter control of the DFT could be obtained, then it may be viable to investigate the development of a method for estimating internal porosity in a fillet weld when primer is used.
- In addition, the introduction of double-sided welding as a variable, which is common in structural welding.
- Introducing other variables such as fit-up gap, would further develop this work.

References

1. Cairns, Jonathan and McPherson, Norman and Galloway, Alexander and MacPherson, Malcolm and McKechnie, Crawford. (2013) *Optimised penetration for fillet welding. In: 17th International Conference on Joining Materials*, JOM 17, 2013-05-05 - 2013- 05-08.

2. British Standards Institution (2017) BS 15614-1, *Specification and qualification of welding procedures for metallic materials - welding procedure test - Part 1: Arc and gas welding of steels and arc welding of nickel and nickel alloys. Available at:* https://www.iso.org/standard/51792.html

3. Cairns, J.W.P. and McPherson, N.A. and Galloway, A.M. (2015) *Identification of key GMAW fillet weld parameters and interactions using artificial neural networks*. Welding and Cutting, 15 (1). pp51-57. ISSN 1612-3433.

4. Boekholt, R. (1996) *Welding mechanisation and automation in shipbuilding worldwide*. Cambridge, Abington Publication, pp1, 133, 136.

5. Cozens, Mark (2002) *Fillet Welded Joints - A Review of the Practicalities*, The Welding Institute, Cambridge. https://www.twi-global.com/technical-knowledge/job-knowledge/fillet-welded-joints-a-review-of-the-practicalities-066

6. British Standards Institution (2013) *BS 2553-5.5 - Welding and Allied Processes - Symbolic representation on drawings - Welded Joints.* Available at: https://www.iso.org/obp/ui/#iso:std:72740:en

7. The Welding Institute Ltd. (2004) *A General Review of the Causes and Acceptance of Shape Imperfections – Part 2,* Cambridge. http://www.twi-global.com/technical-knowledge/job-knowledge/a-general-review-of-the-causes-and-acceptance-of-shape-imperfections-part-2-068/

8. Easterling, K. (1992) *Introduction to the physical metallurgy of welding*. 2nd edn. Butterworths, UK.

9. Grong, Ø. (1994) *Metallurgical Modelling of Welding*, 2nd edn. Norway, Norwegian University of Science and Technology, pp26.

10. British Standards Institution (2015) BS 18491 – Welding and Allied Processes – Guidelines for Measurement of Welding Energies. Available at: https://www.iso.org/obp/ui/#iso:std:iso:tr:18491:ed-1:v1:en

11. Higgins, Raymond A. (2011) *Materials for Engineers and Technicians*, 5th edn. Abington: Routledge, pp.349.

12. The Welding Institute Ltd. (2011) *Materials and their Behaviour*, Cambridge.

13. Davies, A.C. (1992) *The Science and practice of welding Volume 1,* 10th edn. Cambridge: Press Syndicate of the University of Cambridge, pp.94-115.

14. Davies, A.C (1993) *The Science and practice of welding Volume 2*, 10th edn. Cambridge: Press Syndicate of the University of Cambridge, pp.92-119.

15. The Welding Institute Ltd. (2013) *MIG/MAG Welding – Welding Processes and Equipment*, Cambridge.

16. Binzel-Abicor UK (2020) *MIG/MAG Welding Torches.* https://www.binzel-abicor.com/UK/eng/products/manual/migmag-torches/

17. The Welding Institute Ltd. (2013) *Current and Polarity – Welding Processes and Equipment*, Cambridge.

18. Phillips, D.H. (2016) *Welding Engineering an Introduction*, West Sussex, John Wiley & Sons Ltd. pp.9-10.

19. Millar, D.W. (2013) *Modern seamless gas shielded flux cored arc welding (GSFCAW) & gas shielded metal cored arc welding (GSMCAW) wires for high productivity.* Welding and Cutting 12, pp.86-88.

20. Gullco International (2020) *KAT Welding Automation Carriage*, Canada. https://www.gullco.com/welding-automation.html

21. Widgery, D. The Institute of Materials, Minerals and Mining (2005) *New Developments in Advanced Welding*, Cambridge, Woodhead Publishing Ltd, pp31-33, 36.

22. Nittetsu (2010) *Seamless Cored Wire Brochure,* Tokyo, Japan.

23. NST Welding Ltd (2014), *Seamless Cored Wires,* Vikersund, Norway. http://nst.no/dokumenter/diverse/NST%20Digital%20Catalogue%20EN%202016%20web.pdf

24. Myers, D. (2005) *Advantages and Disadvantages of Metal Cored wires*. ESAB Knowledge Centre: https://www.esabna.com/us/en/education/blog/advantages-and-disadvantages-of-metal-cored-wires.cfm

25. Kobelco (2015) *Weld Imperfections and Preventive Measures*, Tokyo, Japan, Kobe Steel. Ltd, pp9-10.

26. The Welding Institute Ltd. (2007) – *CSWIP 3.1 Welding Inspector,* Cambridge.

27. Moore, P. and Booth, G. (2015) *The Welding Engineer's Guide to Fracture and Fatigue*, Cambridge, Woodhead Publishing, pp.143-145.

28. The James F. Lincoln Arc Welding Foundation (2000) *The Procedure Handbook of Arc Welding*, 14th edn, Cleveland, pp11.2-6, 11.2-11.

29. Halmshaw, R. (1997). *Introduction to the Non-Destructive Testing of Welded Joints*. 2nd edn, Cambridge, Abington Publishing, pp. 5-48.

30. British Standards Institution (2013) *BS 17639, Destructive tests on welds in metallic materials - Macroscopic and microscopic examination of welds*, pp.4-5, Available at: https://shop.bsigroup.com/ProductDetail?pid=000000000030273879

31. American Society for Metals, (1976) *Metals Handbook Vol 11, Non-destructive Inspection and Quality Control*, 8th edn, Ohio, USA, ASM Handbook Committee, pp.13-15.

32. Feldt, R.L, Montle, J.F and Skiles, E.W (1969) *Weldable Primer Patent*, Delaware, United States Patent Office.

33. Khanna, A.S (2008) *High Performance Organic Coatings*, Cambridge, Woodhead Publishing Ltd. 1.2, pp.38-42.

34. Khanna, A.S and Kumar, S (2008) *High Performance Organic Coatings*, Cambridge, Woodhead Publishing Ltd. 4.11.1, pp.158.

35. Mallik. B.P. (2008) *High Performance Organic Coatings*, Cambridge, Woodhead Publishing Ltd. 6.7.4, pp.248-249.

36. Kanitkar, S. (2008) *High Performance Organic Coatings*, Cambridge, Woodhead Publishing Ltd. 8, pp.321-323.

37. Bahadori, A. (2015) *Essentials of Coating, Painting and Lining for the Oil and Gas and Petrochemical Industries*, Oxford, Elsevier Publishing Ltd. 10.4, pp.594-597.

38. British Standards Institution (2003) BS 17652-2: Welding – Test for shop primers in relation to welding and allied processes – part 2: Welding properties of shop primers. Available at:
https://www.iso.org/standard/33399.html

39. British Standards Institution (2007) BS 8501-1: Preparation of steel substrates before application of paints and related products. Visual assessment of surface cleanliness. Rust grades and preparation grades of uncoated steel substrates and of steel substrates after overall removal of previous coatings.
https://shop.bsigroup.com/ProductDetail?pid=000000000030172785

40. Lloyds Rules (2016) The manufacture and certification of material – Section 3.8 – Table 3.3.7 Mechanical properties for acceptance purposes. Available at: https://www.lr.org/en-gb/rules-for-the-manufacture-testing-and-certification-of-materials/

Appendices

*Appendix 1 – Iron – Carbon Phase Diagram. Adapted from
The Welding Institute [12].*
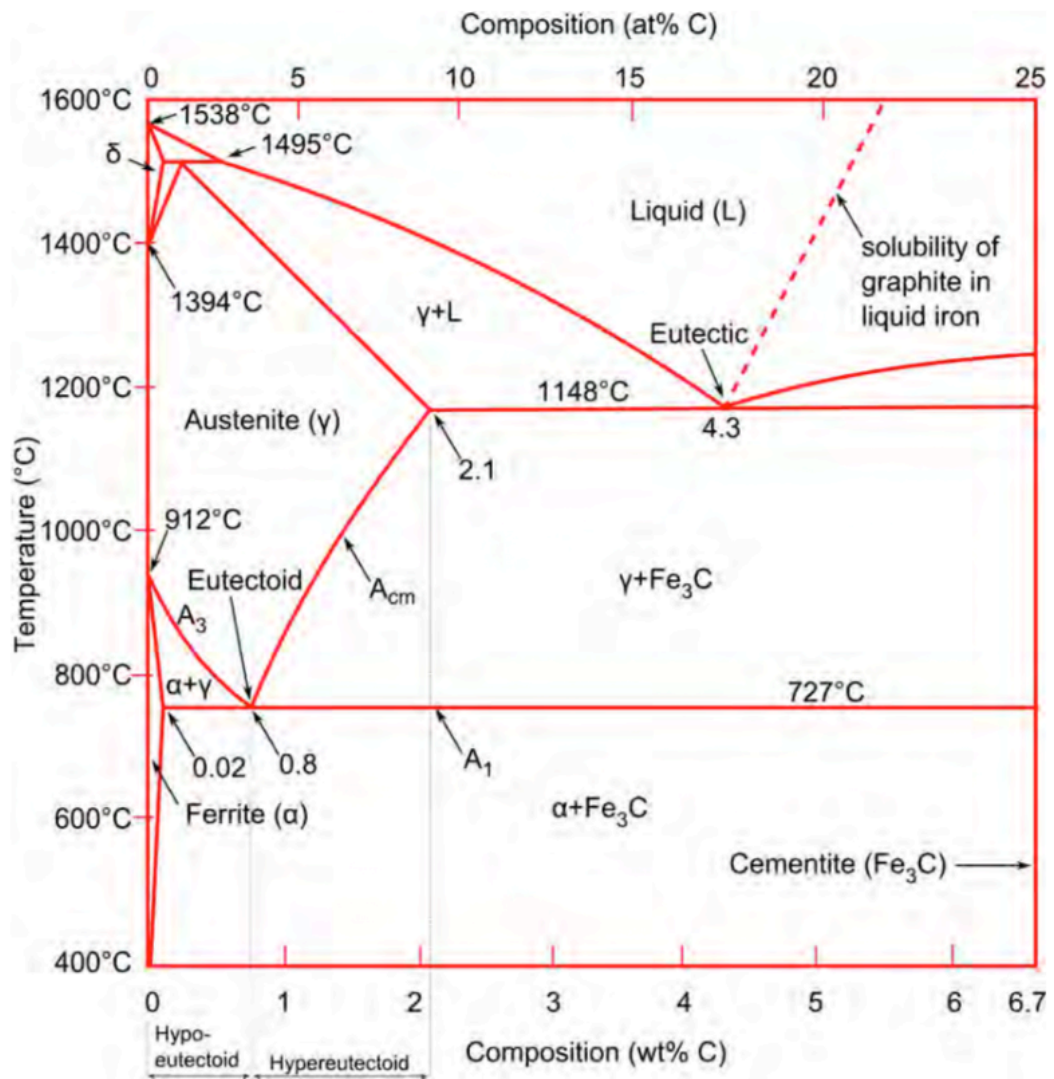
Appendix 2 – Iron – Carbon Phase Diagram. This figure shows the phase transformation in the microstructure as the material cools. Adapted from The Welding Institute [12].
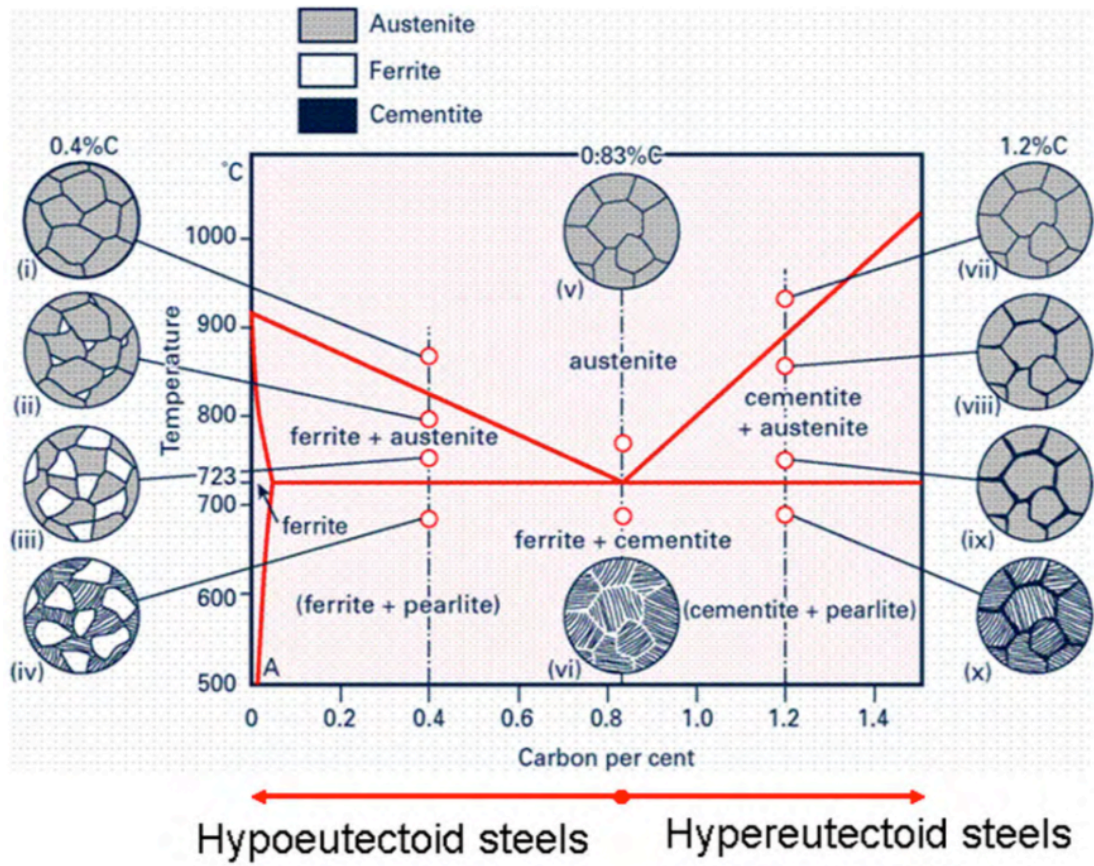
Appendix 3 – An extract from Lloyds Rules for the manufacture and certification of materials. This table gives mechanical acceptance criteria for Lloyds naval grade steels [40].

Grades (see Note 3)	Yield Stress N/mm² min.	Tensile Strength N/mm²	Elongation on $565\sqrt{S_o}$ % min. (see Note 2)	Charpy V-notch impact tests (*see* Notes 3, 4 and 5)					
				Average energy J minimum					
				t ≤50 mm		50 < t ≤70 mm		70 < t ≤100 mm	
				Longitudinal	Transverse	Longitudinal	Transverse	Longitudinal	Transverse
AH 36 DH 36 EH 36 FH 36	355	490-630	21	34	24	41	27	50	34

Impact tests are to be made on the various grades at the following temperatures:

AH grades 0°C
DH grades -20°C
EH grades -40°C
FH grades -60°C

SSAB

	MILL SHEET AND TEST CERTIFICATE	1/4
	LLOYD'S REGISTER EMEA (EN 10 204-3.2/LR)	A 27510 –001 10.07.2015

Tilaaja Purchaser	Vastaanottaja Consignee	Päivämäärä Date
DENT STEEL SERVICES (YORKSHIRE) LTD LOW MOOR STEELWORKS NEW WORKS ROAD, LOW MOOR BD12 0QN BRADFORD GREAT BRITAI	DENT STEEL SERVICES (YORKSHIRE) LTD LOW MOOR STEELWORKS NEW WORKS ROAD, LOW MOOR BD12 0QN BRADFORD GREAT BRITAI	13.07.2015 HEL 1500407/3
Tilaus nro Order No. P069030	Asiakkaan merkki Shipping mark	Valmistajan merkki Mark of the Manufacturer
Tilausvahvistus Order Confirmation 27510		

Todistus Certificate: LR — Laivaus Shipping: EMSDOLLART — Laatuleimaus Quality Stamping: LR DH 36

Toimitustyyppi Delivery type: PART DELIVERY
Sulatus nro levy nro Cast No. Plate No. XXXXX XXX XX XXX

Tuote Product: HEAVY PLATES
Laji Grade: LR DH 36 LR RULES OF MATERIALS CH3:2014
Toleranssit Tolerances: EN 10029:2010 CLASS B/SOCIETY'S RULES
Laatuselvitys Quality Specifications: HIGH STRENGTH STEEL FOR SHIP STRUCTURES

Tarkastajan leima Stamp of Inspector — Vastaanottajan leima Stamp of Surveyor — Muut leimaukset Other Stamps

Positio Item	Mitat mm Dimensions mm			Merkki Marke	Kpl Pos	Paino kg Weight kg	Sulatus levy nro Cast plate No		SP nro UT MT SP No UT MT
FLATNESS DEVIATION MAX. 6 MM/M									
NORMALIZED STEEL PLATES									
SURFACE CONDITION EN 10 163–2:2005 CLASS A1									
001	5.00 X 2000	X	4000		6	1884	30794	533	021
001	5.00 X 2000	X	4000		6	1884	31376	014	014
001	5.00 X 2000	X	4000		6	1884	31376	015	014
SURFACE CONDITION EN 10 163–2:2005 CLASS A1									
002	6.00 X 2000	X	4000		6	2262	33956	010	010
002	6.00 X 2000	X	4000		6	2262	33956	011	010
002	6.00 X 2000	X	4000		6	2262	33956	012	010
002	6.00 X 2000	X	4000		6	2262	33956	013	010
002	6.00 X 2000	X	4000		6	2262	33956	014	010
002	6.00 X 2000	X	4000		6	2262	33956	015	010
002	6.00 X 2000	X	4000		6	2262	33956	016	010
HOT ROLLED STEEL PLATES									

HIGH STRENGTH STEEL FOR SHIP STRUCTURES

Pos. Item	Sulatus, k.erä nro Cast. test No		T-tila Cond	Vetokoe Tensile test												
				K2	°C	RP02 MPa	RT05 MPa	REL MPa	REH MPa	RM MPa 1	2	3	A % 50	80	200	REH /RM
001	30794	021	N	11					429	542			30			
001	31376	014	N	11					410	541			32			
002	33956	010	N	11					409	524			32			
003	33956	042	NR	11					409	538			29			
003	33956	047	NR	11					430	557			30			
003	33956	048	NR	11					451	551			28			
003	33956	058	NR	11					451	555			28			
004	33957	022	NR	11					439	560			27			
005	33761	051	NR	11					457	569			26			
006	33761	051	NR	11					457	569			26			
007	34045	013	NR	11					440	570			27			
008	32610	012	NR	51					432	581			24			

K2: 11=TOP,TRANSV. 51=BOTTOM,TRANSV.

N =NORMALIZED NR=NORMALIZING ROLLING

Pos. Item	Sulatus k.erä nro Cast. test No		Iskukoe Impact test						Sitkeämurtuma Ductile fracture				Erikoiskokeet Special tests			
			K3	°C	1	2	3	Keskiarvo Average	1	2	3	Keskiarvo Average	K4	°C	1	2
001	30794	021	117	–020	117	123	114	118								
001	31376	014	117	–020	120	116	120	119								
002	33956	010	117	–020	149	152	146	149								
003	33956	042	117	–020	204	217	174	198								
003	33956	047	117	–020	220	211	196	209								
004	33957	022	115	–020	159	165	176	167								
005	33761	051	111	–020	220	259	226	235								
006	33761	051	111	–020	220	259	226	235								
007	34045	013	111	–020	196	186	184	189								
008	32610	012	151	–020	137	173	162	157								

K3: 117=CH-V/ISO-V(J),TX10,TOP,LONGIT,KV600 115=CH-V/ISO-V(J),7.5X10,TOP,LONGIT,KV600 111=CH-V/ISO-V(J),10X10,TOP,LONGIT,KV600 151=CH-V/ISO-V(J),1(

Sulatus nro Cast No Schmelzen Nr No de coulén Nº Плавки	Koe nro Test No Prüf Nr. Essai No Nº Пробы	Positio Pos. Pos. Poste Поз	Cekv Ceq Cäq Cëq Cekv	Analyysi % Chemical composition % Chemisch Zusammensetzung % Composition Chimique % Анализ плавки % (*=ppm)													
				C	SI	MN	P	S	AL	NB	V	TI	CU	CR	NI	MO	CA
30794		001	.41	.153	.37	1.40	.009	.005	.034	.009	.009	.005	.025	0.06	0.05	.007	.003
31376		001	.41	.154	.37	1.41	.012	.005	.038	.011	.010	.004	.021	0.05	0.04	.005	.003
33956		002	.40	.143	.38	1.43	.012	.007	.033	.010	.011	.004	.028	0.06	0.04	.008	.000
33956		003	.40	.143	.38	1.43	.012	.007	.033	.010	.011	.004	.028	0.06	0.04	.008	.000
33957		004	.41	.156	.38	1.42	.011	.008	.032	.011	.015	.003	.029	0.05	0.04	.007	.000
33761		005	.41	.154	.45	1.40	.013	.003	.029	.042	.009	.004	.024	0.05	0.04	.006	.002
33761		006	.41	.154	.45	1.40	.013	.003	.029	.042	.009	.004	.024	0.05	0.04	.006	.002
34045		007	.43	.164	.44	1.45	.012	.002	.030	.041	.011	.005	.028	0.06	0.06	.006	.002
32610		008	.43	.165	.48	1.47	.010	.001	.034	.042	.020	.006	.035	0.03	0.04	.006	.002

Appendix 5 – Certified Material Test Report for NSSW SF-1A.

Certified Material Test Report	Hikari Plant
According to EN 10204, type 3.1	Nippon Steel & Sumikin Welding Co., Ltd.
Test Report No. : 1515207V	Purchaser : Norsk Sveiseteknikk AS
Date of issue : January 05, 2016	Purchaser's Spec.No. NSTV-4 Rev.1
	Level of testing : ISO 14344 Schedule 4

1. Materials

Trade Designation	Size	Manufacturing No.	Manufacturing Date
NSSW SF-1A ※	1.2 mm	5Q162FP960	October 06, 2015

※ Applicable code : EN ISO 17632-A-T 42 2 Z P M 1 H5

2. Welding Conditions (Test type : ISO)

Base Metal (mm)	SM490A 20tx250wx300l	Welding Position	Flat	Kind of Gas	80%Ar +20%CO2	Wire extension (mm)	25

	Current DC(+) (A)	Voltage (V)	Travel Speed (cm/min)	Flow Rate of Gas (l/min)	Preheat Temp. (℃)	Interpass Temp. (℃)
	270	27	25	25	22	140〜160
Spec.	270±10	27±2	28±3	20〜25	15 min.	135〜163

3. Test results of All-Weld-Metal (Test type : ISO)

Tension Test	Conditions	Yield Strength (MPa)	Tensile Strength (MPa)	Elongation(%)
	AW	514	575	25
Spec.	AW	420 min.	500〜640	20 min. A5

Impact Test (J)	Conditions	Temp. (℃)	Ind. Value			Ave.
	AW	-20	89	81	86	85
Spec.	AW	-20	32 min.			47 min.

Chemical composition (%)																	
	C	Si	Mn	P	S	Cu											
	0.04	0.54	1.27	0.015	0.006	0.27											
Spec.	0.03/ 0.07	0.30/ 0.70	1.10/ 1.60	0.030 max.	0.025 max.	0.35 max.											

S,P and N of the strip : Below specified maximum.

4. Hydrogen Content of Deposited Metal (Acc. to ISO 3690)

HDM (ml/100g)			Ave.
3.2	3.7	3.6	3.5
Spec.		—	5 max.

Statement :
We hereby certify that the contents of this report are correct and accurate, and all operations performed by us or our subcontractors are in compliance with the requirements of the DATA SHEET No. : NSTV-4 Rev.1

No. 151016HFH (MIT 7854)

Net Weight
5Q162FP960 : 19,500.0 kg

Certified by SHUSHIRO NAGASHIMA
Group Manager, Quality Control Dept.

This is electronically made and is not signed.

Appendix 6 – Certified Material Test Report for NSSW SM-3A.

Certified Material Test Report According to EN 10204,type 3.1	Chiba Plant (Narashino) Nippon Steel & Sumikin Welding Co.,Ltd.
Test Report No.　：　N04567　Rev.1	Purchaser : Norsk Sveiseteknikk AS
Date of issue　　：　November 12, 2015	Purchaser's Spec.No.：　NSTN-07　Rev.0

1.Materials

Trade Designation	Size	Manufacturing No.	Lot No.	Manufacturing Date
NSSW　SM-3A　※	1.2 mm	5X581BW960	5Y251	March 20, 2015
NSSW　SM-3A　※	1.2 mm	5X671BW960	5Y251	March 23, 2015
NSSW　SM-3A　※	1.2 mm	5X701BW960	5Y251	March 24, 2015
NSSW　SM-3A　※	1.2 mm	5X761BW960	5Y251	March 26, 2015
NSSW　SM-3A　※	1.2 mm	5X791BW960	5Y251	March 27, 2015

※　Applicable code : AWS A5.18-2010 E70C-GM, EN ISO 17632-A-T 42 4 Z M M 1 H5

2.Welding Conditions

Base Metal (mm)	KL33 20tx250wx300L	Welding Position	Flat		Hydrogen Content of Deposited Metal	
Current DC(+) (A)	270	Kind of Gas	80%Ar+20%CO$_2$		Acc. To ISO 3690	
Voltage (V)	30	Flow Rate of Gas (l/min)	25		HDM (ml/100g)	Ave.
Travel Speed (cm/min)	30	Preheat/Inter-pass Temp.(℃)	15 / 150±15		1.3, 1.3, 1.2	1.3
Wire extension (mm)	20					

3. Test results of All-Weld-Metal

Tension Test	Conditions	Yield Strength (MPa)	Tensile Strength (MPa)	Elongation(%)
	AW	477	556	27

Impact Test (J)	Conditions	Temp. (℃)	Ind. Value	Ave.
	AW	-40	134, 128, 117	126

・Radiographic Test : A5.18 acceptable

Chemical composition (%)											
C	Si	Mn	P	S	Cu	Ni	Cr	Mo	V	Nb	Ti, B, Al, As, Sb, Pb
0.04	0.51	1.39	0.009	0.013	0.22	0.01	0.01	0.01	0.01	0.01	* * * * * *

*Below specified maximum

Other elements of the Data Sheet : Below specified maximum
S.P and N of the strip : Below specified maximum

Statement：
We hereby certify that the contents of this report are correct and accurate, and all operations performed by us or our subcontractors are in compliance with the requirements of the DATA SHEET No.:
NSTN-07 Rev.0

No. 150825HFH　　　（ MIT　7731 ）

Net Weight

5X581BW960	:	1,775	kg
5X671BW960	:	3,537.5	kg
5X701BW960	:	2,812.5	kg
5X761BW960	:	4,662.5	kg
5X791BW960	:	587.5	kg

Certified by　　　　ISAO　KANAUCHI

Group Manager, Quality Control Dept.

This is electronically made and is not signed.

Appendix 7 – Certified Material Test Report for Lincoln SupraMIG.

Test Report

LINCOLN ELECTRIC
THE WELDING EXPERTS®

Product **SupraMIG**
Size(s) mm **1.2 x 15 Kg Plastic Random**
Item No. **16S1215PR**
Lot/Batch **E1MG170139**

Product Line

Class   AWS A5.18 ER70S-6
ISO14341-A: G 46 4 M21 3Si1 / G42 3 C1 3Si
ISO 14341-A : G42 3 C1 3Si1

Customer Ref **PO- 6334**
Our Reference **0809505789 - 02.03.2017**
Quantity **360.0 SP**
Customer **BHC LIMITED**

EDINBURGH ROAD
CARNWATH ML11 8HS
United Kingdom

Chemical analysis (%)   According to EN10204 2.2

C	Si	Mn	P	S	Cr	Ni	Mo	Cu	V	Al	N	Ti+Zr
0.081	0.86	1.46	0.011	0.007	0.04	0.02	0.01	0.02	<0.01	0.002	0.007	0.008

Mechanical test, Wire. RM (MPa)   According to EN10204 2.2
Tensile testing   **Impact testing**

ReL	Rm	A5	Temp.	KV
MPa	MPa	%	°C	J
502	574	28	-40	102

Remarks

The product identified above has been manufactured, tested and supplied in compliance with a certified ISO 9001 Quality Assurance Programme.

Company
Lincoln Electric UK Limited
Mansfield Road
S26 2BS Aston, Sheffield
United Kingdom

LINCOLN ELECTRIC (UK) LIMITED
QUALITY ASSURANCE

Printed By **Thomas Rooney**
Function
Date **13/MAR/2017**

Cert. No.
00334228
ZEU_CMN , 1

Inspection Certificate 3.1

LINCOLN ELECTRIC

OERLIKON **SAF-FRO**

Product	**OUTERSHIELD 71E-H**
Size(s) mm	**1,2**
Item No.	**900118**
Lot/Batch	**P1FC120142**
Product Line	**FCAW Wire**
Class	**AWS A5.20:E71T-1M-JH4 AWS A5.20 : E71T-1C-H4**
	EN ISO 17632-A: T46 3 P M 1 H5 EN ISO 17632-A

Chemical analysis (%) — According to EN10204 3.1

C	Si	Mn	P	S	Cr	Ni	Mo	Nb	Cu	V	Ti	B
0.040	0.41	1.30	0.016	0.011	0.04	0.03	<0.01	0.02	0.10	0.01	0.030	0.0026
N												
0.005												

Mechanical tests, all weld metal — According to EN10204 2.2
Tensile testing **Impact testing**

Cond.	Temp. °C	Rp0.2 N/mm2	Rm N/mm2	A5 %		Cond.	Temp. °C	KV J	Temp. °C	KV J
AW	RT	581	636	26		AW	-20	127	-30	111

Diffusible hydrogen — According to EN10204 3.1

HDM as Manufactured
4 ml/100g

Remarks

The product identified above has been manufactured, tested and supplied in compliance with a certified ISO 9001 Quality Assurance Programme.

Company		Printed		Cert. No.
Lincoln Electric UK Limited	Harris Calorific International Sp. z o.o. Kierownik Kontroli Jakości *Remigiusz Polaczek* *Remigiusz Polaczek*	By	**Thomas Rooney**	**00617428**
Mansfield Road		Function		ZEU_CMN_FCW , 1
S26 2BS Aston, Sheffield		Date	**21/DEC/2018**	
United Kingdom				

Appendix 9 – NST storage and handling recommendations for seamless flux-cored and metal-cored welding wires. Adapted NST Welding UK Ltd. [23].

Flux cored wires.

NST

Storage and handling.

Storage and handling.
NST and NSSW (Nittetsu) seamless flux and metal cored wires are manufactured in a manner which provides wires with no open seams, preventing moisture from penetrating the wire.
NST/NSSW seamless wires provides the customer with a product that has a guaranteed low hydrogen control (the only point of ingress for moisture is at the start and end of the wire).
The seamless manufacturing process has the additional benefit of enabling the wire to be copper coated, this provides extended shelf life due to rust prevention, prevents down time with liner cleaning and provides excellent electrical pick up from the welding tip (copper to copper).

Method of storage
To ensure the wire is used at its optimum the following guidelines should be observed:
▪ Welding materials shall be stored inside, away from rain, snow and dew.
▪ Welding materials should be stored off the floor, preferably on wooden pallets which enable air circulation to take place (10cm off the floor, and 10cm off the wall).
▪ It is desirable to store materials places where the temperature is below 30°C and the relative humidity is less than 80%.
▪ Environments where rusting tends to occur due to sea breeze, SO2 gas etc., should be avoided.
▪ A plan should be devised to use materials on a first in, first out basis.
▪ The packing shipped from the manufacturer must be kept as it is until just before use.

Period of storage – quality guarantee period
The quality guarantee period of seamless flux cored wire shall be for 24 months after production as long as they have been stored under the conditions specified in "methods of storage" above. However, products can be used even after the lapse of the above mentiond period if no physical or chemical changes such as rusting, discoloration etc. are observed on the surface of the wires.

Handling
It is advised that opened cartons should be used within 5 days.
This period can be extended longer, however wire inspection should take place regularly to check for rust formation (when rust spots are observed the remaining wire should be disposed of).

Hydrogen levels
As part of the manufacturing process hydrogen measurements are taken of all NST and Nittetsu seamless flux cored seamless wires (this data is available on the wire batch certificate).

Aug 2014   REV:7

Perfect Welding   www.nst.no

International.

Interplate 855
IMO Resolution MSC.215 (82) compliant Zinc Silicate Shop Primer

PRODUCT DESCRIPTION	A two pack, zinc silicate shop (pre-construction) primer providing good corrosion protection even after heating upto 800°C and resistance to damage caused by welding, gas cutting and fairing. Suitable for fast welding processes and offers control of secondary surface preparation requirements.
INTENDED USES	As a shop (pre-construction) primer for the protection of steel during fabrication and assembly. Suitable for use with controlled cathodic protection. For use at Newbuilding.

PRODUCT INFORMATION

Colour	NQA855-Red Brown, NQA856-Grey, NQA858-Dark Green (Mercosul - Argentina, Brazil, Chile & Uruguay only)
System Film Thickness	1 coat at 15 microns dry (60 microns wet) per coat
Finish/Sheen	Matt
Part B (Curing Agent)	NQA857
Volume Solids	25% ±2% (ISO 3233:1998)
Mix Ratio	0.67 volume(s) Part A to 1 volume(s) Part B
Specific Gravity	Paste (Part A) 1.894-1.991 Binder (Part B) 0.86-0.89 Mixed Paint 1.274-1.332
Theoretical Coverage	16.7 m²/litre at 15 microns dft, allow appropriate loss factors
Method of Application	Airless Spray, Brush, Conventional Spray, Roller
Flash Point	Part A 5°C; Part B 10°C; Mixed 13°C

Drying Information	5°C	10°C	25°C	35°C
Hard Dry [ISO 9117:90]			5 mins	4 mins
Pot Life	24 hrs	24 hrs	24 hrs	8 hrs

Overcoating Data - see limitations

	Substrate Temperature							
	5°C		10°C		25°C		35°C	
Overcoated By	Min	Max	Min	Max	Min	Max	Min	Max

Note Consult International Paint, minimum of 7 days for appropriate primers.

REGULATORY DATA	**VOC**	628 g/lt as supplied (EPA Method 24) 472 g/kg of liquid paint as supplied. EU Solvent Emissions Directive (Council Directive 1999/13/EC)
		Note: VOC values are typical and are provided for guidance purposes only. These may be subject to variation depending on factors such as differences in colour and normal manufacturing tolerances.

International.

Interplate 855

IMO Resolution MSC.215 (82)
compliant Zinc Silicate Shop Primer

CERTIFICATION

When used as part of an approved scheme, this material has the following certification:

- Weld Fumes - Trace Gas Measurement during Welding (SLV)
- Weld Fumes - Thermal Degradation on Welding (NOHA)
- Weld Quality - Approved for Overweldable Shop Primers (GL)
- Weld Quality - Approval of Prefabrication Primers (LR)
- Weld Quality - Shop Primers for Corrosion Protection of Steel Plates and Structures (DNV)
- Weld Quality - Russian Maritime Register of Shipping
- Weld Quality - Weldable Prefabrication Shop Primer (ABS)

- IMO PSPC Resolution MSC.215 (82) - Det Norske Veritas (DNV)
- IMO PSPC Resolution MSC.215 (82) - Registro Italiano Navale (RINA)
- IMO PSPC Resolution MSC.215 (82) - Lloyds Register (LR)

Consult your International Paint representative for details.

SURFACE PREPARATIONS

Use in accordance with the standard Worldwide Marine Specifications.
All surfaces to be coated should be clean, dry and free from contamination.

NEWBUILDING

Shop primers should be applied using automatic blasting/spraying equipment.
Blast to a minimum of Sa2½ (ISO 8501-1:2007) or St2 for insulation part inside. Steel grit or a mixture of steel grit of particle size 0.6-1.0mm (24-39 mils) and steel shot of particles size 0.6-1.4mm (24-55 mils) are normally used to give a predominantly angular profile.
Apply Interplate 855 before oxidation occurs. If oxidation does occur the entire oxidised area should be reblasted to the standard specified above.

Consult your International Paint representative for specific recommendations.

Cleanliness

All surfaces to be coated must be clean, dry and free from contamination.

Residual dust levels prior to paint application must not exceed rating "1" for dust size classes "3", "4" or "5" (ISO 8502-3:1993).

Residual soluble salt levels prior to coating application must not exceed 50mg/m² as extracted and measured in accordance with ISO 8502-6 (1995) and ISO 8502-9 (1998) respectively.

Surface profile

The surface profile must lie in the range 30-75 microns (ISO 8503-1/2:1988).

NOTE
For use in Marine situations in North America, the following surface preparation standards can be used:
SSPC-SP10 in place of Sa2½ (ISO 8501-1:2007)

X.International.

Interplate 855
IMO Resolution MSC.215 (82)
compliant Zinc Silicate Shop Primer

APPLICATION

Mixing	Material is supplied in 2 containers as a unit. Always mix a complete unit in the proportions supplied. Agitate Paste (Part A) with a power agitator, slowly add binder (Part B) while agitating. Allow to mix for at least 5 minutes, sieve through a 30-60 mesh screen before use. Continue stirring during use.
Thinner	GTA820 (Winter Grade), GTA840 (Summer Grade) Not recommended. Use International GTA820, GTA840 only in exceptional circumstances (max 15% by volume). DO NOT thin more than allowed by local environmental legislation.
Airless Spray	Recommended Tip Range 0.38-0.58 mm (15-23 thou) Total output fluid pressure at spray tip not less than 60 - 100 kg/cm² (850 - 1420 p.s.i.)
Conventional Spray	Use suitable proprietary equipment. Thinning may be required.
Brush	Application by brush is recommended for small areas only. Multiple coats may be required to achieve specified film thickness.
Roller	Application by roller is recommended for small areas only. Multiple coats may be required to achieve specified film thickness. Brush and roller are not suitable for application of full coats. Airless spray should be used for the latter.
Cleaner	International GTA820/GTA840
Work Stoppages and Cleanup	Do not allow material to remain in hoses, gun or spray equipment. Thoroughly flush all equipment with International GTA820/GTA840. Once units of paint have been mixed they should not be resealed and it is advised that after prolonged stoppages work recommences with freshly mixed units. Clean all equipment immediately after use with International GTA820/GTA840. It is good working practice to periodically flush out spray equipment during the course of the working day. Frequency of cleaning will depend upon amount sprayed, temperature and elapsed time, including any delays. Do not exceed pot life limitations. All surplus materials and empty containers should be disposed of in accordance with appropriate regional regulations/legislation.
Welding	In the event welding or flame cutting is performed on metal coated with this product, dust and fumes will be emitted which will require the use of appropriate personal protective equipment and adequate local exhaust ventilation. In North America do so in accordance with instruction in ANSI/ASC Z49.1 "Safety in Welding and Cutting."

SAFETY

All work involving the application and use of this product should be performed in compliance with all relevant national Health, Safety & Environmental standards and regulations.

Prior to use, obtain, consult and follow the Material Safety Data Sheet for this product concerning health and safety information. Read and follow all precautionary notices on the Material Safety Data Sheet and container labels. If you do not fully understand these warnings and instructions or if you can not strictly comply with them, do not use this product. Proper ventilation and protective measures must be provided during application and drying to keep solvent vapour concentrations within safe limits and to protect against toxic or oxygen deficient hazards. Take precautions to avoid skin and eye contact (ie. gloves, goggles, face masks, barrier creams etc.) Actual safety measures are dependant on application methods and work environment.
EMERGENCY CONTACT NUMBERS:
USA/Canada - Medical Advisory Number 1-800-854-6813
Europe - Contact (44) 191 4696111. For advice to Doctors & Hospitals only contact (44) 207 6359191
R.O.W. - Contact Regional Office

LIMITATIONS

Drying times will depend on the substrate temperature and ventilation conditions.
If the relative humidity is below 50%, cure will be retarded.
Pot life may reduce to 8 hours (25°C) as Binder (Part B) approaches the end of its shelf life.
Interplate 855 is not recommended for manual spray application.
At higher dry film thickness, fabrication properties (welding and cutting) may be affected.
Shop primers are not recommended for use as touch-up primers after fabrication.

Film Thickness

Minimum Film Thickness

Film thicknesses below the specified 15 microns may result in premature breakdown of the shop primer and
substrate corrosion, necessitating additional secondary surface preparation.

Maximum Film Thickness

Film thicknesses above the specified 15 microns may adversely affect welding and cutting properties and may affect
the performance of subsequently applied coating systems. Thicknesses above 25 microns should be avoided.

Overcoating information is given for guidance only and is subject to regional variation depending upon local climate
and environmental conditions. Consult your local International Paint representative for specific recommendations.
The temperature of the surface to be coated must be at least 3°C above the dew point. For optimum application
properties bring the material to 21-27°C , unless specifically instructed otherwise, prior to mixing and application.
Unmixed material (in closed containers) should be maintained in protected storage in accordance with the
information given in the STORAGE section of this data sheet.
Technical and application data herein is for the purpose of establishing a general guideline of the coating and proper
coating application guidelines. Test performance results were obtained in a controlled laboratory environment and
International Paint makes no claim that the exhibited published test results, or any other tests, accurately represent
results actually found in all field environments. As application, environmental and design factors can vary
significantly, due care should be exercised in the selection, verification of performance and use of the coating.

Appendix 11 - Steel plate returned from International Paint with shop primer Interplate 855 applied.

Appendix 12 – Elcometer Dry Film Thickness Gauge Calibration Certificate.

Test Certificate
Certificat d'essai • Testzertifikat

elcometer
www.elcometer.com

Certificate Number: 456-SK23908-G
Numéro de Certificat:
Bescheinigungsnummer:

Instrument Part Number: A415CFNFTI
Code Article d'instrument:
Artikelnummer des Geräts:

Instrument Type: Elcometer 415 Model T Dual FNF Paint & Powder Thickness Gauge: 0-1000µm/40mils
Instrument Modèle: Elcometer 415 Modèle T Mixte FNF Jauge de mesure d'épaisseur de peinture et poudre: 0-1000µm/40mils
Gerätetyp: Elcometer 415 Modell T Farb- und Pulverbeschichtungsmessgerät für Eisen & Nichteisen (FNF): 0-1000µm/40mils

Instrument Serial Number: SK23908   **Instrument PCB Serial Number:** SJ05199
Instrument Numéro de Série: Circuit imprimé Numéro de Série:
Seriennummer des Geräts: Seriennummer der Leiterplatte:

Measurement Date: 26/10/2016
Date de Mesure:
Maß-datum:

The instrument was calibrated using a smooth calibration, with the factory zero plate and the thickest certified foil listed below in accordance with Elcometer's Certification Procedure.

L'instrument a été étalonné à l'aide d'un étalonnage lisse, en utilisant une plaque zéro et la feuille d'étalonnage certifié la plus épaisse qui est énumérés ci-dessous, selon les Procédures d'Etalonnage d'Elcometer.

Das Gerät wurde nach einer glatten Kalibriermethode kalibriert durch Einsetzen einer Nullplatte und die dickste zertifizierter Folie, die unten aufgelistet ist. Die Kalibriermethode wurde gemäß Elcometer's Zertifizierungsprotokolls durchgeführt.

Measurement Results: Ferrous • Resultats de Mesure: Ferreux • Messergebnisse: Eisenmetall

Foil / Substrate[1] Feuille d'Etalonnage / Substrat[1] Folie / Untergrund[1]			Actual Measured Value[1] Valeur mesurée exacte[1] Aktuelle Messwert[1]			Allowable Value[1] Valeur admissible[1] Zulässigen Wert[1]			
Value • Valeur • Wert		Serial Number[2] Numéro de Série[2] Seriennummer[2]	µm	mils		µm	mils	
µm	mils								
1013.0	39.88	NA01982	1013.7	39.91	±1%	1002.9 - 1023.1	39.48 - 40.28	Pass • Réussi • Bestanden
128.1	5.04	SE18133	127.0	5.00	±3%	124.3 - 131.9	4.89 - 5.19	Pass • Réussi • Bestanden
0.0	0.00	501154	0.0	0.00	±1µm	-1.0 - 1.0	-0.04 - 0.04	Pass • Réussi • Bestanden
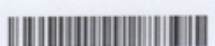
Measurement Results: Non Ferrous • Resultats de Mesure: Non-Ferreux • Messergebnisse: Nichteisenmetall

Foil / Substrate[1] Feuille d'Etalonnage / Substrat[1] Folie / Untergrund[1]			Actual Measured Value[1] Valeur mesurée exacte[1] Aktuelle Messwert[1]			Allowable Value[1] Valeur admissible[1] Zulässigen Wert[1]			
Value • Valeur • Wert		Serial Number[2] Numéro de Série[2] Seriennummer[2]	µm	mils		µm	mils	
µm	mils								
1013.0	39.88	NA01982	1013.3	39.89	±1%	1002.9 - 1023.1	39.48 - 40.28	Pass • Réussi • Bestanden
128.1	5.04	SE18133	128.4	5.05	±3%	124.3 - 131.9	4.89 - 5.19	Pass • Réussi • Bestanden
0.0	0.00	501013	0.8	0.03	±1µm	-1.0 - 1.0	-0.04 - 0.04	Pass • Réussi • Bestanden

Signed on behalf of Elcometer Limited • Signé au nom d'Elcometer Limited • Unterzeichnet im Namen Elcometer Limited

Name: *A Smith*
Nom:
Name: Quality Manager • Responsable Qualité • Qualitätsbetriebsleiter

[1] Measurements taken in microns, mils values are calculated using 1µm = 0.03937mil
[1] Les valeurs sont prises en microns. Les valeurs en 'mils' sont calculées en utilisant 1µm = 0.03937mil
[1] Messwerte sind in Microns gezeigt. Um auf „mils" umzurechnen, benutzen Sie 1µm = 0.03937mil
[2] Certificate Number: 43627
[2] Numéro de Certificat: 43627
[2] Bescheinigungsnummer: 43627

Appendix 13 – Welding Set Calibration Certificate.

PREMIER WELDING LTD
Email: gideon@premierwelding.com

VALIDATION CERTIFICATE

Customer info

Customer: UNIVERSITY OF STRATHCLYDE

Address: GLASGOW

Welding equipment info

		Validation info	
Manufacturer:	Miller	**Validation date:**	20/07/2017
Model:	XMT 304	**Expiration date:**	19/07/2018
Equipment ID:	LF440233A	**Grade of validation:**	Standard
		Validation type:	Accuracy
Kemppi ArcValidator L 650		**Other instruments:**	RESISTIVE LOAD .
Serial number:	2353094		
Type:	Electronically controlled resistor load		

VALIDATION RESULTS

VOLTAGE (V)

Set		Measured				Result			Display			Result
	MIN	#1	mean	#2	MAX		MIN	#1	mean	#2	MAX	
16.5	14.8	18.0	18.1	18.1	18.2	✅	16.0	18.0	18.0	18.0	20.2	✅
20.9	18.8	20.8	20.9	20.9	23.0	✅	18.8	20.7	20.8	20.8	23.0	✅
25.3	22.8	25.3	25.3	25.3	27.8	✅	23.2	25.1	25.1	25.1	27.4	✅
29.6	26.6	29.5	29.5	29.5	32.6	✅	27.4	29.4	29.4	29.4	31.6	✅
34.0	30.6	33.9	33.9	33.9	37.4	✅	31.8	33.3	33.6	33.8	36.0	✅

CURRENT (A)

Set voltage (V)	Measured				Display					Result
	#1	mean	#2		MIN	#1	mean	#2	MAX	
16.5	60	60	60		50	59	59	59	70	✅
20.9	138	138	138		128	138	138	137	148	✅
25.3	226	226	226		216	228	228	228	236	✅
29.6	312	312	312		302	315	315	315	322	✅
34.0	400	400	400		390	402	402	402	410	✅

VALIDATION PARAMETERS

Idle voltage (V)	Supply voltage (V)	Temperature (°C)
85.9	415	20.0
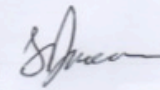
WELDING PROCESS TYPE

MIG/MAG	TIG	MMA
☑		

NOTES
CERT NO. 09698/1 MIG

✅ **PASSED**

21/7/2017
Date

G DUNCAN

Validation is based on EN 50504:2008 standard

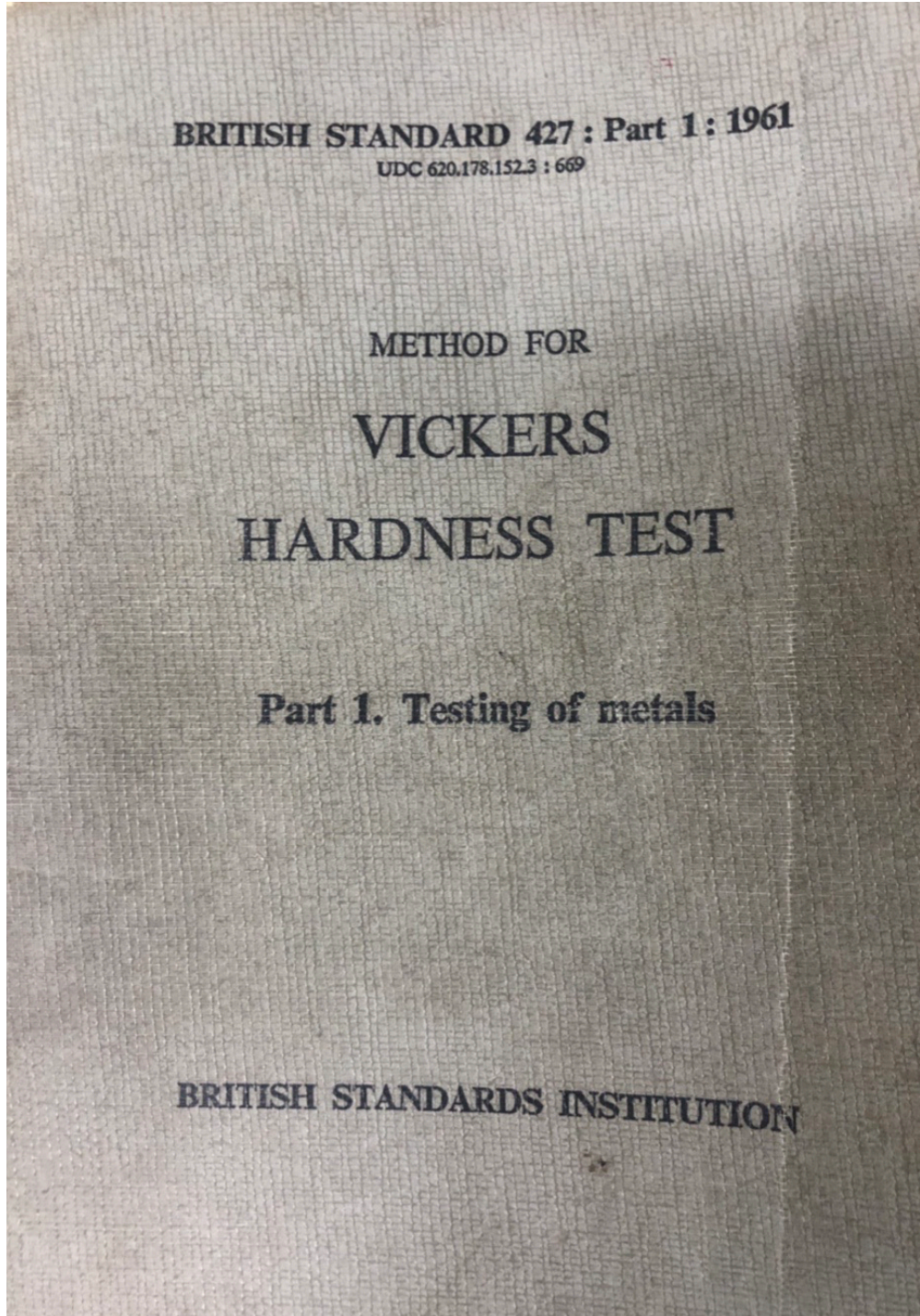*Appendix 14 – British Standard for Vickers Hardness Testing.*

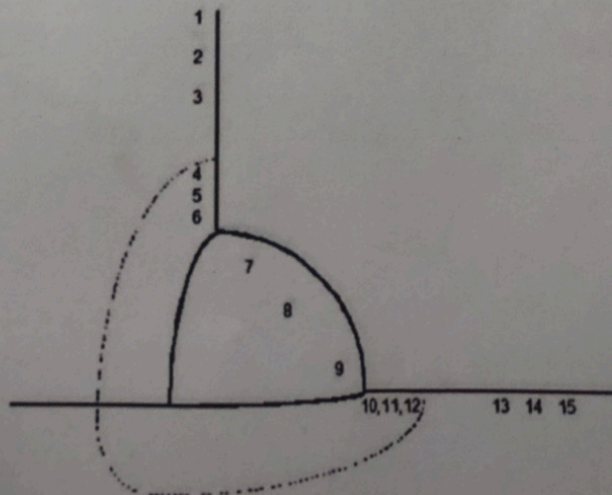**BRITISH STANDARD 427 : Part 1 : 1961**

UDC 620.178.152.3 : 669

METHOD FOR

VICKERS

HARDNESS TEST

Part 1. Testing of metals

BRITISH STANDARDS INSTITUTION

Load = 5 kgf

Diagonal of impression mm	0·000	0·001	0·002	0·003	0·004	0·005	0·006	0·007	0·008	0·009
0·06	2576	2492	2412	2336	2264	2195	2129	2065	2005	1947
0·07	1892	1839	1789	1740	1693	1648	1605	1564	1524	1486
0·08	1449	1413	1379	1346	1314	1283	1254	1225	1197	1171
0·09	1145	1120	1095	1072	1049	1027	1006	985	965	946
0·10	927	909	891	874	857	841	825	810	795	780
0·11	766	753	739	726	713	701	689	677	666	655
0·12	644	633	623	613	603	593	584	575	566	557
0·13	549	540	532	524	516	509	501	494	487	480
0·14	473	466	460	453	447	441	435	429	423	418
0·15	412	407	401	396	391	386	381	376	371	367
0·16	362	358	353	349	345	341	336	332	329	325
0·17	321	317	313	310	306	303	299	296	293	289
0·18	286	283	280	277	274	271	268	265	262	260
0·19	257	254	252	249	246	244	241	239	237	234
0·20	232	229	227	225	223	221	218	216	214	212
0·21	210	208	206	204	202	201	199	197	195	193
0·22	192	190	188	186	185	183	182	180	178	177
0·23	175	174	172	171	169	168	166	165	164	162
0·24	161	160	158	157	156	154	153	152	151	150
0·25	148	147	146	145	144	143	141	140	139	138
0·26	137	136	135	134	133	132	131	130	129	128
0·27	127	126	125	124	123·5	122·6	121·7	120·8	120·0	119·1
0·28	118·3	117·4	116·6	115·8	115·0	114·2	113·4	112·6	111·8	111·0
0·29	110·2	109·5	108·7	108·0	107·3	106·5	105·8	105·1	104·4	103·7
0·30	103·0	102·3	101·7	101·0	100·3	99·7	99·0	98·4	97·7	97·1
0·31	96·5	95·9	95·2	94·6	94·0	93·4	92·9	92·3	91·7	91·1
0·32	90·5	90·0	89·4	88·9	88·3	87·8	87·2	86·7	86·2	85·7
0·33	85·1	84·6	84·1	83·6	83·1	82·6	82·1	81·6	81·2	80·7
0·34	80·2	79·7	79·3	78·8	78·4	77·9	77·4	77·0	76·6	76·1
0·35	75·7	75·3	74·8	74·4	74·0	73·6	73·2	72·7	72·3	71·9
0·36	71·5	71·1	70·8	70·4	70·0	69·6	69·2	68·8	68·5	68·1
0·37	67·7	67·4	67·0	66·6	66·3	65·9	65·6	65·2	64·9	64·5
0·38	64·2	63·9	63·5	63·2	62·9	62·6	62·2	61·9	61·6	61·3
0·39	61·0	60·6	60·3	60·0	59·7	59·4	59·1	58·8	58·5	58·2
0·40	57·9	57·7	57·4	57·1	56·8	56·5	56·2	56·0	55·7	55·4
0·41	55·2	54·9	54·6	54·4	54·1	53·8	53·6	53·3	53·1	52·8
0·42	52·6	52·3	52·1	51·8	51·6	51·3	51·1	50·9	50·6	50·4
0·43	50·1	49·9	49·7	49·5	49·2	49·0	48·8	48·6	48·3	48·1
0·44	47·9	47·7	47·5	47·2	47·0	46·8	46·6	46·4	46·2	46·0

16

Appendix 15 – Vickers Hardness Testing Record Sheet.

Russell Angus Phipps – MPhil Hardness Testing

Weld Sample - 36

Filler - SF-1A

Primer paint thickness - 0-7 μm

Comments -

Indent No.	Position	Hardness No. Hv 5
1	Parent	146
2	Parent	158
3	Parent	166
4	HAZ	182
5	HAZ	227
6	HAZ	271
7	Weld	234
8	Weld	227
9	Weld	223
10	HAZ	252
11	HAZ	223
12	HAZ	210
13	Parent	165
14	Parent	172
15	Parent	174

Appendix 16 – Visible surface breaking pores on tested production panel.

Appendix 17 – HAZ Hardness totalled and averaged to allow comparison.

HAZ Hardness (HV) - Totals & Averages			
Filler Type	DFT Range (μm)	Total Across 4 Indents	Average (*)
SupraMIG	0-7	966	242 (2)
	7.1 - 20	967	242 (2)
	20.1 - 45	949	237 (1)
SF-1A	0-7	973	243 (1)
	7.1 - 20	1040	260 (3)
	20.1 - 45	1033	258 (2)
SM-3A DCEN	0-7	1064	266 (1)
	7.1 - 20	1263	316 (3)
	20.1 - 45	1139	285 (2)
Outershield	0-7	1157	289 (2)
	7.1 - 20	1072	268 (1)
	20.1 - 45	1233	308 (3)
SM-3A DCEP	0-7	1280	320 (2)
	7.1 - 20	1187	297 (1)
	20.1 - 45	1291	323 (3)
* Number in brackets is the order of value starting from lowest to highest.			

Appendix 18 – HAZ area totalled and averaged to allow comparison.

HAZ Area (mm2) - Totals & Averages			
Filler Type	DFT Range (µm)	Total Over 5 Samples (mm2)	Average (*) (mm2)
SupraMIG	0-7	228.3	45.7 (3)
	7.1 - 20	197.9	39.6 (2)
	20.1 - 45	188.1	37.6 (1)
SF-1A	0-7	193.2	38.6 (2)
	7.1 - 20	147.8	29.6 (1)
	20.1 - 45	195.7	39.1 (3)
SM-3A DCEN	0-7	130.9	26.2 (3)
	7.1 - 20	99.3	19.9 (1)
	20.1 - 45	111.6	22.3 (2)
Outershield	0-7	137.6	27.5 (2)
	7.1 - 20	116	23.2 (1)
	20.1 - 45	145.1	29 (3)
SM-3A DCEP	0-7	141	28.2 (1)
	7.1 - 20	146.2	29.2 (2)
	20.1 - 45	149.3	29.9 (3)
* Number in brackets is the order of value starting from lowest to highest.			
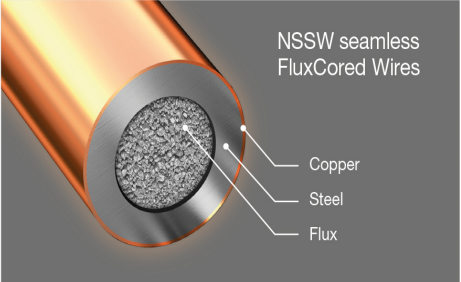
Appendix 19 – Penetration area totalled and averaged to allow comparison.

Penetration Area (mm2) - Totals & Averages			
Filler Type	DFT Range (µm)	Total Over 5 Samples (mm2)	Average (*) (mm2)
SupraMIG	0-7	87.7	17.5 (1)
	7.1 - 20	94.7	18.9 (3)
	20.1 - 45	93.5	18.7 (2)
SF-1A	0-7	77.3	15.5 (1)
	7.1 - 20	79.9	16 (3)
	20.1 - 45	79.8	16 (2)
SM-3A DCEN	0-7	32.8	6.6 (1)
	7.1 - 20	39.1	7.8 (2)
	20.1 - 45	45.2	9 (3)
Outershield	0-7	56.5	11.3 (1)
	7.1 - 20	60.3	12.1 (3)
	20.1 - 45	60.1	12 (2)
SM-3A DCEP	0-7	79.7	15.9 (1)
	7.1 - 20	84.8	17 (3)
	20.1 - 45	81.2	16.2 (2)
* Number in brackets is the order of value starting from lowest to highest.			

Appendix 20 – Porosity Area (mm2) across 4 varied filler types at 3 DFT ranges and the average porosity area at each DFT Range.

Filler Type	Porosity Area Over 70mm Sample (mm2)		
	DFT Range (µm)		
	0-7	7.1 - 20	20.1 - 45
SupraMIG	0	1.3	16.6
SF-1A	0.9	0.9	18.7
Outershield	2.1	9.3	22.6
SM-3A DCEP	0	0	5.7
	Average Porosity Area at DFT Range		
All Fillers	0.8	2.9	15.9

Appendix 21 – Advantages of seamless cored wires, with the copper coating improving conductivity and providing a stable welding arc. Adapted from NSSW [22].

NSSW FCW	Benefits:
✔	**Extremely low hydrogen content**
✔	**Superior wire feeding properties**
✔	**Excellent conductivity and stable arc**
✔	**Reliable quality with no downtime**
✔	**Deep penetration into base material**
✔	**Less cleanup and finishing work**
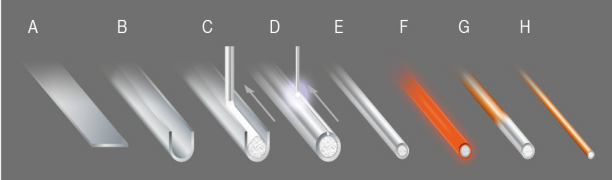
NSSW seamless FluxCored Wires

Copper
Steel
Flux

A B C D E F G H

NSSW ICF Production Process (In-line continuous filling)

A. Strip
B. Roll forming
C. Flux filling
D. Seam welding

E. Drawing
F. Dehydrogenation and annealing
G. Copper plating
H. Drawing and spooling

Appendix 22 – The influence of shop primers on weld quality for mechanized or automated welding – Work by Boekholt, R. [4].

SHIPYARD	No porosity	Yes porosity	BH	PIT		SOLUTION
1 Japan		X	X	X		SPD
2 Japan		X	X	X		
3 Japan		X		X		
4 Japan		X	X			SPD
6 Japan		X	X	X		
7 Japan		X	X	X		SPD
8 Japan		X	X	X		
9 Japan		X	X	X		SPD
10 Japan		X		X		
11 Japan		X		X		
12 Japan		X	X	X		
14 Japan		X	X	X		SPD
15 Japan		X	X	X		
16 Japan		X	X	X		SPD
17 Japan		X	X	X		
18 Japan		X	X	X		SPD
19 Japan		X	X	X		SPD
20 Japan		X	X	X		
21 Japan		X	X	X		SPD
22 Japan		X	X	X		SPD
23 Japan		X	X			
24 Japan		X	X	X		
25 Japan		X		X		SPD
26 Japan		X	X	X		
28 Belgium	X				FCAW 3F	
	X				SMAW 2F	
		X			SAW TWIN	LC
		X			FCAW 2F	
29 Denmark		X				SPD
			Type: zinc silicate			
30 Denmark						
31 Denmark	X				SMAW	
	X				Robotic	
		X		(semi)	FCAW	
		X		(aut.)	FCAW	
		X		(aut.)	CMAW	not possible
			Type: zinc silicate		SAW	SPD
32 Germany			Possible with great expense			
			Type: Iron-Oxide			
33 Germany		X	Type Iron-Oxide			SPD
			Type: Iron oxide			LC
34 Germany		X				LC
			Type: Iron-Oxide Zinc Silicate			
35 Germany		X				
			Type: Lindecote Zinc Silicate			
36 Germany		X				LC
37 Germany		X				LC
			Type: Zinc primer Iron oxide primer			
38 Germany		X				LC
			Type: Sigma Ironside			

39 Spain		X			
			Type: Fe-Epoxy Primer		
40 Spain		X			
			Type: Fe-Epoxy Primer		
41 Spain		X			
			Type: Fe-Epoxy Primer		
42 Spain	X				
43 Spain		X			
			Type: Zinc primer		
45 USA		X			SPD
			Type: Int. Zinc Systems		
46 A Netherlands					
46 B Netherlands					
47 Netherlands		X			SPD
			Type: Sigma Weld MC		
48 Netherlands					
49 Netherlands					
50 Netherlands					
51 Netherlands					
52 Netherlands					
53 Netherlands					
54 Netherlands					
55 Portugal		X			
			Type: Zinc silicate		
56 Portugal		X			
			Type: Zinc silicate		
57 U.K.		X			